ADDIS ABABA INSTITUTE OF TECHNOLOGY
SCHOOL OF GRADUATE STUDIES

DEPARTMENT OF CIVIL ENGINEERING

COMPARISON OF CONVENTIONAL AND MODAL PUSHOVER ANALYSIS OF BUILDINGS

A thesis submitted to the school of Graduate Studies in Partial fulfillment of the Requirements for the Degree of Master of Science in Civil Engineering (Structures)

By

Abdi Mohammed

Advisor: **Dr.-Ing. Adil Zekaria**

March 2012

ADDIS ABABA INSTITUTE OF TECHNOLOGY
SCHOOL OF GRADUATE STUDIES

DEPARTMENT OF CIVIL ENGINEERING

COMPARISON OF CONVENTIONAL AND MODAL PUSHOVER ANALYSIS OF BUILDINGS

A thesis submitted to the school of Graduate Studies in Partial fulfillment of the Requirements for the Degree of Master of Science in Civil Engineering (Structures)

By

Abdi Mohammed

March 2012

Approved by Board of Examiners

Dr.-Ing. Adil Zekaria Advisor	_____ Signature	_____ Date
Dr. Shifferaw Taye External Examiner	_____ Signature	_____ Date
Dr. Esayas Gebreyouhannes Internal Examiner	_____ Signature	_____ Date
Ato Dawit Admasu Chairman	_____ Signature	_____ Date

ACKNOWLEDGEMENTS

I would like to express my sincere appreciation to my advisor Dr.-Ing. Adil Zekaria for the support, guidance, encouragement and insights he provided me throughout the study.

I also extend my gratitude towards all those individuals who had contributed in one way or the other.

Finally, I would like to express my deepest appreciation to my family for their confidence in me and for the support, love and understanding.

TABLE OF CONTENTS

LIST OF TABLES

LIST OF FIGURES

LIST OF NOTATIONS

c = viscous damping coefficient

C_o = modification factor to relate the SDOF spectral displacement to MDOF roof displacement

C_1 = modification factor to relate the expected maximum inelastic SDOF displacement divided by the elastic SDOF displacement

C_2 = modification factor to represent the effect of hysteresis shape on the maximum displacement response

C_3 = modification factor to represent increased displacements due to second-order effects

C_R = ratio of peak deformations of inelastic and corresponding elastic SDOF systems for systems with known yield-strength reduction factor.

$C\mu$ = ratio of peak deformations of inelastic and corresponding elastic SDOF systems for systems with known ductility factor.

d_i = the lateral drift in story *i*

d_r = design interstory drift, evaluated difference of the average lateral displacements at the top and bottom of the storey under consideration

D_n = peak spectral roof displacement of the n^{th} mode SDF system

E_D = energy dissipated through hysteretic behavior

E_S = strain energy at the maximum displacement

g = acceleration of gravity

h_i = height of i^{th} story

k_i = elastic lateral stiffness of the building

k_e = effective lateral stiffness of the building

$[K]$ = stiffness matrix

k = stiffness of SDOF system

$[M]$ = mass matrix

m = mass of SDOF system

p_i = the portion of the total weight of the building

R = ratio of inelastic strength demand to calculated yield strength coefficient

R_y = yield-strength reduction factor

S_a = spectral pseudo-acceleration

S_d = spectral pseudo-displacement

T_e = effective fundamental period

T_o = characteristic period of the response spectrum

T_a = period defined in Newmark–Hall smooth design spectrum

T_b = period defined in Newmark–Hall smooth design spectrum

T_c = period separating acceleration- and velocity-sensitive regions

$T_{c'}$ = transition period in Newmark–Hall Ry –μ– Tn relations

T_n = elastic natural period of vibration

u_{rn} = peak roof of the n^{th} mode MDF system

u_{rjn} = n^{th} mode roof displacement in the j-direction

u = relative displacement between the mass and base of the structure

$\dot{u}$ = velocity of mass with respect to time

$\ddot{u}$ = acceleration of mass with respect to time

V_{by} = base shear at yield

V_i = total calculated lateral shear force in the direction under consideration at story *i*

W = total dead load

ξ = viscous damping

δ = reference displacement of MDOF model

δ_t = target displacement of MDOF model

ζ_{eq} = equivalent damping value

ζ_{eff} = effective damping value

Ω = forcing frequency

κ = damping modification factor

γ = behavior factor

θ_i = story drift sensitivity coefficient

θ_m = the maximum value of θ_i for all stories

ϕ_n = mode shape factor

ϕ_{rn} = amplitude of ϕn at the roof in the direction of the selected pushover curve

ϕ_{rjn} = n^{th} – mode amplitude of mode shape at roof level in the j-direction

Γ_n = modal participation factor for the n^{th} mode SDF system

$\bar{f}_y$ = normalized yield strength

μ = ductility factor

ω_D = natural circular frequency of a damped vibration of a system.

ωn = the natural circular frequency of a system.

ABSTRACT

After revealing the deficiencies of Conventional Pushover Analysis (CPA) method for structures with significant higher modes, Modal Pushover Analysis (MPA) procedures is proposed to overcome this limitation. This study primarily evaluates the effectiveness of MPA compared to conventional pushover analysis in predicting structural response of low and medium rise reinforced concrete buildings, designed as fully ductile moment resisting frame based on the Ethiopian building code. In addition, the values from MPA are compared to that of the Response Spectrum Analysis (RSA) method for better understanding of the methods. For the analysis of the buildings the analytical nonlinear modeling of structural elements are considered which includes failure modes in flexure and shear by the software SAP2000.

The results obtained from MPA are compared to CPA and RSA methods. It is shown that higher results of the story shear, story displacement and inter-story drift ratio can be predicted by the MPA than CPA method. The RSA method generally underestimates the story displacement and inter-story drift ratio as compared to MPA.

KEYWORDS: Modal Pushover Analysis (MPA), higher mode effect, ductile moment resisting RC frame, Conventional Pushover Analysis (CPA), Response Spectrum Analysis (RSA), Seismic Performance Evaluation

1. INTRODUCTION

1.1 Background

Over the past thirty years it has been recognized that damage control must become a more explicit design consideration which can be achieved only by introducing some kind of nonlinear analysis into the seismic design methodology. Following this pushover analysis has been developed over the past twenty years and has become the preferred method of analysis for performance-based seismic design, PBSD and evaluation purposes. It is the method by which the ultimate strength and the limit state can be effectively investigated after yielding, which has been researched and applied in practice for earthquake engineering and seismic design. Nonlinear response history analysis is a possible method to calculate structural response under a strong seismic event. However, due to the large amount of data generated in such analysis, it is not considered practical and PBSE usually involves nonlinear static analysis, also known as pushover analysis. Moreover, the calculated inelastic dynamic response is quite sensitive to the characteristics of the input motions, thus the selection of a suitable representative acceleration time–histories is mandatory. This increases the computational effort significantly. The simplified approaches for the seismic evaluation of structures, which account for the inelastic behaviour, generally use the results of static collapse analysis to define the inelastic performance of the structure. Currently, for this purpose, the nonlinear static procedure (NSP) or pushover analysis described in FEMA-273/356/440, ATC-40/55 and EC8 documents are used. However, the procedure involves certain approximations and simplifications that some amount of variation is always expected to exist in seismic demand prediction of pushover analysis.

Structures are expected to deform inelastically when subjected to severe earthquakes, so seismic performance evaluation of structures should be conducted considering post-elastic behavior. Therefore, a nonlinear analysis procedure must be used for evaluation purpose as post-elastic behavior cannot be determined directly by an elastic analysis. Moreover, maximum inelastic displacement demand of structures should be determined to adequately estimate the seismically induced demands on structures that exhibit inelastic behaviour. Various simplified nonlinear analysis procedures and approximate methods to estimate maximum inelastic displacement demand of structures are proposed by researchers. The widely used simplified nonlinear

analysis procedure, pushover analysis, has also been an attractive subject of study which is mainly appropriate for structures in which higher modes are not predominant, which are not influenced by dynamic characteristics. Although, pushover analysis has been shown to capture essential structural response characteristics under seismic action, the accuracy and the reliability of pushover analysis in predicting global and local seismic demands for all structures have been a subject of discussion.

As conventional (traditional) pushover analysis is widely used for design and seismic performance evaluation purposes, its limitations, weaknesses and the accuracy of its predictions in routine application should be identified by studying the factors affecting the pushover predictions. In other words, the applicability of pushover analysis in predicting seismic demands should be investigated for low, mid and high-rise structures by identifying certain issues such as modeling nonlinear member behavior, computational scheme of the procedure, variations in the predictions of various lateral load patterns utilized in traditional pushover analysis, efficiency of invariant lateral load patterns in representing higher mode effects and accurate estimation of target displacement at which seismic demand prediction of pushover procedure is performed. Following these ,a number of studies have been done and raised doubts on the effectiveness of conventional pushover methods, whereby a constant single-mode incremental force vector is applied to the structure, in estimating the seismic demand/capacity of framed buildings subjected to earthquake action which may lead to inaccurate prediction of deformations when higher modes are important and/or the structure is highly pushed into its nonlinear post-yield range and inaccurate prediction of local damage concentrations, responsible for changing the modal response. After revealing the deficiencies of the conventional pushover methods, efforts have been made to improve these deficiencies. The improved pushover procedures have been proposed to overcome the certain limitations of conventional pushover procedures. Extension of the pushover approach to consider higher modes effects has attracted attention, the effort being to match as closely as possible the results of nonlinear time history analysis.

For the purpose of considering higher mode effects recently some enhanced pushover procedures based on the modal combination concept are developed while the simplicity of the conventional methods is kept (Paret et al.1996; Sasaki et al. 1998; Moghadam 2002; Chopra and Goel 2002; Shakeri et al. 2006). In modal pushover analysis (MPA) proposed by (Chopra

and Goel 2002), multiple pushover analyses with lateral load corresponding to the considered elastic mode shapes are conducted separately, and then the total seismic response is estimated by combining the responses due to each modal load. In fact the total seismic response of the multi degree of freedom system is estimated by combining the responses of multiple single degree freedom system.

Even though in recent years there are great amount of research on modal pushover analysis, little has been done to evaluate the efficiency of modal pushover analysis as compared to conventional pushover analysis procedure for 3D asymmetric reinforced concrete structures. The principal objective of this paper is to study on the conventional and modal pushover analysis for 3D asymmetric reinforced concrete structures and to compare responses from two methods. In addition a detailed dynamic analysis of RC frame building is performed using response spectrum method based on EBCS-8, 1995 provisions to compare with modal pushover analysis. In this paper, the target displacement used for modal pushover analysis was estimated by multiplying the values from the elastic response-spectrum analysis method with inelastic deformation ratio (Chopra and Chintanapakdee 2004).

1.2 Objectives and Scope

This study is concerned with the application of recent development on techniques of pushover analysis proposed by (Chopra and Goal 2002), and recommended by ATC-55, and the effects of higher modes on the results of nonlinear static pushover analysis. The responses of three multistory buildings made of reinforced concrete due to earthquake ground motions are investigated. It aims to encourage the inclusion of performance-based concepts in local seismic codes of design and evaluation.

Mainly, the objectives of this thesis are:

(1) To compare the seismic demands estimated by response spectrum and conventional pushover analysis with that of modal pushover analysis.

(2) To observe the significance of higher mode effects applied during the pushover analysis.

(3) To evaluate the seismic performance of the selected RC buildings designed and detailed according to EBCS, 1995 code provisions.

(4) To plot the pushover curve resulting from the design earthquake forces.

The effect of different distributions of lateral load patterns, soil-structure interaction effect and nonlinear-dynamic analysis of these RC buildings are not performed in this study.

1.3 Thesis Organization

The thesis is divided into six chapters as follows.

Chapter 1: Gives a general introduction, need for the investigation, objective and scope of the investigation and organization of the thesis.

Chapter 2: Presents a review of previous studies in literature concerning performance-based seismic evaluation and design of new or existing structures based on nonlinear static analysis together with the approximations and limitations of the conventional pushover analysis method and recommendations to improved methods of pushover analysis.

Chapter 3: In this chapter, the philosophy of pushover analysis is presented, together with the demonstration of linear and nonlinear static and dynamic methods of structural analysis. The concept of Modal Pushover Analysis (MPA) is described. In addition, various methods used for determination of target displacement and performance point are also illustrated in this chapter.

Chapter 4: Presents non-linear analytical modeling of structural components subjected to earthquake motions. Geometric and material non-linearity property of structural elements is explained. The numerical modeling of the frame buildings using computers is outlined. Nonlinear capabilities using the plastic hinge concept and the tools needed for pushover analysis are also described.

Chapter 5: In this chapter the general sequence of steps needed to perform both conventional and modal pushover analysis is exploited. The results of the analysis are compiled and presented in a suitable format. Comparison between the results obtained from the conventional and modal pushover analyses are carried out. In addition the corresponding results obtained by response spectrum analyses are also presented. The seismic demands: floor displacements profiles, storey shear force and interstorey drift ratios for each RC building are presented and discussed.

Chapter 6: The main conclusion and recommendations that can be drawn from the current study are summarized, and also suggestions for future studies are outlined.

2. LITRATURE REVIEW

Most of the simplified nonlinear analysis procedures utilized for seismic performance evaluation make use of conventional (traditional) pushover analysis and/or equivalent SDOF representation of actual structure. However, conventional pushover analysis afterwards simply called pushover analysis involves certain approximations and simplification, therefore some amount of variation is always expected to exist in seismic demand prediction so that the reliability and the accuracy of the procedure should be identified. For this purpose, researchers investigated various aspects of pushover analysis to identify the limitations and weaknesses of the procedure and proposed improved pushover procedures that consider the effects of lateral load patterns, higher modes, failure mechanisms, etc.

Krawinkler and Seneviratna [17] conducted a detailed study that discusses the advantages, disadvantages and the applicability of conventional pushover analysis by considering various aspects of the procedure. The basic concepts and main assumptions on which the pushover analysis is based, target displacement estimation of MDOF structure through equivalent SDOF domain and the applied modification factors, importance of lateral load pattern on pushover predictions, the conditions under which pushover predictions are adequate or not and the information obtained from pushover analysis were identified. Local and global seismic demands were calculated from pushover analysis results at the target displacement associated with the individual records. The comparison of pushover and nonlinear dynamic analysis results showed that pushover analysis provides good predictions of seismic demands for low-rise structures having uniform distribution of inelastic behaviour over the height. It was also recommended to implement pushover analysis with caution and judgment considering its many limitations since the method is approximate in nature and it contains many unresolved issues that need to be investigated.

İnel, Tjhin and Aschheim [16] conducted a study to evaluate the accuracy of various lateral load patterns used in current pushover analysis procedures. First mode, inverted triangular, rectangular, "code", adaptive lateral load patterns and multimode pushover analysis were studied. Pushover analyses using the indicated lateral load patterns were performed on four buildings consisting of 3- and 9-story regular steel moment resisting frames designed as a part of SAC joint venture (FEMA-355C) and modified versions of these buildings with a weak first

story. Peak values of story displacement, interstory drift, story shear and overturning moment obtained from pushover analyses at different values of peak roof drifts representing elastic and various degrees of nonlinear response were compared to those obtained from nonlinear dynamic analysis. Simplified inelastic procedures were found to provide very good estimates of peak displacement response for both regular and weak-story buildings. However, the estimates of interstory drift, story shear and overturning moment were generally improved when multiple modes were considered. The results also indicated that simplifications in the first mode lateral load pattern can be made without an appreciable loss of accuracy.

Sasaki, Freeman and Paret [24] proposed Multi-Mode Pushover (MMP) procedure to identify failure mechanisms due to higher modes. The procedure uses independent load patterns based on higher modes besides the one based on fundamental mode. A 17-story steel frame damaged by 1994 Northridge earthquake and a 12-story steel frame damaged by 1989 Loma Prieta earthquake were evaluated using MMP. For both frames, pushover analysis based only on first mode load pattern was inadequate to identify the actual damage. However, pushover results of higher modes and/or combined effect of 1st mode and higher modes matched more closely the actual damage distribution. It was concluded that MMP can be useful in identifying failure mechanisms due to higher modes for structures with significant higher-order modal response.

Moghadam [19] proposed a procedure to quantify the effects of higher mode responses in tall buildings. A series of pushover analysis is performed on the buildings using elastic mode shapes as load pattern. Maximum seismic responses are estimated by combining the responses from the individual pushover analyses. The proposed combination rule is that response for each mode is multiplied by mass participating factor for the mode considered and contribution of each mode is summed. The procedure was applied to a 20-story steel moment resisting frame to assess the accuracy of the procedure. Pushover analyses for first three modes were performed on the frame and the responses for each mode were combined to estimate the final response. Comparison of estimated displacements and inter-story drifts with the mean of maximum responses resulted from six nonlinear dynamic analysis indicated a good correlation. Another important observation, resulting from the work of (Moghadam and Tso 1996, 1997), is the effect of the distribution of the lateral loads along the height on the torsional response of the building. It was shown that using the modal load pattern produces results more accurate than a triangular or uniform distribution. In the same work the estimation of the target displacement is

done using the results of a spectral dynamic analysis, which along with the previous observation suggest that a spectral dynamic elastic analysis provides very useful information relevant to the inelastic torsional response of a building.

Chopra and Goel [8] developed an improved pushover analysis procedure called Modal Pushover Analysis (MPA) which is based on structural dynamics theory. Firstly, the procedure was applied to linearly elastic buildings and it was shown that the procedure is equivalent to the well known response spectrum analysis. Then, the procedure was extended to estimate the seismic demands of inelastic systems by describing the assumptions and approximations involved. Earthquake induced demands for a 9-story SAC building were determined by MPA, nonlinear dynamic analysis and pushover analysis using uniform, "code" and multi-modal load patterns. The comparison of results indicated that pushover analysis for all load patterns greatly underestimates the story drift demands and lead to large errors in plastic hinge rotations. The MPA was more accurate than all pushover analyses in estimating floor displacements, story drifts, plastic hinge rotations and plastic hinge locations. While in all previous methods modal superposition is carried out at the level of loading, in MPA, pushover analyses are carried our separately for each significant mode, and the contributions from individual modes to calculated response quantities (displacements, drifts, etc.) are combined using an appropriate combination rule (SRSS or CQC). Although, theoretically, superposition of modal responses does not apply in the inelastic range of the response (modes are not uncoupled anymore), (Chopra and Goel 2002) have shown that the error, taking the results of inelastic time-history analysis as the benchmark, is typically smaller than in the case that superposition is carried out at the level of loading. MPA results were also shown to be weakly dependent on ground motion intensity based on the results obtained from El Centro ground motion scaled by factors varying from 0.25 to 3.0. It was concluded that by including the contributions of a sufficient number of modes (two or three), the height-wise distribution of responses estimated by MPA is generally similar to the 'exact' results from nonlinear dynamic analysis when compared with the other load distributions.

Chintanapakdee and Chopra [5] evaluated the accuracy of MPA procedure for a wide range of buildings and ground motions. Generic one-bay frames of 3, 6, 9, 12, 15- and 18-stories with five strength levels corresponding to SDOF-system ductility factors of 1, 1.5, 2, 4 and 6 were utilized. Each frame was analysed by a set of 20 large magnitude small- distance records

obtained from California earthquakes. Median values of story drift demands from MPA and nonlinear dynamic analyses were calculated and compared. It was shown that with two or three modes included, MPA predictions were in good correlation with nonlinear dynamic analyses and MPA predicted the changing height-wise variation of demand with building height and SDOF-system ductility factor accurately. The bias and dispersion in MPA estimates of seismic demands were found to increase for longer-period frames and larger SDOF-system ductility factor although no perfect trends were observed. It was also illustrated that the bias and dispersion in MPA estimates of seismic demand for inelastic frames were larger than those for elastic systems due to additional approximations involved in MPA procedure. Finally, the MPA procedure was extended to estimate seismic demand of inelastic systems with seismic demand being defined by an elastic design spectrum.

3. METHODS OF STRUCTURAL ANALYSIS

Among the engineering community involved with the development of seismic design procedures, there is a general belief that the conventional elastic design and analysis methods cannot capture many important aspects that control the seismic performance of structures in severe earthquakes. Moreover, another powerful tool, inelastic time-history analysis, is computationally expensive and not feasible for many cases. Nowadays, engineers are seeking a technique, which would solve the drawbacks described above. The search for a more useful and rational design process is a big issue for the future. Design has always been a compromise between simplicity and reality. The latter term, reality, seems to be very complex due to big uncertainties in imposed demands and available capacities. The first term, simplicity, is a necessity driven by computational cost and at the same time the limited ability to implement complexity with available knowledge and tools.

The estimation of demands can be accomplished using a variety of available procedures. The primary objective is to determine forces and deformations both at the global and at the local level when the structure is subjected to seismic loads that characterize the hazard at the building site. As such, there are four possible methods to analyze a mathematical model of a building structure. They may be classified into two broad categories depending on the treatment of the response or the treatment of the loads. The former category results in the distinction between linear and nonlinear methods of analysis, while the latter distinguishes static and dynamic application of the seismic loads.

Linear static and dynamic procedures (LSP and LDP): These procedures are recommended for regular buildings where issues such as torsion and high-mode effects are negligible. The expectation is that the computed displacements using linear equivalent elastic stiffness are approximately equal to the actual displacements that may occur inelastically under the design loads. FEMA-356 lists specific criteria to limit the use of such procedures. Linear procedures are not recommended in ATC-40.

Nonlinear static and dynamic procedures (NSP and NDP): Nonlinear procedures are generally applicable for all buildings with the exception that NSP is limited to buildings where high-mode effects are small. Again, the FEMA document has explicit guidelines to determine if

higher modes play an important role in the response: high-mode effects are deemed significant if the shear in any story resulting from a modal analysis considering modes required obtaining 90% mass participation exceeds the corresponding story shear considering first-mode response only by a factor of 1.3.

3.1 Elastic Methods of Analysis

Performance based design and assessment in structural engineering is becoming more important in the past several years. The decision of the analysis method for performance-based assessment is being a new topic and linear elastic methods of analysis have been used for a long time. The force demand on each component of the structure is obtained and compared with available capacities by performing an elastic analysis. Elastic analysis methods include code static lateral force procedure, code dynamic procedure and elastic procedure using demand-capacity ratios. These methods are also known as force-based procedures which assume that structures respond elastically to earthquakes. In code static lateral force procedure, a static analysis is performed by subjecting the structure to lateral forces obtained by scaling down the smoothened soil-dependent elastic response spectrum by a structural system dependent force reduction factor, "R". In this approach, it is assumed that the actual strength of structure is higher than the design strength and the structure is able to dissipate energy through yielding.

In code linear dynamic procedure, force demands on various components are determined by an elastic dynamic analysis. Linear dynamic analysis procedures include response spectrum analysis and time history analysis. The former is a method for obtaining an approximate solution of the coupled, second-order, linear differential equations of motion under forced vibration. The response spectrum analysis begins with determining the natural frequencies and mode shapes via an eigenvalue analysis. The coupled equations of motion are then decoupled via a modal transformation wherein the principle of orthogonality of the mode shapes with respect to the mass, damping, and stiffness matrices is applied. Each decoupled equation corresponds to the equation of motion of a single-degree-of-freedom (SDOF) system associated with a mode of vibration. The peak response of each single degree-of- freedom system is obtained through the use of elastic-response spectra. Since the peak response in each mode does not occur at the same time, the peak response with contributions from all modes is estimated via the application of modal combination rules that are based on random vibration theory.

Time history analysis provides a method for obtaining the “exact” response of a structure as a function of time, whereas response spectrum analysis results in estimates of peak response. The response-history is normally determined using step-by-step numerical integration of the equation of motion. Consequently, time history analysis is performed using computer software where the ground acceleration is divided into small time steps and the response is calculated at the end of each time step while satisfying dynamic equilibrium. In general, the ground acceleration is only available at discrete points in time separated by a fixed time step while the solution may be sought at points in time other than at integer multiples of the time step. Thus, the ground acceleration must be interpolated, with linear interpolation often being adequate.

In demand/capacity ratio (DCR) procedure, the force actions are compared to corresponding capacities as demand/capacity ratios. Demands for DCR calculations must include gravity effects. While code static lateral force and code dynamic procedures reduce the full earthquake demand by an R-factor, the DCR approach takes the full earthquake demand without reduction and adds it to the gravity demands. DCRs approaching 1.0 (or higher) may indicate potential deficiencies.

Elastic methods can predict elastic capacity of structure and indicate where the first yielding will occur, however they don’t predict failure mechanisms and account for the redistribution of forces that will take place as the yielding progresses. Therefore, if not used with caution real deficiencies present in the structure could be missed.

Modal response spectrum is applicable when the structure remains almost elastic or when expected plastic deformations (ductility) are uniformly distributed all over the height of the structure. (Toprak et al, 2008).

Though, inelastic methods are more realistic means of assessing the deformational state in structures subjected to strong ground motion compared to simple linear analysis, linear analysis is still applying in a design office environment for design of new and assessment of existing buildings. (Papanikolaou et al, 2005).

The elastic analysis procedure give accurate results for service level earthquake and acceptable results in the presence of some amount of yielding and force redistribution, but care must be taken to ensure the elastic analysis procedures are not invalid. (Willford et al, 2008).

The pushover analysis method is superior over the conventional dynamic analysis method recommended by the code for seismic evaluation of structures. The response spectrum method underestimates the response of the model in comparison with modal pushover analysis. (Chandrasekaran et al, 2006).

In general, response spectrum analysis method can give acceptable results when expected inelastic deformations are uniformly distributed all over the height of the structure and the structure remains almost elastic, i.e. the level of expected damage when the cracking, yielding, or other forms of nonlinearity are considered to be slight to moderate. Stiffness reduction factors are used to approximate expected nonlinearities in a system. In this study response spectrum analysis is performed to see the deficiencies of elastic systems as compared to modal pushover analysis and to have the better understanding about nonlinear analysis methods.

3.1.1 Response Spectrum Method (RSM)

The response spectrum is simply a plot of the peak or steady-state response (displacement, velocity or acceleration) of a series of oscillators of varying natural frequency, which are forced into motion by the same base vibration or shock. The resulting plot can then be used to pick off the response of any linear system, given its natural frequency of oscillation. One such use is in assessing the peak response of buildings to earthquakes. Response spectra can also be used in assessing the response of linear systems with multiple modes of oscillation (multi-degree of freedom systems), although they are only accurate for low levels of damping. Model analysis is performed to identify the modes, and the response in that mode can be picked from the response spectrum. This peak response is then combined to estimate a total response. The earthquake spectrum, on the other hand, is an average of a number of earthquake records modified for site-specific conditions and then smoothed out for design purposes which are specified by the appropriate building code.

3.2. Inelastic Methods of Analysis

Structures suffer significant inelastic deformation under a strong earthquake and dynamic characteristics of the structure change with time. Inelastic analytical procedures accounting for the above properties are required to investigate the performance of the structure. Inelastic analytical procedures help to understand the actual behavior of structures by identifying failure modes and the potential for progressive collapse. Inelastic analysis procedures basically include

inelastic time history analysis and inelastic static analysis which is also known as pushover analysis.

The inelastic time history analysis is the most accurate method to predict the force and deformation demands at various components of the structure. However, the use of inelastic time history analysis is limited because dynamic response is very sensitive to modeling and ground motion characteristics. It requires proper modeling of cyclic load deformation characteristics considering deterioration properties of all important components. Also, it requires availability of a set of representative ground motion records that accounts for uncertainties and differences in severity, frequency and duration characteristics. Moreover, computation time, time required for input preparation and interpreting voluminous output make the use of inelastic time history analysis impractical for seismic performance evaluation.

3.2.1 Pushover Analysis

Regarding the inelastic behavior of structures at low performance levels and the complexity associated with the nonlinear time history analysis, in recent years nonlinear static procedure (NSP) as a simple tool has been developed for estimating seismic demands in the inelastic structure. Therefore the NSP so-called pushover analysis has played an important role in the development of performance-based earthquake engineering concepts in guideline documents and codes (e.g. ATC-40, 1996; FEMA-356, 2000; Erocode-8, 2002). Pushover analysis is an approximate analysis method in which the structure is subjected to monotonically increasing lateral forces with an invariant height-wise distribution until a target displacement is reached. Pushover analysis can provide an insight into the structural aspects, which control performance during severe earthquakes. The analysis provides data on the strength and ductility of the structure, which cannot be obtained by elastic analysis. The pushover procedure consists of two parts. First, a target displacement for the building is established. The target displacement is an estimation of the top displacement of the building when exposed to the design earthquake excitation. Then a pushover analysis is carried out on the building until the top displacement of the building equals to the target displacement (Tso and Moghadam 1998). The extent of damage in the building at this target displacement level is considered representative of damage the building will experience when subjected to the design level ground shaking. The original pushover procedure does not account for the three-dimensional effects. The first study to use

pushover analysis for asymmetrical buildings involves the use of 3-D inelastic programs (Moghadam and Tso 1996). An alternative approach to pushover analysis of asymmetric buildings uses the results of elastic dynamic analyses of the building to obtain the target displacements and load distributions for pushover analysis (Tso and Moghadam 1997).

In pushover analyses, both the force distribution and target displacement are based on very restrictive assumptions, i.e. a time-independent displacement shape. Thus, it is in principle inaccurate for structures where higher mode effects are significant, and it may not detect the structural weaknesses that may be generated when the structure's dynamic characteristics change after the formation of the first local plastic mechanism.

Pushover analysis can be performed as force-controlled or displacement controlled. The method used in nonlinear static analysis is based on the Newton-Raphson method, and it supports the methods of load control or displacement control. In force-controlled pushover procedure, full load combination is applied as specified, i.e, force-controlled procedure should be used when the load is known (such as gravity loading). Nonlinear static analysis can be used to create initial conditions based on gravity loads for the subsequent pushover analysis. In creating the initial conditions of the gravity loads, performing nonlinear static analysis can reflect the nonlinear behavior, which may take place in the process.

A two or three dimensional model which includes bilinear or trilinear load-deformation diagrams of all lateral force resisting elements is first created and gravity loads are applied initially. A predefined lateral load pattern which is distributed along the building height is then applied. The lateral forces are increased until some members yield. The structural model is modified to account for the reduced stiffness of yielded members and lateral forces are again increased until additional members yield. The process is continued until a control displacement at the top of building reaches a certain level of deformation or structure becomes unstable. To evaluate whether a structure is adequate to sustain a certain level of seismic loads, its capacity has to be compared with the demand corresponding to a scenario event. The roof displacement is plotted with base shear to get the global capacity curve.

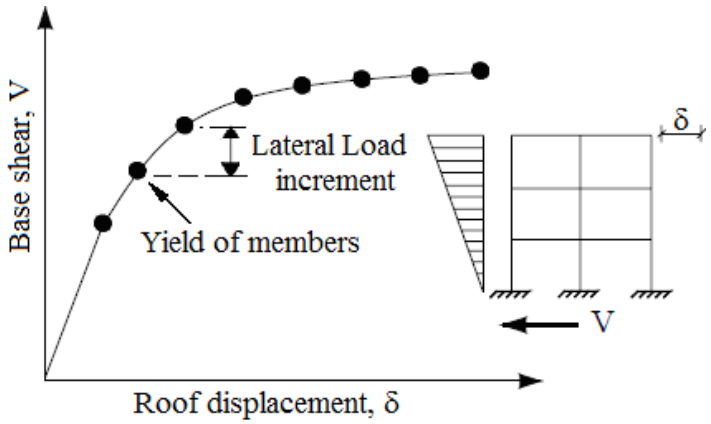

Figure 3.1. Typical global pushover curve of the structure

Generally, pushover analysis is performed as displacement-controlled proposed to overcome these problems. In displacement-controlled procedure, specified drifts are sought (as in seismic loading) where the magnitude of applied load is not known in advance. The magnitude of load combination is increased or decreased as necessary until the control displacement reaches a specified value. Generally, roof displacement at the center of mass of structure is chosen as the control displacement.

The internal forces and deformations computed at the target displacement are used as estimates of inelastic strength and deformation demands that have to be compared with available capacities for a performance check.

3.2.2 Limitations of Conventional Pushover Analysis

Although pushover analysis has advantages over elastic analysis procedures, underlying assumptions, the accuracy of pushover predictions and limitations of current pushover procedures must be identified. The estimate of target displacement, selection of lateral load patterns and identification of failure mechanisms due to higher modes of vibration are important issues that affect the accuracy of pushover results.

Target displacement is the global displacement expected in a design earthquake. Most of the time, roof displacement at mass center of the structure is used as target displacement. The accurate estimation of target displacement associated with specific performance objective affect the accuracy of seismic demand predictions of pushover analysis.

In pushover analysis, the target displacement for a multi degree of freedom (MDOF) system is usually estimated as the displacement demand for the corresponding equivalent single degree of

freedom (SDOF) system. The basic properties of an equivalent SDOF system are obtained by using a shape vector which represents the deflected shape of the MDOF system. Most of the researchers recommend the use of normalized displacement profile at the target displacement level as a shape vector but iteration is needed since this displacement is not known a priori but elastic response spectrum can be used as first trial. Thus, a fixed shape vector, elastic first mode, is used in conventional pushover analysis without regards to higher modes by most of the approaches. Moreover, hysteretic characteristics of MDOF should be incorporated into the equivalent SDOF model, if displacement demand is affected from stiffness degradation or pinching, strength deterioration, P-Δ effects. Lateral loads represent the likely distribution of inertia forces imposed on structure during an earthquake. The distribution of inertia forces vary with the severity of earthquake and with time during earthquake.

However, in pushover analysis, generally an invariant lateral load pattern is used that the distribution of inertia forces is assumed to be constant during earthquake and the deformed configuration of structure under the action of invariant lateral load pattern is expected to be similar to that experienced in design earthquake. As the response of structure, thus the capacity curve is very sensitive to the choice of lateral load distribution, selection of lateral load pattern is more critical than the accurate estimation of target displacement.

3.3. The Role and Use of Nonlinear Analysis in Seismic Design

Buildings are usually designed for seismic resistance using elastic analysis; most will experience significant inelastic deformations under large earthquakes. Modern performance-based design methods require ways to determine the realistic behavior of structures under such conditions.

Nonlinear analyses involve significantly more effort to perform and should be approached with specific objectives in mind. Typical instances where nonlinear analysis is applied in structural earthquake engineering practice are to: (1) assess and design seismic retrofit solutions for existing buildings; (2) design new buildings that employ structural materials, systems, or other features that do not conform to current building code requirements; (3) assess the performance of buildings for specific owner/stakeholder requirements.

3.4 Methods of nonlinear static analysis to evaluate seismic performance

Many methods were presented to apply the Nonlinear Static Procedure (NSP) to structures. The commonly used methods can be listed as

(1) The Capacity Spectrum Method (CSM) (ATC, 1996).

(2) The Displacement Coefficient Method (DCM) (FEMA-273/356, 1997).

(3) Modal Pushover Analysis (MPA) (Chopra, 2002)

3.4.1 The Capacity Spectrum Method (CSM)

Capacity Spectrum Method is one of the most popular methods utilized for a quick estimate to evaluate the seismic performance of structures. The method is recommended by ATC-40 [1] as a displacement-based design and assessment tool for structures. The method was developed by Freeman and it has gone through several modifications since then. The most recent three versions (Procedures A, B and C) of Capacity Spectrum Method are presented in detail in ATC-40. The method requires construction of a structural capacity curve and its comparison with the estimated demand response spectrum, both of which are expressed in Acceleration-Displacement Response Spectrum (ADRS) format.

Design Response Spectra

The selection of a performance objective involves the specification of a hazard level. Unless ground motion time histories are used in a dynamic time-history analysis, it is customary to specify the hazard in terms of a response spectrum. The generation of the ground motion hazard spectrum is a function of several parameters, most of which pertain to site characteristics.

In the absence of ground motion time histories, both ATC-40 and FEMA-356 have presented a procedure to construct the elastic design spectra.

Generating the Design Spectrum

Elastic design site response spectra are described by a standard (two domain) shape defined by the coefficients C_A and Cv. Elastic response spectra are described by a standard shape to simplify the application of these spectra to nonlinear static analysis procedures. The procedure to construct the elastic design spectrum can be summarized as shown in Figure 3.2.

ATC-40 Provisions for Generating the Design Spectrum

C_A - a site response coefficient, simply the effective peak acceleration (EPA) at the site

C_V - a coefficient when divided by the period defines the acceleration in the constant velocity domain.

ATC-40 provides the three options when developing the elastic design spectra. But SAP2000 uses the site seismic coefficients given in Table 3.2.

To use Table 3.2, it is first necessary to determine the shaking intensity, which is defined as the product of three quantities: Z * E *N = zone factor*earthquake hazard level*near source factor. Using the shaking intensity value, the corresponding site response coefficients C_A and C_V are obtained for a known soil profile. The response spectrum can now be easily generated as indicated in Figure 3.2.

Table 3.1. Average soil properties used to establish soil profile from ATC-40

TABLE 3.1 Average Soil Properties Used to Establish Soil Profile

Soil profile type	Soil profile name	Shear wave velocity (m/s)	Standard penetration test (blows/30 cm)	Undrained shear strength (kPa)
S_A	Hard rock	>1520	n/a	n/a
S_B	Rock	760–1520	n/a	n/a
S_C	Very dense soil	365–760	>50	>2
S_D	Stiff soil	180–365	15–150	1–2

Note: n/a, not applicable.

Table 3.2. ATC-40 specifications for developing hazard spectrum

TABLE 3.2 ATC-40 Specifications for Developing Hazard Spectrum

		Shaking intensity, *ZEN*					
Soil profile		0.075	0.150	0.200	0.300	0.400	>0.400
S_B	C_A	0.08	0.15	0.20	0.30	0.40	1.0∗*ZEN*
	C_V	0.08	0.15	0.20	0.30	0.40	1.0∗*ZEN*
S_C	C_A	0.09	0.18	0.24	0.33	0.40	1.0∗*ZEN*
	C_V	0.13	0.25	0.32	0.45	0.56	1.4∗*ZEN*
S_D	C_A	0.12	0.22	0.28	0.36	0.44	1.1∗*ZEN*
	C_V	0.18	0.32	0.40	0.54	0.64	1.6∗*ZEN*

Notes: Z = zone factor (IBC-2000: e.g., Zone 4 = 0.4g); E = 0.5 (SE), 1.0 (DE), and 1.25 (Zone 4) and 1.50 (Zone 3) (ME); N = near source factor (typically, N = 1 for faults not capable of producing events with maximum moment magnitude M > 6.5 and faults with slip rates less than 2 mm/year). Linear interpolation is permitted for intermediate values.

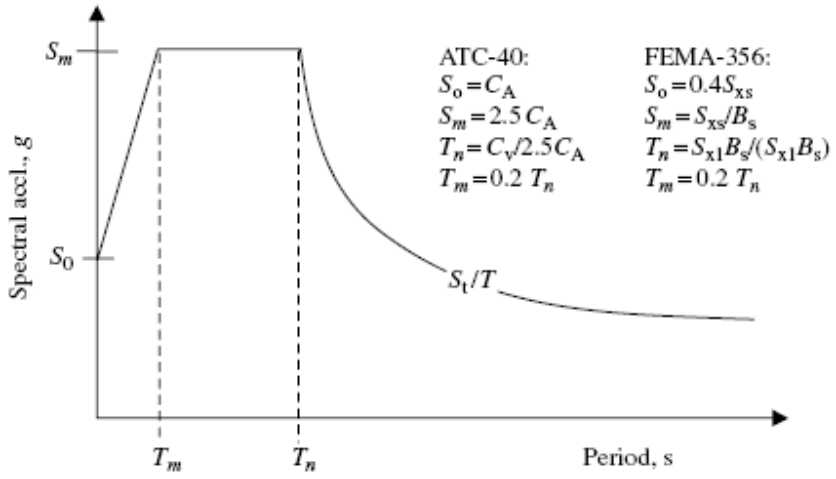

Figure 3.2. ATC-40 and FEMA-356 representation of the 5% damped response spectrum

If the elastic design spectrum is used to create the demand spectrum, the overlay is valid only if the structural response is also elastic. Hence, the next step in the process is to reduce the elastic response spectrum to an inelastic spectrum using the concept of equivalent damping. Using the fundamental principles of structural mechanics, the equivalent damping ζ_{eq} associated with dissipated energy during inelastic response is given by

$$\zeta_{eq} = 1/(\Omega/\omega)(1/4\pi)(E_D/E_S) \quad (3.1)$$

Where (Ω/ω) is the ratio of the forcing frequency to the natural frequency of the system, E_D is the energy dissipated through hysteretic behavior, and E_S is the strain energy at the maximum displacement. If it is assumed that the peak response is associated with the resonant frequency, then the ratio $(\Omega/\omega) = 1.0$.

The ATC-40 methodology for estimating the equivalent viscous damping is derived for a bilinear capacity curve, therefore, it is necessary to transform the capacity curve into bilinear form.

The elastic design spectrum already incorporates 5% damping; hence the equivalent damping from inelastic behavior must be added to the elastic viscous damping. For behavior other than bilinear hysteresis, a modification factor κ is introduced.

The final damping value incorporating elastic damping, equivalent inelastic damping, and general hysteretic behavior is given by

$$\zeta_{eff} = \kappa\zeta_{eq} + 0.05 \quad (3.2)$$

Finally, the elastic spectrum is transformed into a reduced spectrum for the damping ratio ζ_{eff}. The intersection of the capacity and demand in the AD format defines the maximum displacement demand of SDOF which is then transformed back to evaluate the expected response of the building.

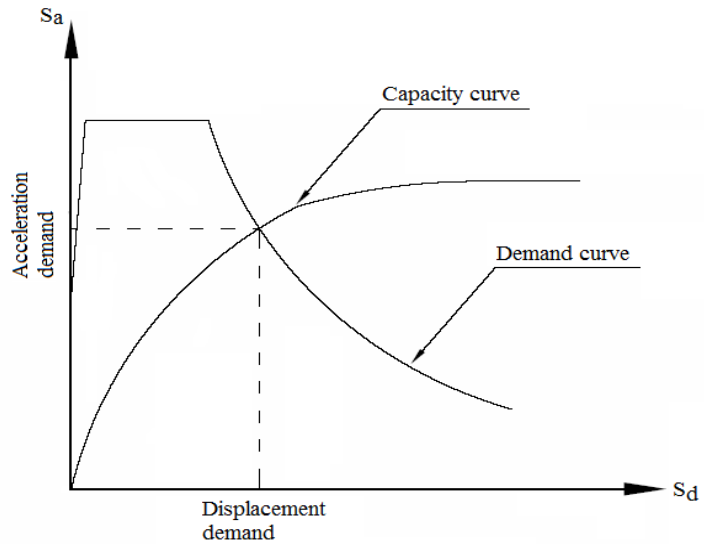

Figure 3.3. Graphical representation of capacity spectrum method

The ADRS format was introduced that the spectral accelerations are plotted against spectral displacements with radial lines representing the period, T. The demand (inelastic) response spectrum accounting for hysteretic nonlinear behaviour of structure is obtained by reducing elastic response spectrum with spectral reduction factors which depend on effective damping. A performance point that lies on both the capacity spectrum and the demand spectrum (reduced for nonlinear effects) is obtained for performance evaluation of the structure. The dependence of spectral reduction factors on structural behaviour type (hysteretic properties) and ground motion duration; and the approximations involved in determination of these characteristics are the main weaknesses of the method.

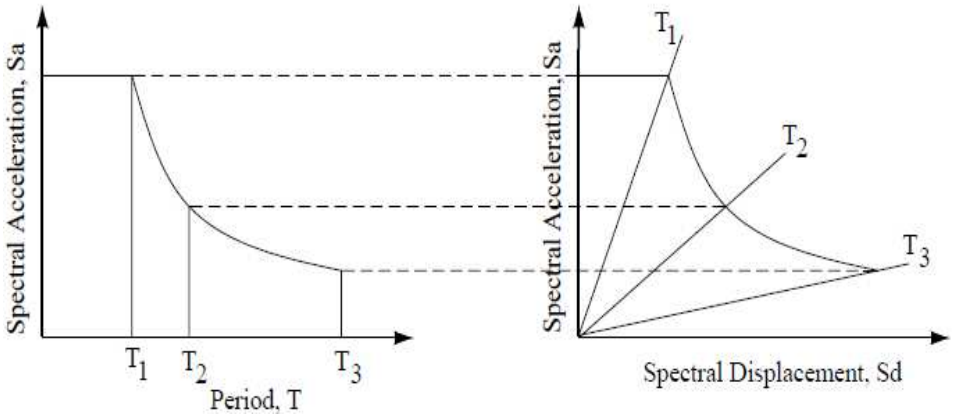

Standard Spectrum (Sa vs T) ADRS Spectrum (Sa vs Sd)

Figure 3.4. Response Spectrum in Standard and ADRS Format

In this paper the response spectrum coefficients are found from the above Table 3.2 of ATC-40 for stiff soil class (SD), which corresponds with soil class B in EBCS-8, 1995 code as:

CA = 0.0153 and Cv = 0.0227 for PGA = 0.1g, i.e. ZEN = 0.1

3.4.2 Displacement Coefficient Method (DCM)

Displacement Coefficient Method described in FEMA-356 [14] is a non-iterative approximate procedure based on displacement modification factors. The expected maximum inelastic displacement of nonlinear MDOF system is obtained by modifying the elastic spectral displacement of an equivalent SDOF system with a series of coefficients. It combines the POA with a modified version of the equal displacement approximation, according to which the linear elastic spectral displacement or the spectral acceleration, corresponding to the effective period and damping of the equivalent SDOF system, is corrected by some factors. These factors were obtained for regular frame buildings. Among its advantages is that the DCM provides a direct numerical procedure to define displacement demand and needs no conversions in spectral format. The target displacement δ_t in FEMA-376 is given by:-

$$\delta_t = C_o C_1 C_2 C_3 S_a \frac{T_e^2}{4\pi^2} g \qquad (3.3)$$

where *T*e, is the effective fundamental period (in seconds) of the building in the direction under consideration, *Sa* is the response spectrum acceleration (in *g*) at the effective fundamental

period and damping ratio of the building in the direction under consideration; and g is the gravity acceleration. To convert elastic demand thus obtained to inelastic demand, the displacement quantity is multiplied by the corrective factors Co, C1, C2 and C3, the minimum prescribed value of these factors being unity. Where factor, Co = Modification factor that relates the elastic response of a SDF system to the elastic displacement of the MDF building at the control node, C1 = Modification factor that relates the maximum inelastic and elastic displacement, stemming from the $R - \mu - T$ relationship it reflects the ratio of the peak displacement of the inelastic system to that of the corresponding elastic system with the same unyielding period of vibration, C2 = Modification factor to represent the effects of pinched hysteretic shape, stiffness degradation, and strength deterioration, and C3 = Modification factor to represent increased displacement due to P-delta effects. The major drawback of FEMA 376 is that such a simple product formulation may not correctly reflect the three distinct failure effects of the actual nonlinear behaviors of structures (ATC-55, 2002).

3.4.3 Modal Pushover Analysis (MPA) method

The results of elastic dynamic analyses of the building can be used to obtain the target displacements and load distributions to pushover analysis of asymmetric buildings (Tso and Moghadam 1997). This analysis is called response-spectrum-based pushover analysis which takes into account the higher modal and three-dimensional effects induced by torsion. The results of target displacement from of RSA can be multiplied by inelastic deformation ratio to obtain the target displacement for modal pushover analysis method.

The computational effort involved in MPA including the first few two or three modes is comparable to that required in FEMA procedures using two or three lateral-force distributions. With the roof displacement determined from the elastic design spectrum and empirical equations for the ratio of peak deformations of inelastic and elastic systems, pushover analysis for each mode requires computational effort similar to one FEMA force distribution.

3.5 Modal Pushover Analysis (MPA) Procedure

The modal pushover analysis (MPA) procedure, which includes the contributions of all significant modes of vibration, estimates seismic demands much more accurately than current pushover procedures used in structural engineering practice. Chopra and Goel [9] developed MPA procedure to account for the effects of higher modes on structural response and for the

redistribution of inertial forces during progressive yielding. The procedure retains the conceptual simplicity of current procedures of invariant load distributions. When applied to elastic systems, the MPA procedure is equivalent to standard response spectrum analysis (RSA), now common in structural engineering practice. The MPA procedure for estimating seismic demands is extended to unsymmetric-plan buildings. In this procedure, the seismic demand due to individual terms in the modal expansion of the effective earthquake forces is determined by non-linear static analysis using the inertia force distribution for each mode, which for unsymmetric buildings includes two lateral forces and torque at each floor level. These 'modal' demands due to the first few terms of the modal expansion are then combined by the CQC rule to obtain an estimate of the total seismic demand for inelastic systems. Modal pushover analysis (MPA) utilizes the concept of modal combinations through several pushover analyses using invariant load patterns based on elastic mode shapes where the total response is determined with combination of each mode at the end.

Chopra and Goel [9] extended the elastic RSA procedure to estimate the seismic demands of inelastic systems by identifying the assumptions and the approximations involved.

The procedure consists of the following steps:

Details of MPA procedure are illustrated as a series of following steps (Chopra, A.K. and Goel R.K., 2002):

1. Compute the natural frequencies, ωn, and mode shapes, ϕn. These properties are determined with eigen analysis of the linearly-elastic structure for the first few important modes. It is necessary to be normalized mode-shape ϕn, so that the roof component of ϕn equals to unity ($\phi n = 1$).

2. Develop the base-shear – roof displacement (*Vbn - urn)* pushover curve for the nth mode employing the load distribution $Sn^* = M \phi n$

3. Idealize the pushover curve as a bilinear curve (Figure 3.6).

4. Transform the idealized pushover curve into the *Fsn/Ln - Dn* relation (Figure 3.6) by utilizing formulas as follow:

$$\frac{F_{sny}}{Ln} = \frac{V_{bny}}{M_n^*} \quad , \qquad D_{ny} = \frac{u_{rny}}{\Gamma_n \phi_{rn}} \tag{3.4}$$

Where:

$$\Gamma_n = \frac{\phi_n^T mi}{\phi_n^{|T} m \phi_n} \qquad L_n = \phi_n^T mi \qquad M_n^* = L_n \Gamma_n \tag{3.5}$$

Γn : modal participation factor for the n-th mode

ϕrn : amplitude of ϕn at the roof in the direction of the selected pushover curve

Dn : peak spectral roof displacement

5. Compute the peak deformation, *Dn*, of the nth mode inelastic SDF system (Figure 3.7) with force deformation relation of Figure-3.6 by solving Equation:

$$\ddot{D}n + 2\zeta_n \omega_n \dot{D}_n + \frac{F_{sn}}{L_n} = -\ddot{u}_g(t) \tag{3.6}$$

For an SDF system with known Tn and ζn; Dn can be computed from non-linear RHA, inelastic design spectrum, or elastic design spectrum in conjunction with empirical equations for the ratio of deformations of inelastic and elastic systems

6. Calculate the peak roof displacement *urno* in the direction of the selected pushover curve associated with related to the nth-“mode” inelastic SDF system from:

$$Urno = \Gamma_n \phi_{rn} D_n \tag{3.7}$$

For Asymmetric building the peak roof displacement is determined from

$$u_{rxn} = \Gamma_n \phi_{rxn} D_n \qquad u_{ryn} = \Gamma_n \phi_{ryn} D_n \qquad u_{r\theta n} = \Gamma_n \phi_{r\theta n} D_n \tag{3.8}$$

7. Compute other favorite responses, *rno*, at *urno*

8. Repeat Steps 3 to 7 for as many modes as required for sufficient accuracy.

9. Calculate the total response by combining the contribution of peak “modal” responses using pertinent combination rule such as SRSS and CQC.

The procedure involves certain approximations and assumptions that coupling among modal coordinates due to yielding of the structure is neglected while calculating the peak roof displacement, urno and superposition of peak modal responses to obtain the total peak response is utilized although superposition is valid only for elastic systems. Also, the total response is approximated by using an appropriate modal combination rule to combine the peak modal responses.

MPA using only one mode determines adequately the seismic demands, as long as the response of the frame is elastic. For higher levels of intensity, one mode is adequate for the lower stories, but higher modes need to be considered to capture demands at the upper stories in order to avoid stability problems. This is due to the fact that higher mode effects are more critical at upper stories.

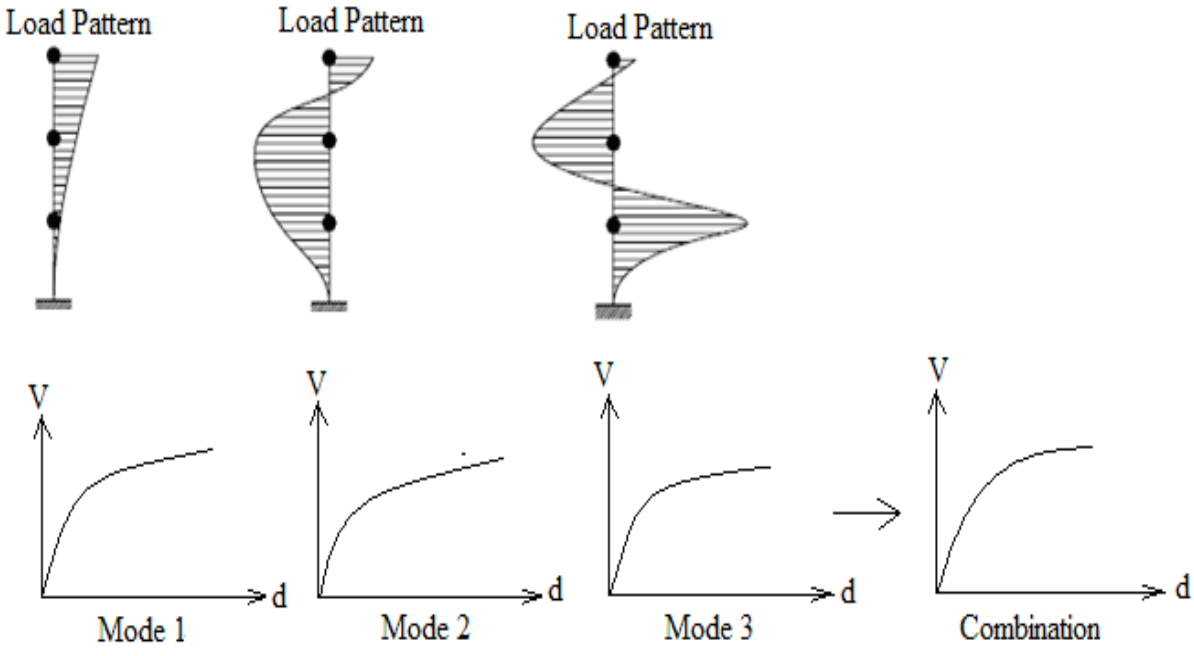

Figure 3.5. Combination of modal pushover curves

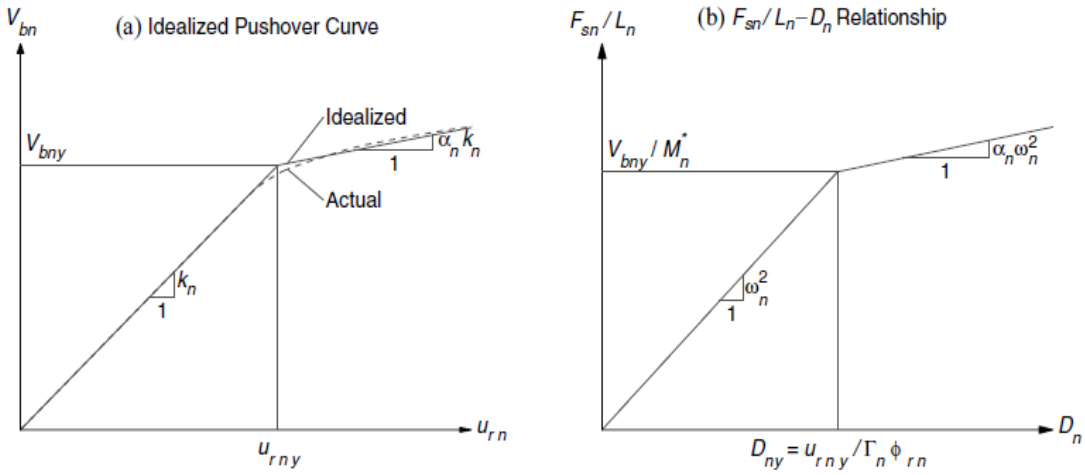

Figure 3.6. Properties of the nth-"mode" inelastic SDF system from the pushover Curve (Chopra, A.K. and Goel , R.K., 2002)

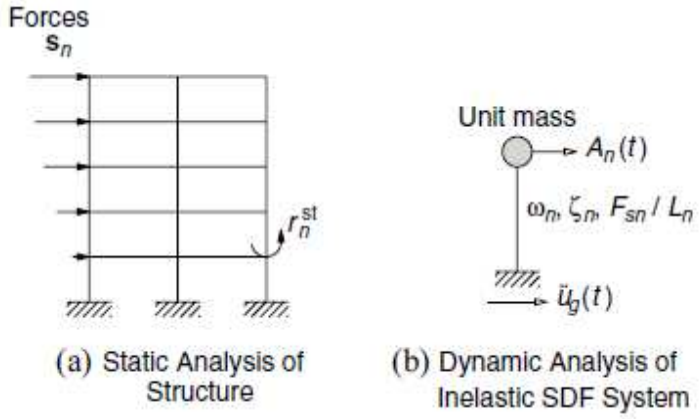

Figure 3.7. Conceptual explanation of uncoupled modal RHA of inelastic MDF systems (Chopra, A.K. and Goel, R.K., 2002)

For an inelastic system, no invariant distribution of forces will produce displacements proportional to the n-th elastic mode. Therefore, the three components of roof displacement of an inelastic system will not simultaneously reach the values given by Equation (3.8). One of the two lateral components will be selected as the controlling displacement; the choice of the component would be the same as the dominant motion in the mode being considered.

3.6. Seismic Demand, Target Displacement and Performance Point

The seismic demand on a structure is usually expressed in the form of a design spectrum according to the prevailing seismic code and including all structural and zoning parameters. The seismic demand is also related to the nonlinear behavior of the structure and is obtained iteratively. The intersection of the demand spectrum with the nonlinear pushover response is called “Performance Point’’ or “Target displacement”. It corresponds to the state the structure is expected to reach under the considered earthquake. Depending on the position and state of the performance point (with respect to the actual pushover curve), the analyst may decide on how safe or vulnerable the structure is and where possible strengthening should be performed.

3.6.1 Determination of Target Displacement

The fundamental question in the execution of the pushover analysis is the magnitude of the target displacement at which seismic performance evaluation of the structure is to be performed. The target displacement serves as an estimate of the global displacement of the structure is expected to experience in a design earthquake. It is the roof displacement at the center of mass of the structure. The extent of damage experienced by the structure at this target displacement is considered representative of the damage experienced by the building when subjected to design level ground shaking. In the pushover analysis it is assumed that the target displacement for the MDOF structure can be estimated as the displacement demand for the corresponding equivalent SDOF system transformed to the SDOF domain through the use of a shape factor. This assumption, which is always an approximation, can only be accepted within limitations and only if great care is taken in incorporating in the predicted SDOF displacement demand all the important ground motion and structural response characteristics that significantly affect the maximum displacement of the MDOF structure. Inherent in this approach is the assumption that the maximum MDOF displacement is controlled by a single shape factor without regards to higher mode effects. Under the Non-linear Static Procedure, a model directly incorporating inelastic material response is displaced to a target displacement, and resulting internal deformations and forces are determined. The mathematical model of the building is subjected to monotonically increasing lateral forces or displacements until either a target displacement is exceeded, or the building collapses. The target displacement is intended to represent the maximum displacement likely to be experienced during the design earthquake.

The target displacement is determined from the elastic response spectrum in Annex A of EBCS-8, 1995 based on a generalized SDOF system equivalence. The target displacement determined in this way is multiplied latter by inelastic deformation ratio to come up with inelastic target displacement.

The method consists of the following steps:

- Transformation of the MDOF system to an equivalent SDOF system
- Determination of an equivalent idealized elasto-perfectly plastic system
- Determination of the target displacement for the equivalent system
- Transformation to the MDOF system
- Multiplying by inelastic deformation ratio

In modal pushover analysis procedure the seismic demands due to individual terms in the modal expansion of the effective earthquake forces are determined by a pushover analysis using the inertia force distributions associated with each mode up to a ‘‘modal’’ target displacement.

The target roof displacement in all of these pushover procedures is determined from the peak deformation of an inelastic single-degree-of-freedom system with its force-deformation relation defined from the pushover curve.

4. MODELING OF STRUCTURAL ELEMENTS

4.0 General

Pushover analysis is numerically demanding and may cause numerical difficulties for the software used to run the analysis if our model is complex. Simplifying the model as much as possible is helpful in completing the run and reducing the run time. As the analysis process may usually involve several runs to evaluate effect of the various parameters, it is important to be able to complete a pushover run in less time. Any linear elements should be modeled with least possible amount of meshing. Hinges should be assigned to any location where nonlinear behavior is expected, even when nonlinear behavior is later not observed at some of these locations. Having more hinges than necessary does not slow down analysis and it ensures that nonlinear behavior is captured.

The key step for the entire analysis is identification of the primary structural elements, which should be completely modeled in the analysis. Secondary elements, which do not significantly contribute to the building's lateral force resisting system, do not need to be included in the analysis. A model with some elements that yield much earlier compared to the rest may be numerically difficult to run. This may happen when elements that are not the main components of lateral system, are modeled with hinges. As these elements are expected to yield early in an earthquake, an easy solution may be to model them as pin-ended. However, building behavior should be verified to not have changed significantly in this process. This may be done by comparing the capacity curves for the model with pin-ended element to that of the original model. Furthermore, these elements should be detailed to yield in a ductile manner.

Rigid end offsets significantly influence model behavior and force distribution between elements. In shear wall buildings where pushover model uses frame elements to model shear walls, the clear span of spandrels and any slender columns formed due to wall openings is usually much smaller than the center to- center span. These elements should be modeled with rigid end offsets and nonlinear hinges should be assigned outside of the offset.

4.1. Types of inelastic Structural Analysis Models

Inelastic structural component models can be differentiated by the way that plasticity is distributed through the member cross section and along its length. Figure 4-1 shows a comparison of five idealized model types for simulating the inelastic response of beam-columns. Several types of structural member (e.g., beams, columns, braces, and some flexural walls) can be modeled using the concepts illustrated in Figure 4-1:

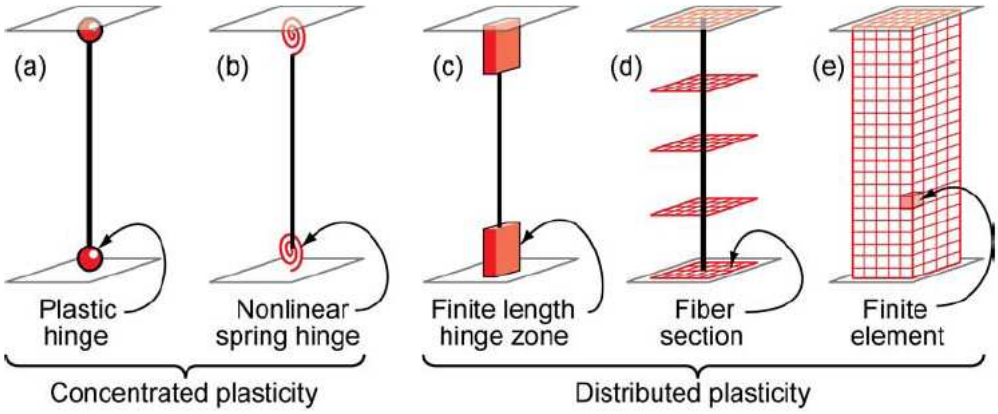

Figure 4.1. Types of inelastic structural models from NEHRP Seismic Design Technical Brief No. 4.

The simplest models concentrate the inelastic deformations at the end of the element, such as through a rigid-plastic hinge (Figure 4.1a) or an inelastic spring with hysteretic properties (Figure 4.1b). By concentrating the plasticity in zero-length hinges with moment-rotation model parameters, these elements have relatively condensed numerically efficient formulations.

The finite length hinge model (Figure 4.1c) is an efficient distributed plasticity formulation with designated hinge zones at the member ends. Cross sections in the inelastic hinge zones are characterized through either nonlinear moment-curvature relationships or explicit fiber-section integrations that enforce the assumption that plane sections remain plane. The inelastic hinge length may be fixed or variable, as determined from the moment-curvature characteristics of the section together with the concurrent moment gradient and axial force. Integration of deformations along the hinge length captures the spread of yielding more realistically than the concentrated hinges, while the finite hinge length facilitates calculation of hinge rotations.

The fiber formulation (Figure 4-1d) models distribute plasticity by numerical integrations through the member cross sections and along the member length. Uniaxial material models are defined to capture the nonlinear hysteretic axial stress-strain characteristics in the cross sections. The plane-sections-remain-plane assumption is enforced, where uniaxial material "fibers" are numerically integrated over the cross section to obtain stress resultants (axial force and moments) and incremental moment-curvature and axial force-strain relations. The cross section parameters are then integrated numerically at discrete sections along the member length, using displacement or force interpolation functions (Kunnath et al. 1990, Spacone et al. 1996). Distributed fiber formulations do not generally report plastic hinge rotations, but instead report strains in the steel and concrete cross section fibers. The calculated strain demands can be quite sensitive to the moment gradient, element length, integration method, and strain hardening parameters on the calculated strain demands. Therefore, the strain demands and acceptance criteria should be benchmarked against concentrated hinge models, for which rotation acceptance criteria are more widely reported.

The most complex models (Figure 4.1e) discretize the continuum along the member length and through the cross sections into small (micro) finite elements with nonlinear hysteretic constitutive properties that have numerous input parameters. This fundamental level of modeling offers the most versatility, but it also presents the most challenge in terms of model parameter calibration and computational resources. As with the fiber formulation, the strains calculated from the finite elements can be difficult to interpret relative to acceptance criteria that are typically reported in terms of hinge rotations and deformations.

Concentrated and finite length hinge models (Figures 4.1a through Figure 4.1c) may consider the axial force-moment (*P-M*) interactions through yield surfaces. On the other hand, fiber (Figure 4.1d) and finite element (Figure 4.1e) models capture the *P-M* response directly. Note that while the detailed fiber and finite element models can simulate certain behavior more fundamentally, they are not necessarily capable of modeling other effects, such as degradation due to reinforcing bar buckling and fractures that can be captured by simpler phenomenological models interpreted relative to acceptance criteria that are typically reported in terms of hinge rotations and deformations.

Some types of concentrated hinge models employ axial load-moment (*P-M*) yield surfaces. Whereas these models generally do a good job at tracking the initiation of yielding under axial load and bending, they may not capture accurately the post-yield and degrading response. On the other hand, some hinge elements with detailed moment-rotation hysteresis models may not capture *P-M* interaction, except to the extent that the moment-rotation response is defined based on average values of axial load and shear that are assumed to be present in the hinge.

4.1.1 Distributed Versus Concentrated Plastic Hinge

While distributed plasticity formulations (Figures 4.1c through 4.1e) model variations of the stress and strain through the section and along the member in more detail, important local behaviors, such as strength degradation due to local buckling of steel reinforcing bars or flanges, or the nonlinear interaction of flexural and shear, are difficult to capture without sophisticated and numerically intensive models. On the other hand, phenomenological concentrated hinge/spring models (Figure 4.1a and 4.1b), may be better suited to capturing the nonlinear degrading response of members through calibration using member test data on phenomenological moment-rotations and hysteresis curves. Thus, when selecting analysis model types, it is important to understand (1) the expected behavior, (2) the assumptions, and (3) the approximations inherent to the proposed model type. While more sophisticated formulations may seem to offer better capabilities for modeling certain aspects of behavior, simplified models may capture more effectively the relevant feature with the same or lower approximation. It is best to gain knowledge and confidence in specific models and software implementations by analyzing small test examples, where one can interrogate specific behavioral effects.

In concentrated plasticity approach, the effect of material yielding is “lumped” into a dimensionless plastic hinges (Figure 4-1a). Regions in the frame elements other than at the plastic hinges are assumed to behave elastically, and if the cross-section forces are less than cross-section plastic capacity, elastic behavior is assumed. When the steady-forces reach the yield surface, a plastic hinge is formed which follow the nonhardening plasticity flow rules. To develop the incremental elasto-plastic relations, following standard practices of the non hardening plasticity flow theory, the incremental elastoplastic stiffness matrix can be generated. The plastic hinge approach eliminates the integration process on the cross section and permits

the use of fewer elements for each member, and hence greatly reduces the computing effort. However, the method has been shown to overestimate the limit load in the case of reinforced concrete structures, where spread of plasticity effects is very significant.

4.1.2 Frame Hinge Properties

SAP2000 introduces the capability of providing plastic hinges at discrete user defined hinges along the clear length of a frame element. The plastic hinge represents the post-yield behavior in one or more degree of freedom. Uncoupled moment, torsion, axial force and shear hinges are available to be modeled along the frame element. Also, a P-M2-M3 hinge which yields based on the interaction of axial force and bending moments at the hinge location can be modeled. More than one type of hinge can exist at the same location, for example, the user might assign both M3 (moment) and V2 (shear) hinge to the same end of a frame element. In the analytical modeling used in SAP2000 software the hysteretic response of the concentrated plasticity at ends of a member can be described by a moment curvature relationship. The program can specify for each material one or more stress-strain curves that are used to generate nonlinear hinge properties in frame elements. The different curves can be used for different parts of a frame cross section.

For nonlinear analysis automatic hinge properties and user-defined hinge properties can be assigned to frame elements. When automatic or user-defined hinge properties are assigned to a frame element, the program automatically creates a generated hinge property for each and every hinge. User-defined hinge properties can either be based on a hinge property generated from automatic property, or they can be fully user-defined. A generated property can be converted to user-defined, and then modified and re-assigned to one or more frame elements. Automatic hinge properties are based upon a simplified set of assumptions that may not be appropriate for all structures. You may want to use automatic properties as a starting point, and then convert the corresponding generated hinges to user-defined and explicitly override calculated values as needed.

The main reason for the differentiation between defined (automatic and user-defined) properties and generated properties is that typically the hinge properties are section dependent. Thus it would be necessary to define a different set of hinge properties for each different frame section type in the model. This could potentially mean that you would need to define a large number of hinge properties. The definition of user-defined hinge properties requires moment–curvature

analysis of each element. For a particular axial force, moment-rotation (*M-θ)* characteristic of a frame member with lumped plasticity gives a measure of rotation ductility capacity of the member.

In SAP2000, the default-hinge model assumes the same deformation capacity for all columns regardless of their axial load and their weak and strong axis orientation. It takes the average values of hinge properties instead of carrying out detailed calculation for each member. But, the hinge properties depend on the type of element, material property, shear span ratio and the axial load on the element. To account for this, in the present study, user-defined hinge properties obtained from the yield, plastic and ultimate rotation characteristics (θ_y, θ_p, θ_{ult}) of typical elements are estimated. Using this method, the inelastic hinge effects of beams and columns of the buildings are analysed. The force-deformation behaviour of hinges such as IO, LS and CP are defined and also incorporated in the software. The input required for SAP2000 is moment-rotation relationship instead of moment-curvature. Also, moment rotation data have been reduced to five-point input that brings some inevitable simplifications. Plastic hinge length is used to obtain ultimate rotation values from the ultimate curvatures. Several plastic hinge lengths have been proposed in the literature (Park and Paulay, 1975; Priestley et al, 1996). In this study plastic hinge length definition given in Eqn. 4.2 which is proposed by (Priestley et al, 1996) is used.

$$Lp = 0.08L_i + 0.022\, f_{yh}\, \phi_{bl} \geq 0.044\, f_{yh}\, \phi_{bl} \qquad (4.1)$$

Where: Lp = the plastic hinge length

L_i = the distance from critical section of the plastic hinge to the point of contraflexure

ϕ_{bl} = the diameter of longitudinal reinforcement

fyh = the yield strength of transverse reinforcement

In existing reinforced concrete buildings, especially with low concrete strength and/or insufficient amount of transverse steel, shear failures of members should be taken into consideration. For this purpose, shear hinges are introduced for beams and columns. Because of brittle failure of concrete in shear, no ductility is considered for this type of hinges. Shear hinge properties are defined such that when the shear force in the member reaches its strength, member fails immediately.

The moment is assumed to vary linearly along the beams and columns with a contra flexure point at the middle of the members. Based on this assumption, the relationship between curvature and rotation at yield is obtained as follows;

$$\theta_y = \frac{L.\varphi_y}{6} \qquad (4.2)$$

Where L= member length;

φ_y = Curvature at yield and

θ_y = Rotation at yield

$$\theta_p = (\varphi_{ult} - \varphi_y) l_p \qquad (4.3)$$

Where l_p = Plastic hinge length

φ_{ult} = Ultimate curvature

θ_p = Plastic rotation

Rotation value at ultimate moment is obtained by adding plastic rotation to the yield rotation.
In the models considered for this study, the moment-curvature response of the cross-section is determined and transformed in to moment-rotation. The results are then used as an input to change the generated hinges to user defined hinge properties option in SAP2000.

4.2. Modeling of Structural Components

4.2.1 Material Nonlinearity

Beam and Columns

Beam-columns are commonly modeled using either concentrated hinges or fiber-type elements. While the fiber elements generally enable more accurate modeling of the initiation of inelastic effects (steel yielding and concrete cracking) and spread of yielding, their ability may be limited to capture degradation associated with bond slip in concrete joints and local buckling and fracture of steel reinforcing bars and steel members.

Shear Walls

Reinforced concrete shear walls are commonly employed in seismic lateral-force-resisting systems for buildings. They may take the form of isolated planar walls, flanged walls (often C-, I- or T-shaped in plan) and larger three dimensional assemblies such as building cores. Nearby

walls are often connected by coupling beams for greater structural efficiency where large openings for doorways are required. The seismic behavior of shear walls is often distinguished between slender (ductile flexure governed) and squat (shear governed) according to the governing mode of yielding and failure. In general, it is desirable to achieve ductile flexural behavior, but this is not possible in circumstances such as (1) short walls with high shear-to-flexure ratios that are susceptible to shear failures, (2) bearing walls with high axial stress and/or inadequate confinement that are susceptible to compression failures, and (3) in existing buildings without seismic design and detailing.

Slender concrete shear walls detailed to current seismic design requirements, having low axial stress, and designed with sufficient shear strength to avoid shear failures, perform in a similar manner to reinforced concrete beam-columns. Ductile flexural behavior with stable hysteresis can develop up to hinge rotation limits that are a function of axial load and shear in the hinge region. Simple slender walls (including coupled walls) can be modeled as vertical beam-column elements with lumped flexural plastic hinges at the ends with reasonable accuracy and computational efficiency. The modeling parameters and plastic rotation limits of ASCE 41 may be used for guidance. The following points should be noted: The lumped hinge models are only suitable for assessing performance within such allowable plastic hinge rotation limits as stable hysteresis occurs, considering axial and shear forces in the hinge.

Nonlinearity only arises at the designated hinge(s), and equivalent flexural and shear stiffness must be specified for elastic elements outside of the hinge. ASCE 41 provides guidance on effective stiffness parameters that account for flexural and shear cracking to handle typical cases (i.e., planar walls with typical reinforcement, wall proportions, and gravity stresses). Beam-column elements are more problematic to use in three-dimensional wall configurations with significant bi-directional interaction, particularly if the wall system is subjected to torsion.

Modeling of Shear Walls as Equivalent frame Method

In modeling shear walls, each planar wall in the assembly is replaced with a column having the same mechanical properties of the wall as in the equivalent frame method. In order to ensure the vertical compatibility of the displacements, the rigid beams at floor levels are rigidly connected to each other at the corners. In addition, the ends of the rigid beams that are connected to each other are released (disconnected) from the connection joint only for torsional moments. In

another words, the transfer of torsional moments between rigid beams is prevented. The rigid link elements used to connect the beams to the wall element are modeled as rigid beam with end offset properties activated along the entire length of the element, which implies so high values for the section stiffness that the beam can be assumed as fully rigid. In Figure 4.2, the connection details of orthogonal shear walls are given. In three dimensional analyses of shear wall assemblies modeled by the conventional equivalent frame model, serious errors occur especially in the analysis of assemblies subjected to torsion. The stiffness of the structural system becomes stiffer than with finite element modeling. Releasing the ends of the rigid beams from the connection joint decreases the torsional stiffness of the shear wall assembly.

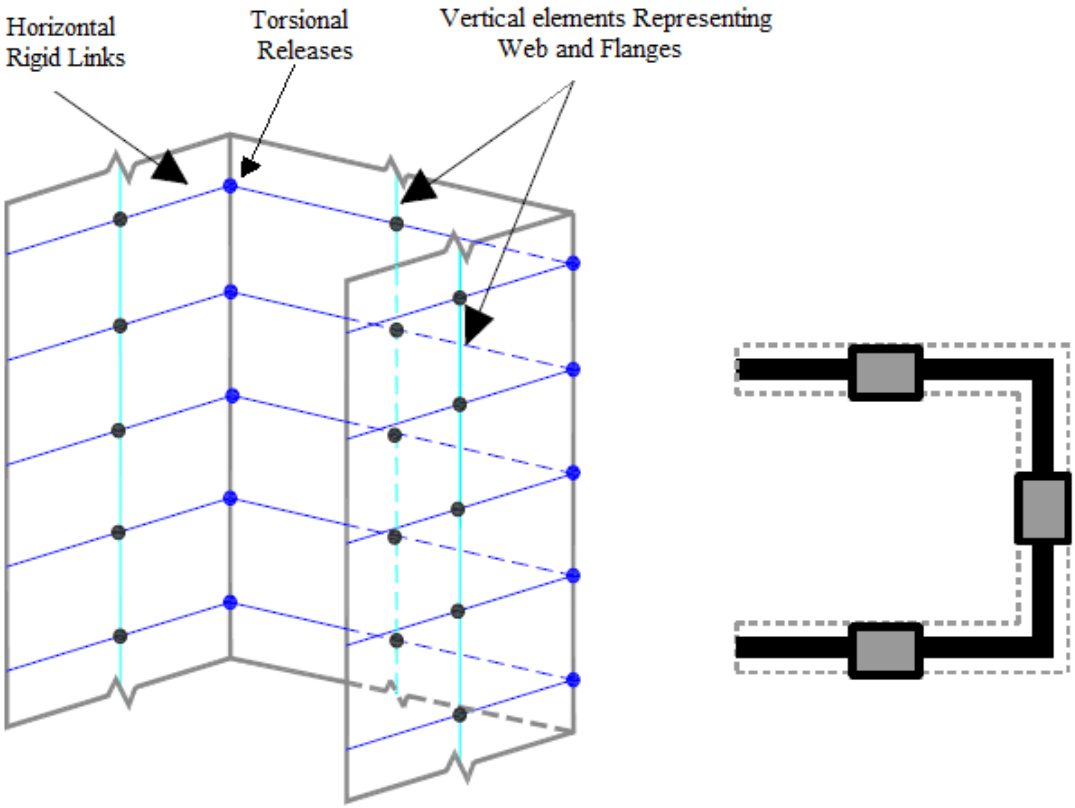

Figure 4.2. Model scheme used to represent U-shape wall system (Beyer *et al*. 2008)

Given that all shear walls in the building are slender with wall height-to-length ratio well above three and therefore seismic response of the shear walls is expected to be dominated by flexure, as well as because modeling nonlinear behavior in SAP2000 pushover analysis is limited to frame elements, the shear walls were modeled as equivalent frame elements. In order to provide connectivity between walls, the equivalent frames were connected at the floor level with rigid

links on the side of the wall without any opening, or with beams with rigid end offsets to model spandrels above wall openings. Figure 4.3 illustrates this modeling technique for the longitudinal walls in the middle core.

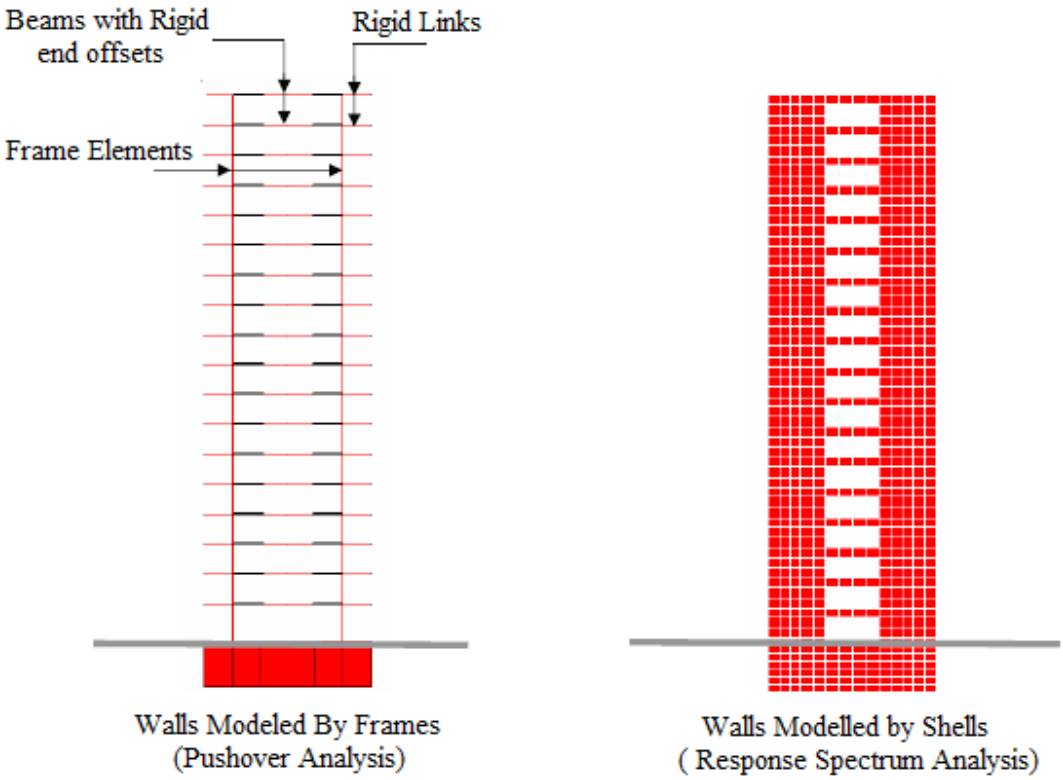

Figure 4.3. Shear wall modeling in pushover and response spectrum analyses (Rana *et al*. 2004)

Nonlinear Behavior of Structural Elements

The nonlinear behavior of a building structure depends on the nonlinear responses of the elements that are used in the lateral force resisting system. Therefore, before applying any nonlinear analysis method on a building structure, the nonlinear behavior of such elements must be clearly described and evaluated.

ATC-40 and FEMA-356 codes define the acceptance criteria depending on the plastic hinge rotations by considering various performance levels. In Figure 4.4, the five points (A, B, C, D and E) which are used to define the hinge rotation behavior of RC members and the acceptance criteria on a force versus deformation diagram are given. In this diagram, points marked as IO, LS and CP represent immediate occupancy, life safety and collapse prevention, respectively.

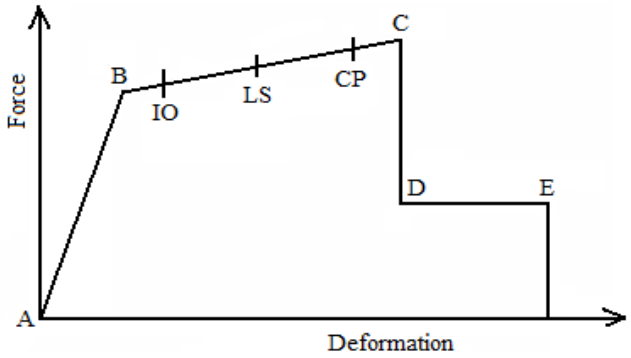

Figure 4.4. Acceptance criteria on a force versus deformation diagram

In this study, the hinge properties are determined according to FEMA-356 [14].

4.2.2. Geometric Nonlinearity

Geometric nonlinearity is the change in the elastic load-deformation characteristics of the structure caused by the change in the structural shape due to large deformations. It is caused by gravity loads acting on the deformed configuration of the structure, leading to an increase of internal forces in members and connections. It plays a fundamental role in the global response of the structure when the occurrences of large deformation in the structural elements induce displacements not more proportional to the loads effectively applied. Involving both local and global aspects, three are the most important sources of geometric nonlinearities: the beam-column effects, the large displacement/rotation effects and the P-delta effects. These geometric nonlinear effects are typically distinguished between *P*-δ effects, associated with deformations along the members, measured relative to the member chord, and *P*-Δ effects, measured between member ends and commonly associated with story drifts in buildings. In buildings subjected to earthquakes, *P*-Δ effects are much more of a concern than *P*- δ effects, and provided that members conform to the slenderness limits for special systems in high seismic regions. *P*- δ effects do not generally need to be modeled in nonlinear seismic analysis. On the other hand, *P*-Δ effects must be modeled as they can ultimately lead to loss of lateral resistance, ratcheting (a gradual build up of residual deformations under cyclic loading), and dynamic instability. Large lateral deflections (Δ) magnify the internal force and moment demands, causing a decrease in the effective lateral stiffness. With the increase of internal forces, a smaller proportion of the structure's capacity remains available to sustain lateral loads, leading to a reduction in the effective lateral strength.

Shown in Figure 4.6 is an idealized base shear versus drift curve of a cantilever structure with and without *P*-Δ effects. If the gravity load is large the stiffness reduction is significant and contributes to loss of lateral resistance and instability. Therefore the gravity load-deformation (*P*-Δ) effect must be considered directly in the analysis, whether static or dynamic. This means that the gravity loads of the entire building must be present in the analysis, and appropriate *P*-Δ analysis techniques should be introduced in the structural model (Wilson 2002; Powell 2010). For nonlinear seismic analyses, ASCE 7 specifies a gravity load combination of 1.0*D* + 0.5*L*, where D is the building dead load and *L* is the specified live load, including allowance for live load reduction. In this paper the gravity load combination of 1.0D + 0.3L from Euro codes of dwellings and similar buildings is used.

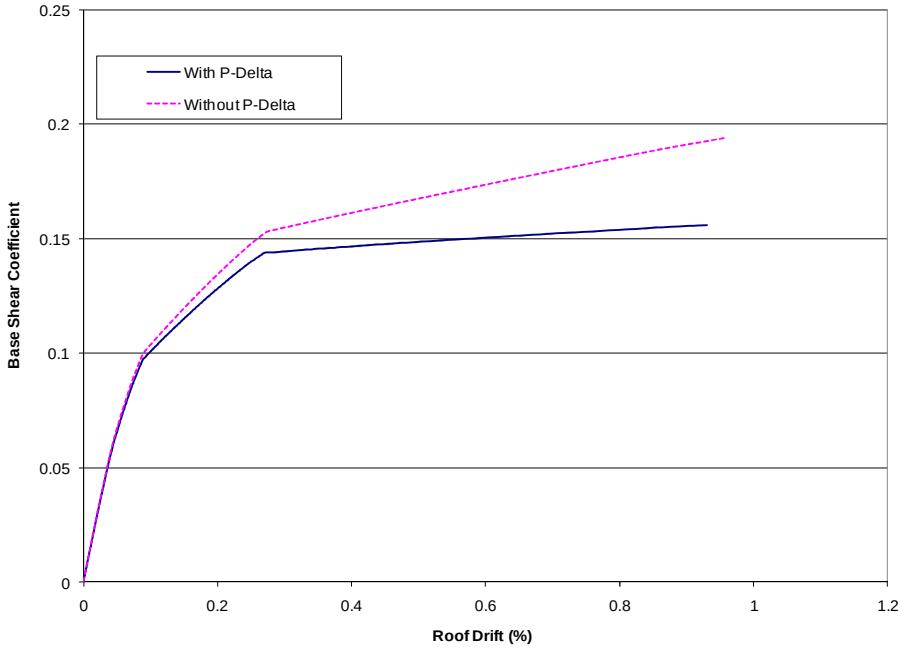

Figure 4.5. Typical Pushover curve with and without P- Δ effect

4.3 Descriptions of the Analyzed Buildings

In this study three buildings are selected, five storey low cost house, ten storey hotel and ten storey mixed use building. In the third building, irregularity in plan and elevation exists as shown in Figure 4.8. The structural system used for these buildings is taken as concrete moment-resisting space frames (MRSF), and the soil type is considered as class B. The ductility class of the building is taken as “medium”, (DM). Furthermore, the design acceleration has

been taken as 0.1g which corresponds to that used for very high seismic zone (Zone 4) in EBCS-8, 1995.

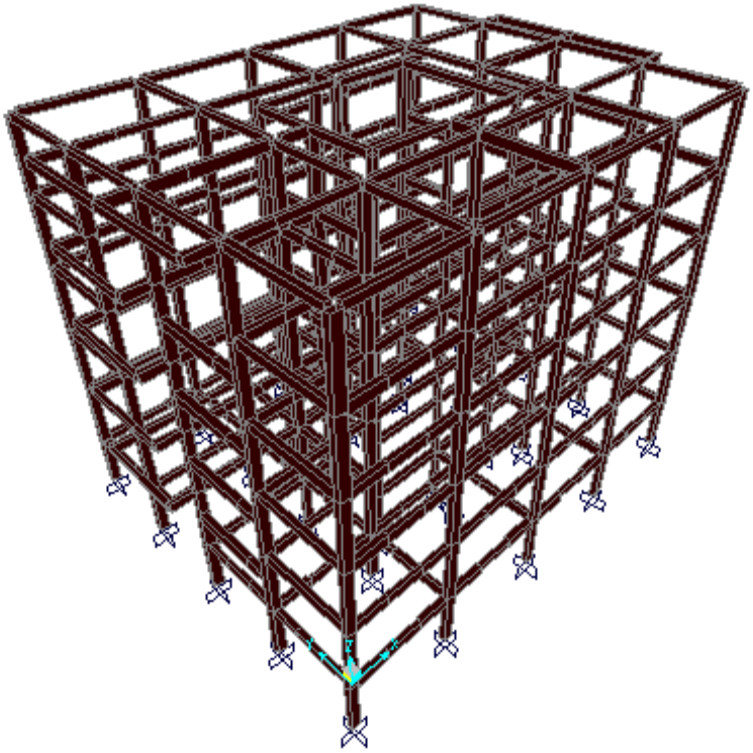

(a)

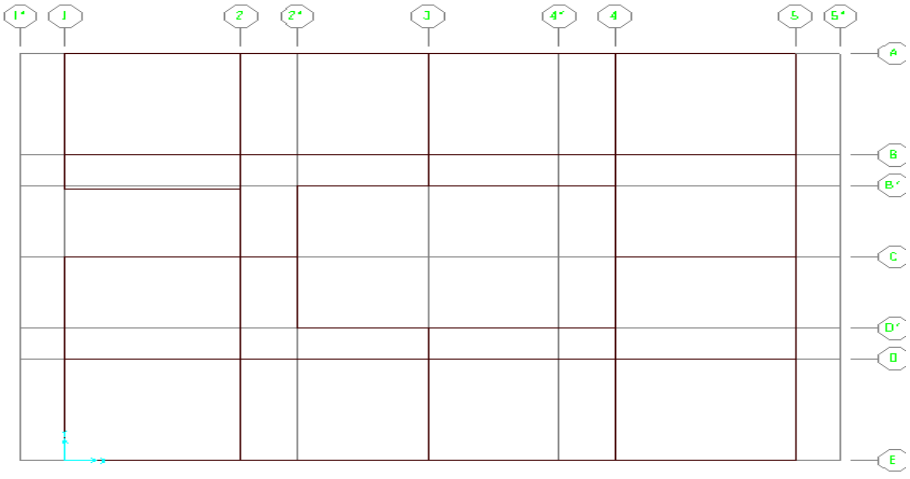

(b)

Figure 4.6. Three dimensional and plan view of five storey RC building

a) Three dimensional view b) Typical plan view

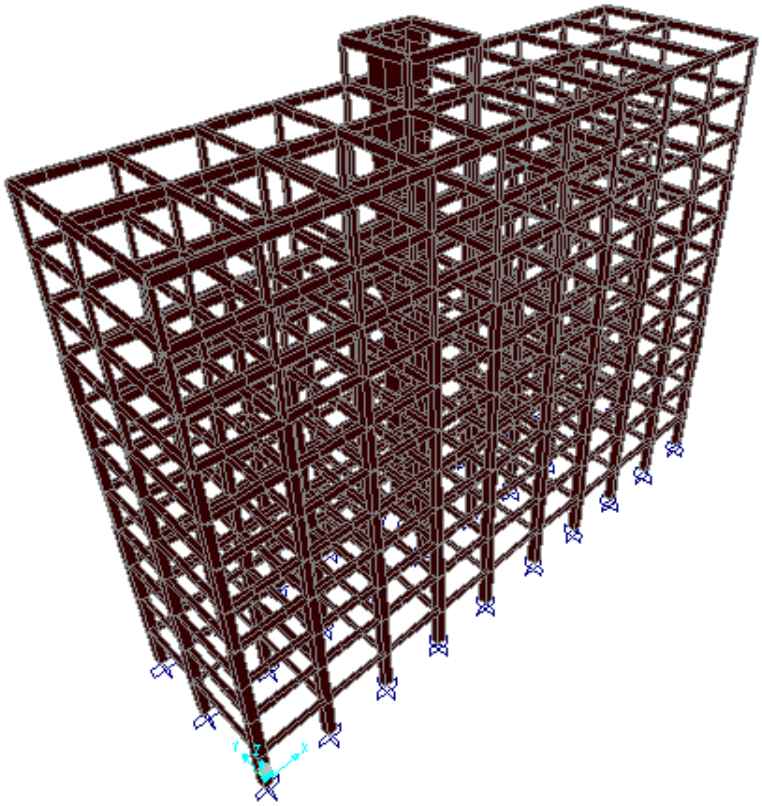

a)

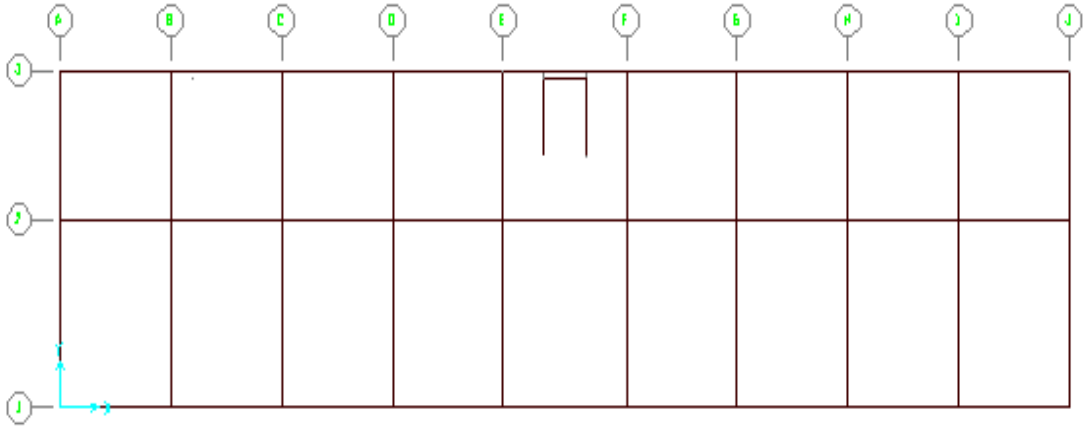

(b)

Figure 4.7. Three dimensional and plan view of ten storey RC building

a) Three dimensional view b) Typical plan view

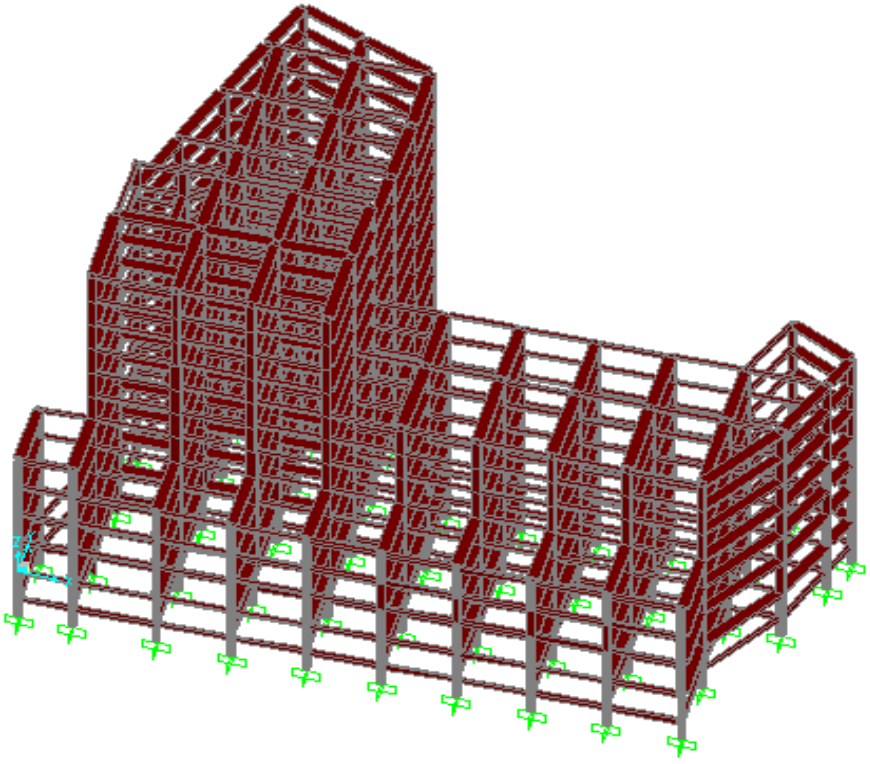

a)

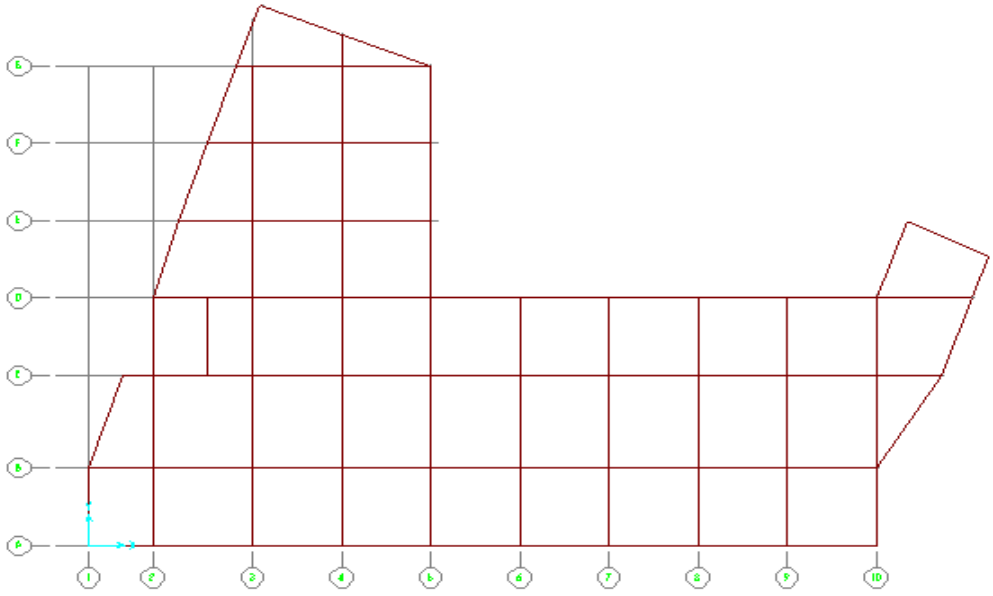

b)

Figure 4.8. Three dimensional and plan view of B + nine storey RC building

a) Three dimensional view b) Typical plan view

4.3.1 Dynamic properties of the Buildings

Table 4.1 Dynamic properties of five storey RC building

		Modal Participation Mass Ratio				Modal Participation Factors	
Mode	Period	Ux	Uy	Sum Ux	Sum Uy	UX	UY
1	0.82	0.00	0.69	0.00	0.69	0.04	15.04
2	0.63	0.00	0.03	0.00	0.73	0.43	3.33
3	0.58	0.74	0.00	0.74	0.73	15.57	0.15
4	0.26	0.00	0.11	0.74	0.84	0.03	6.06
5	0.21	0.00	0.00	0.74	0.84	0.11	1.10
6	0.19	0.11	0.00	0.85	0.84	5.98	0.02
7	0.15	0.00	0.06	0.85	0.91	0.01	4.57
8	0.12	0.00	0.00	0.85	0.91	0.03	0.69
9	0.11	0.05	0.00	0.91	0.91	4.22	0.01
10	0.10	0.00	0.04	0.91	0.95	0.01	3.64
11	0.08	0.00	0.00	0.91	0.95	0.00	0.77
12	0.08	0.00	0.02	0.91	0.97	0.01	2.35

Table 4.2 Dynamic properties of ten storey RC building

		Modal Participation Mass Ratio				Modal Participation Factors	
Mode	Period	Ux	Uy	Sum Ux	Sum Uy	UX	UY
1	2.08	0.00	0.73	0.00	0.73	0.07	75.45
2	1.88	0.05	0.00	0.05	0.74	20.30	4.85
3	1.69	0.70	0.00	0.76	0.74	73.92	1.26
4	0.70	0.01	0.01	0.77	0.74	9.73	7.64
5	0.68	0.00	0.13	0.77	0.87	3.74	31.86
6	0.60	0.11	0.00	0.88	0.87	28.96	1.76
7	0.39	0.00	0.00	0.88	0.87	-6.02	1.27
8	0.33	0.00	0.05	0.88	0.92	1.90	18.83
9	0.30	0.04	0.00	0.92	0.92	17.66	1.76
10	0.26	0.00	0.00	0.93	0.92	3.82	0.55
11	0.20	0.00	0.00	0.93	0.92	1.13	1.49
12	0.19	0.00	0.02	0.93	0.94	1.25	12.70

Table 4.3 Dynamic properties of B + Nine storey RC building

		Modal Participation Mass Ratio				Modal Participation Factors	
Mode	Period	Ux	Uy	Sum Ux	Sum Uy	UX	UY
1	1.48	0.62	0.01	0.62	0.01	41.32	5.81
2	1.29	0.04	0.56	0.66	0.57	11.36	39.08
3	0.96	0.04	0.17	0.70	0.74	9.85	21.90
4	0.52	0.10	0.00	0.80	0.74	16.99	1.25
5	0.44	0.00	0.07	0.80	0.81	1.66	14.13
6	0.41	0.01	0.02	0.81	0.82	4.29	6.20
7	0.29	0.03	0.01	0.84	0.83	9.41	4.48
8	0.26	0.01	0.02	0.85	0.85	6.06	7.91
9	0.24	0.00	0.01	0.85	0.86	2.83	6.32
10	0.17	0.03	0.00	0.88	0.86	8.63	1.03
11	0.16	0.00	0.03	0.88	0.89	1.52	8.69
12	0.15	0.00	0.00	0.88	0.89	2.05	2.72

4.3.2 Columns and Beams Cross Sectional Dimensions and Reinforcements for the RC Buildings

I. For Five Storey Building

Table 4.4 Dimensions and reinforcements used in five storey RC building model for columns

Section Name	Column Dimensions		Column Longitudinal Reinforcement	Transverse reinforcement
	bw (cm)	h (cm)		
CL Section 1-1	25	40	10 ϕ 20	ϕ 6 c/c 200
CL Section 2-2	25	40	8 ϕ 16	ϕ 6 c/c 200
CL Section 3-3	25	40	8 ϕ 14	ϕ 6 c/c 200
CL Section 4-4	25	40	6 ϕ 14	ϕ 6 c/c 200
CL Section 5-5	25	40	8 ϕ 20	ϕ 6 c/c 200
CL Section 6-6	25	25	4 ϕ 16	ϕ 6 c/c 200
CL Section 7-7	25	25	4 ϕ 14	ϕ 6 c/c 200

Table 4.5 Dimensions and reinforcements used in five storey RC building model for beams

Section Name	Beam Dimensions		Beam reinforcement		Transverse reinforcement
	bw (cm)	h (cm)	Top	Bottom	
GB section A-A	25	40	2 ϕ 12 + 1 ϕ 14	2 ϕ 12	ϕ 8 c/c 180
GB section B-B	25	40	2 ϕ 12	2 ϕ 12	ϕ 8 c/c 180
GB section C-C	25	40	2 ϕ 12 + 2 ϕ 14	2 ϕ 12	ϕ 8 c/c 180
GB section D-D	25	40	3 ϕ 12	2 ϕ 12	ϕ 8 c/c 180
GB section E-E	20	40	3 ϕ 12	2 ϕ 12	ϕ 8 c/c 180
GB section F-F	20	40	2 ϕ 12	2 ϕ 12	ϕ 8 c/c 180
GB section G-G	20	40	2 ϕ 12 + 1 ϕ 14	2 ϕ 12	ϕ 8 c/c 180
GB section H-H	20	40	2 ϕ 12 + 2 ϕ 14	2 ϕ 12	ϕ 8 c/c 180
FB section A-A	20	40	4 ϕ 12	3 ϕ 14	ϕ 8 c/c 130
FB section B-B	20	40	5 ϕ 14	3 ϕ 14	ϕ 8 c/c 130
FB section C-C	20	40	3 ϕ 14 + 3 ϕ 16	4 ϕ 16	ϕ 10 c/c 100
FB section D-D	20	40	7 ϕ 16	3 ϕ 14	ϕ 10 c/c 100
FB section E-E	20	40	6 ϕ 16	4 ϕ 16	ϕ 10 c/c 100
FB section F-F	20	40	3 ϕ 16 + 2 ϕ 14	4 ϕ 16	ϕ 10 c/c 100
FB section G-G	20	40	3 ϕ 14 + 3 ϕ 14	2 ϕ 12	ϕ 8 c/c 180
FB section H-H	20	40	4 ϕ 14	4 ϕ 14	ϕ 8 c/c 180
FB section I-I	20	40	4 ϕ 14	3 ϕ 14	ϕ 10 c/c 100
FB section J-J	20	40	2 ϕ 14	2 ϕ 14	ϕ 8 c/c 180
FB section K-K	20	40	2 ϕ 14	2 ϕ 14	ϕ 8 c/c 180
TTB section A-A	20	30	2 ϕ 12	2 ϕ 12	ϕ 8 c/c 180
TTB section B-B	20	30	2 ϕ 12 + 3 ϕ 14	2 ϕ 12	ϕ 8 c/c 180
Lading Beam	25	40	3 ϕ 14	3 ϕ 14	ϕ 8 c/c 180

II. For Ten Storey Building

Table 4.6 Dimensions and reinforcements used in ten storey RC building model for beams

Section Name	Beam Dimensions		Beam reinforcement		Transverse reinforcement
	bw (cm)	h (cm)	Top	Bottom	
GB section 1-1	25	40	2 ϕ 12 + 1 ϕ 14	2 ϕ 12	ϕ 8 c/c 180
GB section 2-2	25	40	2 ϕ 12	2 ϕ 12	ϕ 8 c/c 180
FB section 1-1	30	50	5 ϕ 16	3 ϕ 16	ϕ 8 c/c 100
FB section 2-2	30	50	2 ϕ 16	3 ϕ 16	ϕ 8 c/c 200
FB section 3-3	30	50	9 ϕ 16	7 ϕ 16	ϕ 8 c/c 100
FB section 4-4	30	50	2 ϕ 16	7 ϕ 16	ϕ 10 c/c 200
FB section 5-5	30	50	7 ϕ 16	7 ϕ 16	ϕ 10 c/c 100
FB section 6-6	30	50	2 ϕ 16	4 ϕ 16	ϕ 10 c/c 200
FB section 7-7	30	50	6 ϕ 16	4 ϕ 16	ϕ 10 c/c 100
LB	30	50	4 ϕ 20	6 ϕ 20	ϕ 8 c/c 100
WB	30	50	4 ϕ 16	6 ϕ 16	ϕ 8 c/c 100

Table 4.7 Dimensions and reinforcements used in ten storey RC building model for columns

Section Name	Column Dimensions		Column Longitudinal Reinforcement	Transverse reinforcement
	bw (cm)	h (cm)		
CL Section 1-1	60	60	20 ϕ 24	ϕ 10 c/c 100 + ϕ 10 c/c 200
CL Section 2-2	60	60	20 ϕ 20	ϕ 10 c/c 100 + ϕ 10 c/c 200
CL Section 3-3	50	50	12 ϕ 20	ϕ 10 c/c 100 + ϕ 10 c/c 200
CL Section 4-4	30	30	8 ϕ 16	ϕ 8 c/c 100 + ϕ 8 c/c 200
CL Section 5-5	60	60	16 ϕ 20	ϕ 10 c/c 100 + ϕ 10 c/c 200
CL Section 6-6	50	50	16 ϕ 20	ϕ 10 c/c 100 + ϕ 10 c/c 200
CL Section 7-7	50	50	8 ϕ 16	ϕ 8 c/c 100 + ϕ 8 c/c 200
CL Section 8-8	60	60	16 ϕ 16	ϕ 10 c/c 100 + ϕ 10 c/c 200
CL Section 9-9	50	50	12 ϕ 16	ϕ 10 c/c 100 + ϕ 10 c/c 200
Equivalent Column (2-3)	137	137	34 ϕ 10	ϕ 8 c/c 200
Equivalent Column (E-F)	112.5	112.5	24 ϕ 10	ϕ 8 c/c 200

III. For B + Nine Storey Building

Table 4.8 Dimensions and reinforcements used in B+nine storey RC building model for beams

Section Name	Column Dimensions		Column Longitudinal Reinforcement	Transverse reinforcement
	bw (cm)	h or D (cm)		
CL Section 1-1	60	70	20 ϕ 24	ϕ 8 c/c 200
CL Section 1'-1'	Circular	75	24 ϕ 24	ϕ 8 c/c 200
CL Section 1''-1''	60	70	24 ϕ 24	ϕ 8 c/c 200
CL Section 2-2	60	70	16 ϕ 24	ϕ 8 c/c 200
CL Section 2'-2'	60	70	20 ϕ 24	ϕ 8 c/c 200
CL Section 3-3	60	60	16 ϕ 20	ϕ 8 c/c 200
CL Section 4-4	50	50	12 ϕ 20	ϕ 8 c/c 200
CL Section 5-5	50	50	8 ϕ 20	ϕ 8 c/c 200
CL Section 6-6	50	50	20 ϕ 24	ϕ 8 c/c 200
CL Section 6'-6'	Circular	65	24 ϕ 24	ϕ 8 c/c 200
CL Section 7-7	50	50	16 ϕ 24	ϕ 8 c/c 200
CL Section 8-8	50	50	16 ϕ 20	ϕ 8 c/c 200
CL Section 9-9	40	50	16 ϕ 20	ϕ 8 c/c 200
CL Section 10-10	40	50	14 ϕ 20	ϕ 8 c/c 200
CL Section 10'-10'	Circular	55	16 ϕ 20	ϕ 8 c/c 200
CL Section 11-11	40	50	12 ϕ 20	ϕ 8 c/c 200
CL Section 11'-11'	Circular	55	14 ϕ 20	ϕ 8 c/c 200
CL Section 12-12	40	50	10 ϕ 20	ϕ 8 c/c 200
CL Section 13-13	40	50	8 ϕ 20	ϕ 8 c/c 200
CL Section 14-14	40	50	8 ϕ 16	ϕ 8 c/c 200
CL Section 15-15	50	50	8 ϕ 16	ϕ 8 c/c 200
CL Section 17-17	Circular	55	12 ϕ 20	ϕ 8 c/c 200
CL Section 18-18	40	40	8 ϕ 20	ϕ 8 c/c 200
CL Section 19-19	40	40	8 ϕ 16	ϕ 8 c/c 200
CL Section 20-20	30	30	4 ϕ 16	ϕ 8 c/c 200
CL Section 21-21	Circular	50	14 ϕ 20	ϕ 8 c/c 200
CL Section 22-22	Circular	50	12 ϕ 20	ϕ 8 c/c 200
CL Section 23-23	Circular	50	10 ϕ 20	ϕ 8 c/c 200
CL Section 24-24	Circular	50	8 ϕ 16	ϕ 8 c/c 200
CL Section 25-25	Circular	60	20 ϕ 24	ϕ 8 c/c 200

Table 4.9 Dimensions and reinforcements used in B+nine storey RC building model for beams

Section Name	Beam Dimensions		Beam reinforcement		Transverse reinforcement
	bw (cm)	h (cm)	Top	Bottom	
BFB section A-A	25	50	3 ϕ 14	2 ϕ 14	ϕ 8 c/c 180
FB section A-A1	30	30	3 ϕ 14 + 2 ϕ 16	3 ϕ 14	ϕ 8 c/c 180
FB section A-A2	30	30	5 ϕ 14	3 ϕ 14	ϕ 8 c/c 180
FB section B-B1	30	30	5 ϕ 20	4 ϕ 20	ϕ 8 c/c 180
FB section B-B2	25	40	2 ϕ 12 + 1 ϕ 14	2 ϕ 12	ϕ 8 c/c 180
FB section C-C1	30	80	7 ϕ 20	5 ϕ 20	ϕ 10 c/c 150
FB section C-C2	30	80	6 ϕ 16	5 ϕ 16	ϕ 10 c/c 150
FB section C-C3	30	80	5 ϕ 20 + 4 ϕ 24	9 ϕ 20	ϕ 10 c/c 150
FB section D-D1	25	50	6 ϕ 16	3 ϕ 16	ϕ 8 c/c 180
FB section D-D2	30	80	3 ϕ 16 + 3 ϕ 20	5 ϕ 16	ϕ 10 c/c 150
GB section D-D3	30	50	5 ϕ 14	3 ϕ 14	ϕ 10 c/c 150
FB section E-E1	30	80	4 ϕ 16 + 3 ϕ 20	7 ϕ 16	ϕ 10 c/c 150
FB section E-E2	30	50	6 ϕ 16	5 ϕ 16	ϕ 10 c/c 150
FB section F-F1	30	80	7 ϕ 16	6 ϕ 16	ϕ 10 c/c 150
FB section F-F2	30	80	4 ϕ 20 + 4 ϕ 16	7 ϕ 16	ϕ 10 c/c 150
FB section G-G1	30	80	10 ϕ 20	7 ϕ 20	ϕ 10 c/c 150
Lading Beam	25	40	4 ϕ 16	4 ϕ 16	ϕ 8 c/c 180

5. PUSHOVER ANALYSIS OF BUILDINGS AND COMPARISONS

The pushover analysis can be used to evaluate the expected performance of a structural system by estimating its strength and deformation demands for design earthquakes by means of static inelastic analysis, and comparing these demands with available capacities at the performance levels of interest. It refers to an analysis procedure whereby an incremental-iterative solution of the static equilibrium equations has been carried out to obtain the response of a structure subjected to monotonically increasing lateral load pattern. The structural resistance is evaluated and the stiffness matrix is updated at each increment of the forcing function, up to convergence. The solution proceeds until (i) a predefined performance limit state is reached, (ii) structural collapse is observed or (iii) the program fails to converge. In this manner, each point in the resulting displacement vs. base shear capacity curve represents an effective and equilibrated stress state of the structure, i.e. a state of deformation that bears a direct correspondence to the applied external force vector.

The NSPs are generally believed to be superior than Linear Elastic Procedures (LSPs), such as the classic equivalent static lateral force procedures and modal superposition techniques, because they explicitly consider inelasticity of yielding-expected structural components in resisting moderate and large earthquake intensities. Furthermore, the NSPs are more appealing than Nonlinear Dynamic Procedures (NDPs), which are considered to be the most sophisticated of all available seismic analysis methods, as they yield single-valued estimates of response quantities (e.g., lateral displacements, interstory drifts, member forces and moments, and plastic hinge rotations) for design or evaluation. In pushover analysis, the seismic demands are estimated by the nonlinear static analysis of structure subjected to monotonically increasing lateral forces varying through the height of the structure. The analysis is carried out by applying the gravity loads followed by lateral loading along a direction starting at the end of the gravity push. The structure is pushed until either a predetermined target displacement is reached or it collapse. The reliable post-yield material model and inelastic member deformations are extremely important in the nonlinear analysis. The evaluation is based on an assessment of important parameters, including global drift, inter-storey drift, inelastic element deformations (either absolute or normalized with respect to a yield value), deformations between elements, and element and connection forces (for elements and connections that cannot sustain inelastic

deformations). The inelastic static pushover analysis can be viewed as a method for predicting seismic force and deformation demands, which accounts in an approximate manner for the redistribution of internal forces occurring when the structure is subjected to inertia forces that no longer can be resisted within the elastic range of structural behaviour. The two key steps in applying this method, i.e. lateral force distribution and target displacement are based on the assumption that the structure's response is mainly from the fundamental mode, and that the mode shapes remain unchanged after structure gets into the inelastic region.

5.1. Static Nonlinear Pushover Analysis

Nonlinear static pushover analysis has become the most commonly used method to determine the nonlinear behavior of the building structures in the recent years. In this simplified method, a capacity curve is obtained which shows the relation of base shear and roof displacement. This curve represents the behavior of the building structure under increasing base shear forces. As the capacities of the members of the lateral force resisting system exceed their yield limits during the increasing of the base shear forces, the slope of the force-deformation curve will change, and hence the nonlinear behavior can be represented. In the pushover analysis, the applied lateral forces to a model are increased in a regular manner depending on the initial load pattern. Member forces are calculated for each step and the stiffness of the members whose capacities are exceeded is changed according to the hinge properties in the next step of the analysis. This process ends when the structure becomes unstable.

The pushover analysis can be performed considering the control over the force or displacement. Force control option is useful when the magnitude of the load is known clearly, and the structure is expected to support that load. The displacement control is useful when the magnitude of the load is unknown and displacements are searched.

In this study, due to its simplicity and its computation power SAP2000 [10] computer software is utilized to carry out the pushover analyses.

5.1.1 Purpose of Non-linear Static Push-over Analysis

The purpose of pushover analysis is to evaluate the expected performance of structural systems by estimating performance of a structural system by estimating its strength and deformation demands in design earthquakes by means of static inelastic analysis, and comparing these

demands to available capacities at the performance levels of interest. The evaluation is based on an assessment of important performance parameters, including global drift, interstory drift, inelastic element deformations (either absolute or normalized with respect to a yield value), deformations between elements, and element connection forces (for elements and connections that cannot sustain inelastic deformations), The inelastic static pushover analysis can be viewed as a method for predicting seismic force and deformation demands, which accounts in an approximate manner for the redistribution of internal forces that no longer can be resisted within the elastic range of structural behavior. The pushover is expected to provide information on many response characteristics that cannot be obtained from an elastic static or dynamic analysis.

The following are the examples of such response characteristics:

• The realistic force demands on potentially brittle elements, such as axial force demands on columns, force demands on brace connections, moment demands on beam to column connections, shear force demands in deep reinforced concrete spandrel beams, shear force demands in unreinforced masonry wall piers, etc.

• Estimates of the deformations demands for elements that have to form inelastically in order to dissipate the energy imparted to the structure.

• Consequences of the strength deterioration of individual elements on behavior of structural system.

• Consequences of the strength deterioration of the individual elements on the behaviour of the structural system.

• Identification of the critical regions in which the deformation demands are expected to be high and that have to become the focus through detailing.

• Identification of the strength discontinuities in plan elevation that will lead to changes in the dynamic characteristics in elastic range.

• Estimates of the interstory drifts that account for strength or stiffness discontinuities and that may be used to control the damages and to evaluate P-Delta effects.

• Verification of the completeness and adequacy of load path, considering all the elements of the structural system, all the connections, the stiff nonstructural elements of significant strength, and the foundation system.

The last item is the most relevant one as the analytical model incorporates all elements, whether structural or non structural, that contribute significantly to the lateral load distribution. Load transfer through across the connections through the ductile elements can be checked with realistic forces; the effects of stiff partial-height infill walls on shear forces in columns can be evaluated; and the maximum overturning moment in walls, which is often limited by the uplift capacity of foundation elements can be estimated.

5.1.2 Steps in pushover Analysis

The following steps are included in the pushover analysis. Steps 1 through 4 discuss creating the computer model, step 5 runs the analysis, and steps 6 through 10 review the pushover analysis results.

1. Create the basic computer model (without the pushover data) in the usual manner using the graphical interface of SAP2000 makes this a quick and easy task.
2. Define properties and acceptance criteria for the pushover hinges.
3. The program includes several built-in default hinge properties that are based on average values from ATC-40 for concrete members and average values from FEMA-273 for steel members.
4. Locate the pushover hinges on the model by selecting one or more frame members and assigning them one or more hinge properties and hinge locations considering end-offsets.
5. Define the pushover load cases. In SAP2000 more than one pushover load case can be run in the same analysis. Also a pushover load case can start from the final conditions of another pushover load case that was previously run in the same analysis.

Typically the first pushover load case is used to apply gravity load and then subsequent lateral pushover load cases are specified to start from the final conditions of the gravity pushover. Pushover load cases can be force controlled, that is, pushed to a certain defined force level, or they can be displacement controlled, that is, pushed to a specified displacement. Typically a gravity load pushover is force controlled and lateral pushovers are displacement controlled.

6. Run the basic static analysis and, if desired, dynamic analysis. Then run the static nonlinear pushover analysis.
7. Display the pushover curve
8. Display the capacity spectrum curve.

We can interactively modify the magnitude of the earthquake and the damping information on this form and immediately see the new capacity spectrum plot.

The performance point for a given set of values is defined by the intersection of the capacity curve and the single demand spectrum curve. Also, the file menu in this display allows you to print the coordinates of the capacity curve and the demand curve as well as other information used to convert the pushover curve to Acceleration-Displacement Response Spectrum (ADRS) format.

9. Review the pushover displaced shape and sequence of hinge formation on a step-by-step basis.

10. Review member forces on a step-by-step basis.

11. Output for the pushover analysis can be printed in a tabular form for the entire model or for selected elements of the model. The types of output available in this form include joint displacements at each step of the pushover, frame member forces at each step of the pushover, and hinge force, displacement and state at each step of the pushover.

5.1.3 Effective Stiffness Factors

It is necessary to define effective elastic properties to define the elastic part of the lumped-plasticity model since the elastic part of the member cracks when the member enters in to inelastic range. Hence, the stiffness reduction factors were used to reduce the gross stiffness properties of the beams and the columns and the reduced stiffness were used to define the effective stiffness model and the lumped-plasticity model. The effective rigidity assumed for each member of the structure should be consistent with its intended behaviour and the models used. For lumped plasticity elements, it is recommended (Kappos, 1986; Paulay and Priestley, 1992; Penelis and Kappos, 1997; ASCE, 2000) to use 30% to 50% of the gross flexural rigidity (*EIg*) for beams, 40% to 60% *EIg* for the walls, and 60% to 80% *EIg* for columns (in compression), to account for member cracking, which is different in each type of member; the higher values for columns and walls apply for high axial compression. The approximate component initial effective stiffness values according to ATC-40; 0.5EI and 0.70EI for beams and columns, respectively, are used in this study.

5.2 Modal Pushover Analysis

The Modal Pushover Analysis (MPA) is based on performing a nonlinear static analysis, ("Push Over type" with a special distribution of lateral forces) and also in using, in an approximate manner, the classic theory of structural dynamics, that includes the contributions of the different natural vibration modes for elastic behavior. Based on these assumptions, it allows determining the resisting capacity of the structure and provides information of the nonlinear behavior of the elements under extreme earthquake loading. The earthquake loading is considered acting in equivalent single degree of freedom (SDOF), systems that have a nonlinear behavior curve that is based on the "pushover curves" obtained from the analysis of the multiple degrees of freedom (MDOF) system with lateral distributions of force that are proportional to the corresponding elastic vibration mode shapes. The "pushover curves" for each mode shape are assumed to be bilinear, and are then transformed to a force-deformation relationship, different for each mode. Once the behavior curves for each of the modes are obtained, the nonlinear response of the equivalent nonlinear SDOF systems are computed and afterwards their maximum values are used to estimate the overall maximum values for each response quantities (Storey shear, displacements, drifts, etc.) are combined using an appropriate combination rule (SRSS or CQC). The response spectrum based modal roof displacement for significant modes in each direction is given in Table (5.1-5.6) for five, ten and B+ nine storey RC buildings respectively.

The MPA procedure was implemented originally for symmetric building and then extended to unsymmetric systems. For unsymmetric systems, mode(s) is replaced by 'modal' pair(s). In an unsymmetric-plan building the non-linear static procedure leads to two pushover curves corresponding to the two lateral directions, x and y. It would be natural to use the x (or y) pushover curve for a mode in which the x (or y) component of displacements is dominant compared to their y (or x) component (Chopra and Goel, 2004). In practical application of MPA, the roof displacement for each modal pushover analyses can be estimated from elastic spectrum defining the seismic hazard multiplied by the inelastic deformation ratio (Chopra, 2004).

5.2.1 Modal displacements of the RC Buildings at the Roof level

The modal elastic roof displacement is determined from elastic response spectrum scaled to PGA of 0.1g in both X and Y direction.

I) Modal displacement for five storey building at roof level

Table 5.1 Roof displacement for five storey RC building in X-direction

Mode	ω_n	$T_{n(sec)}$	Sd(t)	A_n=Sd(t)*PGA	Dn =A/ω_n^2	Γ_n	ϕ_{jn}	$U_{jn}=\Gamma_n\phi_{jn}D_n$ (cm)
1	10.740	0.585	2.500	2.453	0.021	15.719	0.086	2.888
2	14.645	0.429	2.500	2.453	0.011	1.320	0.016	0.023
3	19.923	0.315	2.500	2.453	0.006	0.717	0.030	0.013

Table 5.2 Roof displacement for five storey RC building in Y-direction

Mode	ω_n	$T_{n(sec)}$	Sd(t)	A_n=Sd(t)*PGA	Dn =A/ω_n^2	Γ_n	ϕ_{jn}	$U_{jn}=\Gamma_n\phi_{jn}D_n$ (cm)
1	7.387	0.850	1.780	1.746	0.032	14.767	0.066	3.119
2	13.605	0.462	2.500	2.453	0.013	0.201	0.042	0.011
3	15.660	0.401	2.500	2.453	0.010	1.538	0.039	0.060

II. Modal displacement for ten storey building at roof level

Table 5.3 Roof displacement for ten storey RC building in X-direction

Mode	ω_n	$T_{n(sec)}$	Sd(t)	A_n=Sd(t)*PGA	Dn =A/ω_n^2	Γ_n	ϕ_{jn}	$U_{jn}=\Gamma_n\phi_{jn}D_n$ (cm)
1	3.423	1.836	0.827	0.811	0.069	67.710	0.017	8.158
2	7.774	0.808	1.860	1.825	0.030	13.122	0.008	0.313
3	10.674	0.589	2.500	2.500	0.022	29.760	0.016	1.051

Table 5.4 Roof displacement for five storey RC building in Y-direction

Mode	ω_n	$T_{n(sec)}$	Sd(t)	A_n=Sd(t)*PGA	Dn =A/ω_n^2	Γ_n	ϕ_{jn}	$U_{jn}=\Gamma_n\phi_{jn}D_n$ (cm)
1	2.795	2.248	0.676	0.663	0.085	73.295	0.019	11.822
2	9.511	0.660	2.310	2.266	0.025	34.737	0.018	1.539
3	21.248	0.296	2.500	2.453	0.005	18.264	0.014	0.141

III. Modal displacement for B + nine storey building at roof level

Table 5.5 Roof displacement for B + nine storey RC building in X-direction

Mode	ω_n	$T_{n(sec)}$	Sd(t)	A_n=Sd(t)*PGA	Dn =A/ω_n^2	Γ_n	ϕ_{jn}	$U_{jn}=\Gamma_n\phi_{jn}D_n$(cm)
1	4.236	1.483	1.100	1.079	0.060	41.320	0.028	6.958
2	12.037	0.522	2.500	2.500	0.017	17.000	0.045	1.320
3	4.859	1.293	1.230	1.207	0.051	11.360	0.013	0.755

Table 5.6 Roof displacement for B + nine storey RC building in Y-direction

Mode	ω_n	$T_{n(sec)}$	Sd(t)	A_n=Sd(t)*PGA	Dn =A/ω_n^2	Γ_n	ϕ_{jn}	$U_{jn}= \Gamma_n\phi_{jn}D_n$(cm)
1	4.859	1.293	1.230	1.207	0.051	39.100	0.030	5.996
2	6.524	0.963	2.500	2.453	0.058	21.900	0.007	0.921
3	14.184	0.443	2.500	2.453	0.012	14.130	0.033	0.568

5.2.2 Inelastic Deformation Ratio

The estimates of the target displacements need be based on some form of empirical rule so as to correlate the elastic displacement with the inelastic displacement. Previous studies (Veletsos et al.1960, Veletsos et al. 1965, Newmark et al. 1973, Clough et al. 1993 and Chopra 1995) showed that in the medium- and long period range the inelastic displacement is almost equal to the elastic displacement. In the short-period range it has been observed that the inelastic displacement is generally larger than the elastic displacement; however in this region the principle of conservation of energy can be used by which the monotonic force-displacement diagram of the elastic system up to the maximum deformation is the same as that of an elastic-perfectly-plastic system (Miranda et al. 1994).

The peak deformation ratio of inelastic and corresponding elastic single-degree-of- freedom systems ($C\mu$) for systems with known ductility factor (μ) is given by

$$C_\mu = \begin{cases} \mu & T_n < T_a \\ \mu/\sqrt{2\mu-1} & T_b < T_n < T_{c'} \\ 1 & T_n > T_c \end{cases} \qquad (5.1)$$

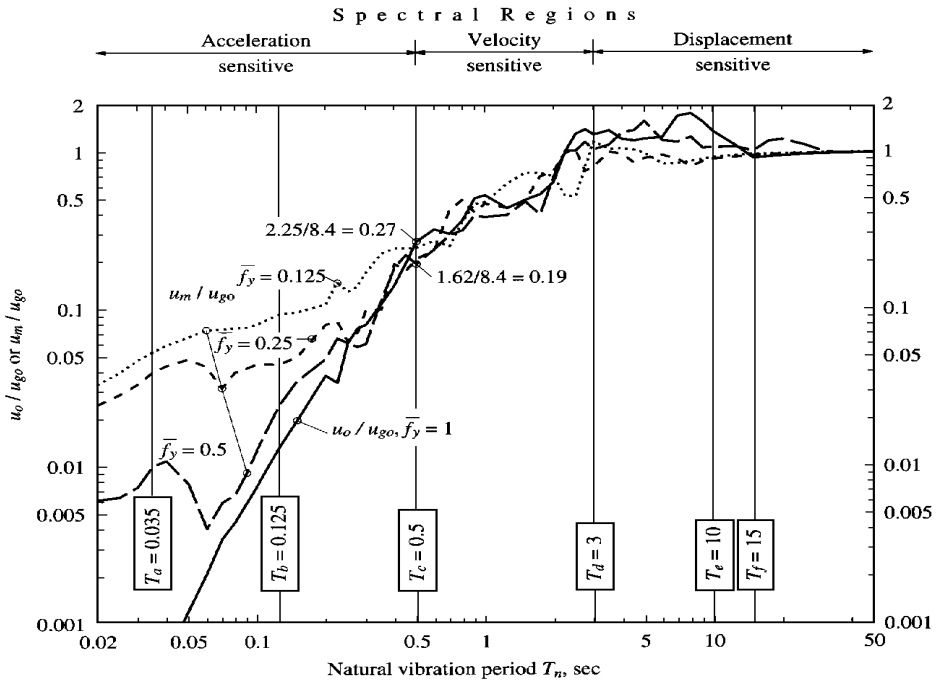

Figure 5.1. Peak deformation of elastoplastic systems and corresponding linear systems due to EI Centro ground motion; for $\bar{f}_y$=1, 0.5, 0.25, 0.125 (Chopra, 2001)

Where $T_{c'} = T_c\sqrt{2\mu - 1}/\mu$

Tn = elastic natural vibration period

Ta,Tb,Tc are periods defined in Newmark–Hall design spectrum Figure 5.1.

As an alternative to the empirical equations for the inelastic deformation ratio, *Ry* –μ– *Tn* relations can be used to estimate the peak deformation of an inelastic SDF system (Chopra and Goel 1999; Fajfar 2000), but this indirect method is slightly biased towards underestimating the deformation (Miranda 2001), Therefore in this paper equations are used to determine the inelastic deformation ratio.

For the buildings under consideration the ductility factor was determined from EBCS-8 considering ductility class medium as γ = 0.30, but ductility factor μ=1/γ = 1/0.30 = 3.33

Therefore, the inelastic deformation ratio was determined using value of μ= 3.33. The inelastic deformation ratio (Cμ) corresponds to C1 in FEMA-273 (1997) Displacement coefficient method.

5.2.3 Determination of modal target displacement at roof level

The modal target displacement for MPA was determined from response spectrum analysis by multiplying the elastic deformation with modification coefficient; called response spectrum based modal pushover analysis. The coefficient Cμ which relates the maximum inelastic and elastic displacement of single degree of freedom system is determined by using the empirical formula given by equation 5.1. The effort of considering nonlinearity in determining the target displacement in each mode in MPA leads to a better prediction of floor displacement and drift ratio.

5.2.4 Modification Coefficients to Determine Target Displacement for Inelastic Systems

Table 5.7 Coefficients relating inelastic to elastic displacements for five storey building

In X-direction			In y-direction		
Mode	Modal period (Tn)	Cμ	Mode	Modal period (Tn)	Cμ
1	0.585	1.00	1	0.850	1.00
2	0.429	1.40	2	0.462	1.40
3	0.315	1.40	3	0.401	1.40

Table 5.8 Coefficients relating inelastic to elastic displacements for ten storey building

In X-direction			In y-direction		
Mode	Modal period (Tn)	Cμ	Mode	Modal period (Tn)	Cμ
1	1.836	1.00	1	2.248	1.00
2	0.808	1.00	2	0.660	1.00
3	0.589	1.00	3	0.296	1.40

Table 5.9 Coefficients relating inelastic to elastic displacements for B+nine storey building

In X-direction			In y-direction		
Mode	Modal period (Tn)	Cμ	Mode	Modal period (Tn)	Cμ
1	1.483	1.00	1	1.293	1.00
2	1.293	1.00	2	0.963	1.00
3	0.522	1.40	3	0.443	1.40

5.2.5 Determination of modal target displacements

Table 5.10 Values of the target roof displacements for MPA of five storey building

Direction of Excitation	Mode 1 $\delta t = C\mu \times Ujn$ (cm)	Mode 2 $\delta t = C\mu \times Ujn$ (cm)	Mode 3 $\delta t = C\mu \times Ujn$ (cm)
X	2.888	0.033	0.019
Y	3.119	0.016	0.084

Table 5.11 Values of the target roof displacements for MPA of ten storey building

Direction of Excitation	Mode 1 $\delta t = C\mu \times Ujn$ (cm)	Mode 2 $\delta t = C\mu \times Ujn$ (cm)	Mode 3 $\delta t = C\mu \times Ujn$ (cm)
X	8.158	0.313	1.051
Y	11.822	1.539	0.197

Table 5.12 Values of the target roof displacements for MPA of B+ nine storey building

Direction of Excitation	Mode 1	Mode 2	Mode 3
	$\delta t = C\mu \times Ujn$ (cm)	$\delta t = C\mu \times Ujn$ (cm)	$\delta t = C\mu \times Ujn$ (cm)
X	6.958	1.320	1.057
Y	5.996	0.921	0.796

5.3 Comparison of Responses from the Analysis

In this section, conventional and modal pushover analysis has been performed for reinforced buildings located in Ethiopia (Zone 4 of PGA= 0.1g). In addition Response spectrum analysis was also performed. Results of these analyses have been presented and compared to each other.

To estimate the seismic demands, the contribution of the first three significant 'modal' pairs was included in the pushover analysis of the buildings. The combined values of story shear, floor displacements and storey drifts were computed including one, two, or three 'modal' pairs (or modes for symmetric building). Figure (5.2-5.10) shows the floor displacements, inter-storey drift ratio and storey shear demands for the 5, 10 and B+9 storey building together with the value determined by RSA of the system. The values of lateral displacements, inter-storey drifts and storey shears were computed at the floor levels for the two analysis directions (X and Y) and compared with each other.

The results show that the first 'modal' pair alone is inadequate in estimating the interstorey drifts and storey shear, especially in the upper stories of the buildings Figure (5.2-5.10). Including the response contributions of higher 'modal' pairs improves the storey shear and storey drifts for all buildings, but the floor displacements are affected only in irregular B+9 building, implying that contributions of the higher modal pairs to floor displacements are negligible for regular or approximately regular buildings. Two 'modal' pairs suffice, implying that the contribution of the third 'modal' pair is negligible in all the cases. The results show higher 'modal' pairs contribute to the seismic demands for the 10-storey regular and B+9 storey irregular buildings and only MPA is able to capture these effects. For two regular buildings the mass participating factor in the first mode is generally ≥70% in X and Y directions (Table 4.1-4.2) which means that the dynamic response will be dominated by the first mode, in this case it is expected that the conventional pushover analysis will yield realistic results, which is not the case in irregular building (Table 4.3). In addition, the PGA cannot push the buildings far into the inelastic range; therefore the responses will be dominated by the first mode. With sufficient number of 'modal' pairs included, the height-wise distribution of storey shear and storey drifts estimated by MPA is generally superior to the first 'modal' pair result.

5.3.1 Floor Displacements and Inter-Storey Drift Ratios

a) Floor Displacements

The floor displacement is given by

$$U_{jxn}(t) = \Gamma_n \phi_{jxn} D_n(t) \qquad U_{jxn}(t) = \Gamma_n \phi_{jxn} D_n(t) \tag{5.2}$$

b) Inter-Storey Drift Ratios

The storey drifts in the x and y directions defined at the CM is given by

$$\Delta_{jxn}(t) = \Gamma_n(\phi_{jxn} - \phi_{j-1,xn}) D_n(t) \qquad \Delta_{jyn}(t) = \Gamma_n(\phi_{jyn} - \phi_{j-1,yn}) D_n(t) \tag{5.3}$$

The inter storey drift ratio (%) is given by

$$(\Delta_{jxn}(t)/h_j)x100 \qquad (\Delta_{jyn}(t)/h_j)x100 \tag{5.4}$$

Where the subscripts x and y show the responses are in X and Y direction respectively.
On the structural level, the inter-storey drift ratio is one of the simplest and most essential damage indicators.

Table 5.13 Inter Storey drift limits for different performance level

Inter-storey Displa-cement Limits	Performance Level		
	Immediate Occupancy	Life Safety	Collapse Prevention
$(\Delta_i / h_i)x100$	1.0	2.0	3.0

5.3.2 Requirement for serviceability limit state

According to EBCS-8, 1995 section 2.4.3.2. For buildings having non-structural elements of brittle materials attached to the structure, the requirements for serviceability limit states is considered satisfied if the inter-storey drifts (%) are limited to :

$$\frac{d_r}{h} x100 \leq 1.0 \qquad (5.5)$$

Where: dr = design interstorey drift, evaluated difference of the average lateral displacements at the top and bottom of the storey under consideration, and

h = Storey height

Therefore the maximum allowable design interstorey drift ratio (%) for both regular 5 and 10-storey building and B+9 storey irregular building is given as:

$d \leq 1.0$ for serviceability limit state

5.3.3 Comparison of floor displacements

In order to assess various analysis methods, the variations of displacements along the height of the buildings using the specified methods of analyses are obtained and compared with one another. Floor displacements for the 5, 10 and B+9 storey building are shown in Figure 5.2, 5.3 and 5.4 respectively. As shown in these figures, the conventional pushover, modal pushover and response spectrum analysis provides more or less similar results, except in Y-direction of irregular B+9 storey building where the first mode mass participation factor is 56% only. The higher modes contribution in MPA to the floor displacement in low to medium rise regular buildings is very small and can be ignored in practice, but it may be very important as shown in 5.4(b) for buildings in which higher modes are very significant. The values of MPA have been extracted from the first three significant modes where as in RSA twelve and above modes were included. The floor displacements obtained from MPA method is generally higher than that of

RSA method except at the upper few stories where the displacement from latter method is greater in most of the cases. This condition occurs since the contribution of higher modes to the top storey displacements is considerable which is not fully included in MPA, and also the building is not pushed far into inelastic range.

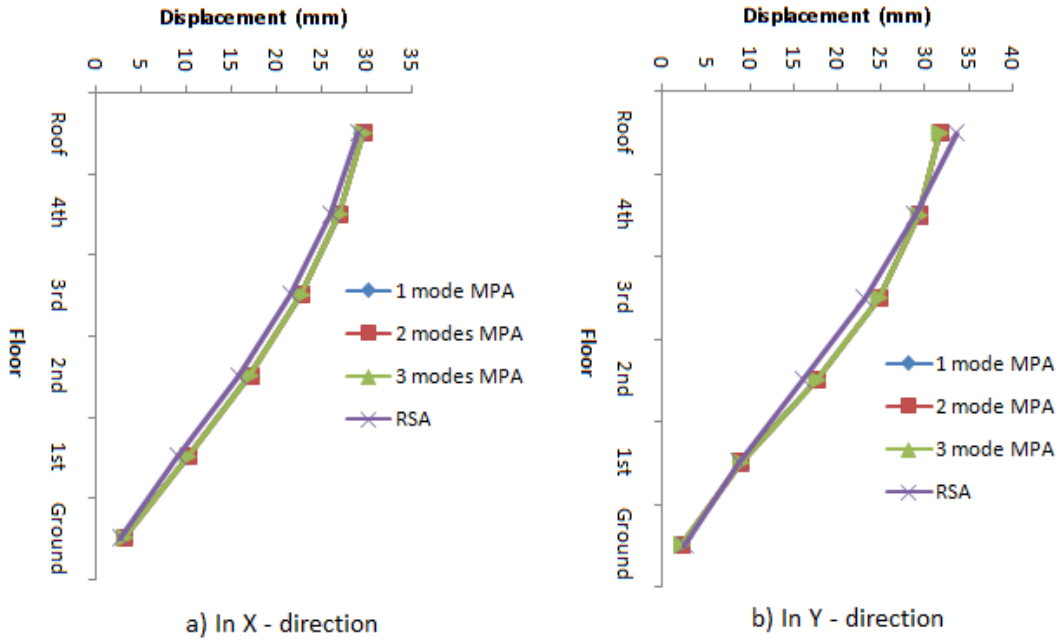

Figure 5.2. Storey displacement profile for five storey RC building

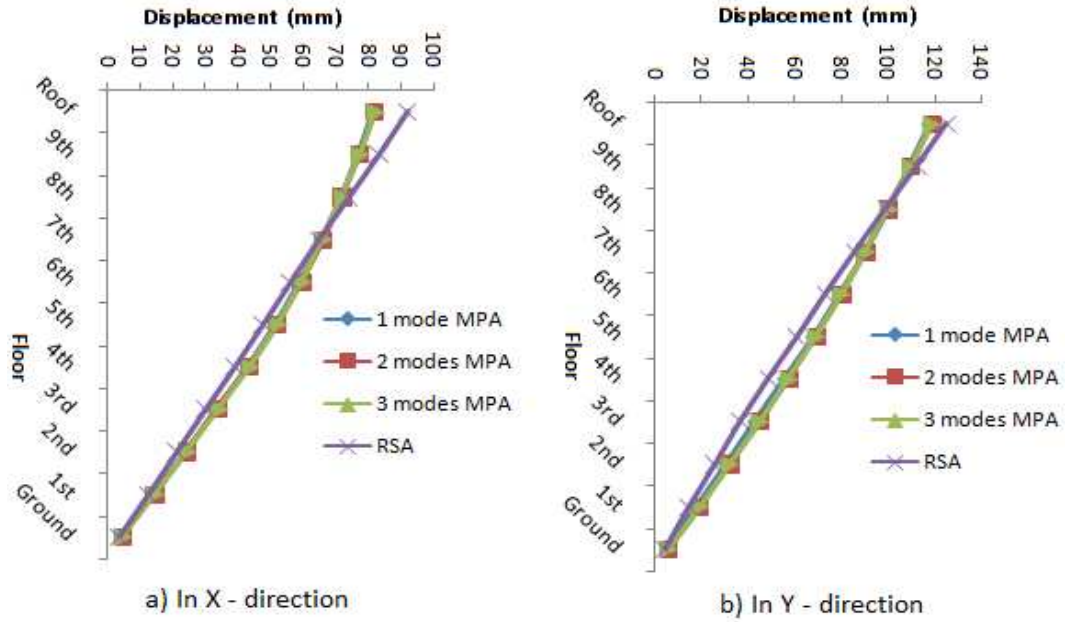

Figure 5.3. Storey displacement profile for ten storey RC building

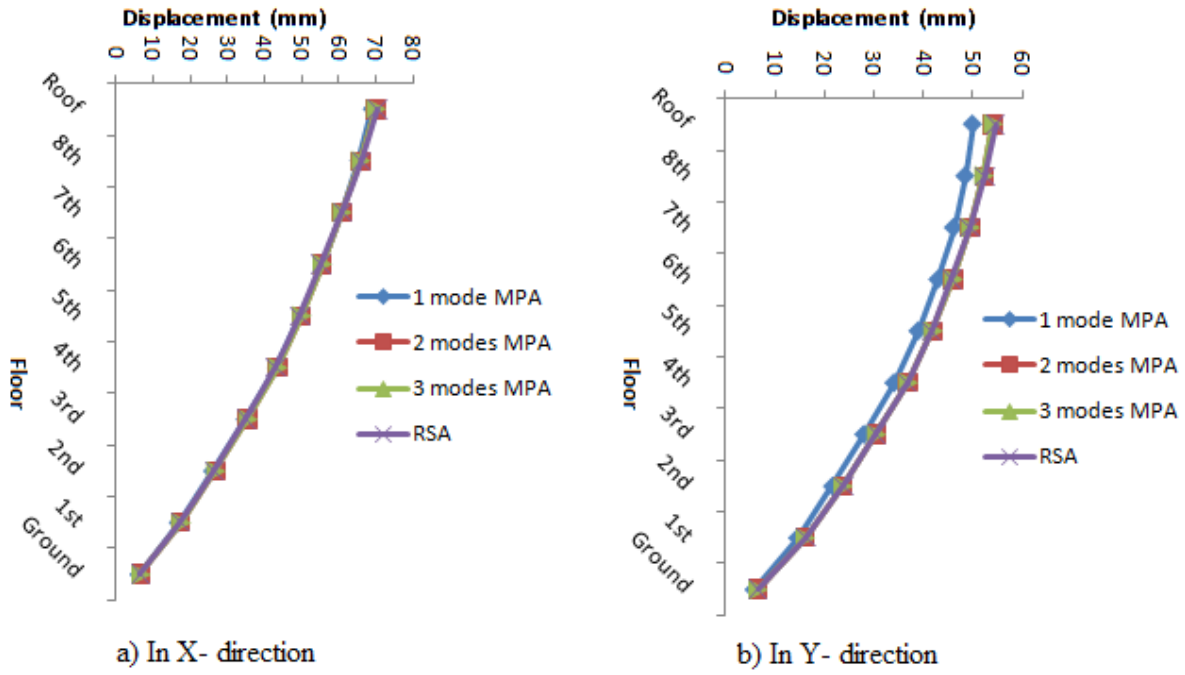

Figure 5.4. Storey displacement profile for B+ nine storey RC building

5.3.4 Comparison of Inter-story drift Ratios

The inter-storey drift ratio is one of the simplest and most essential damage indicators of the structures. The Inter-storey drift limit for different performance level is shown in Table 5.13. The Inter-storey drift ratios for the 5, 10 and B+9 storey building are shown in Figure 5.5, 5.6 and 5.7 respectively for the specified methods of analysis under consideration. From the MPA results it can be observed that the contribution of higher modes to inter-storey drift ratio for 5-storey RC building is very small, but for both regular 10 and irregular B+9 storey RC buildings the contribution is higher. The results show that the contribution of higher modes to inter-storey drift ratio increases with increasing number of stories and/or period, and level of irregularities. From the figure below it can be observed that the RSA method generally underestimates the inter-storey drift ratio as compared to MPA. The modal pushover analysis gave better results of inter-story drift ratio than conventional pushover analysis. For 5, 10 and B+9-storey building the calculated maximum inter-storey drift (%) is 0.476, 0.574 and 0.275 respectively, which is less than 1.0. So all building met the criteria for serviceability limit state of inter-storey drift.

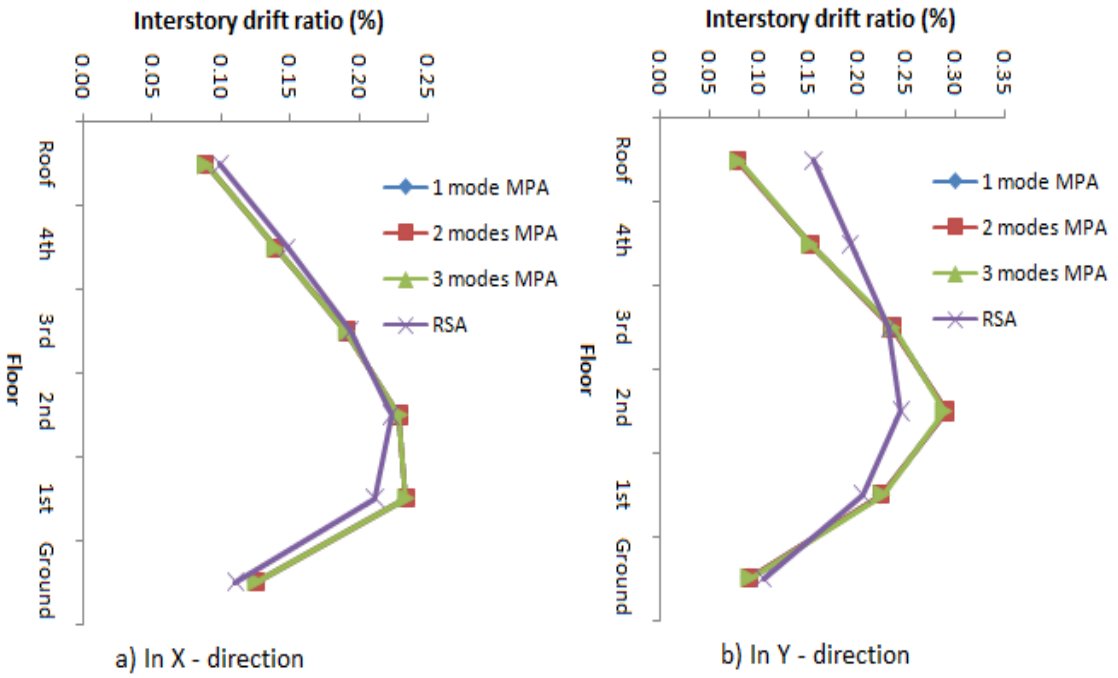

Figure 5.5. Inter-storey drift ratio profile for five storey RC building

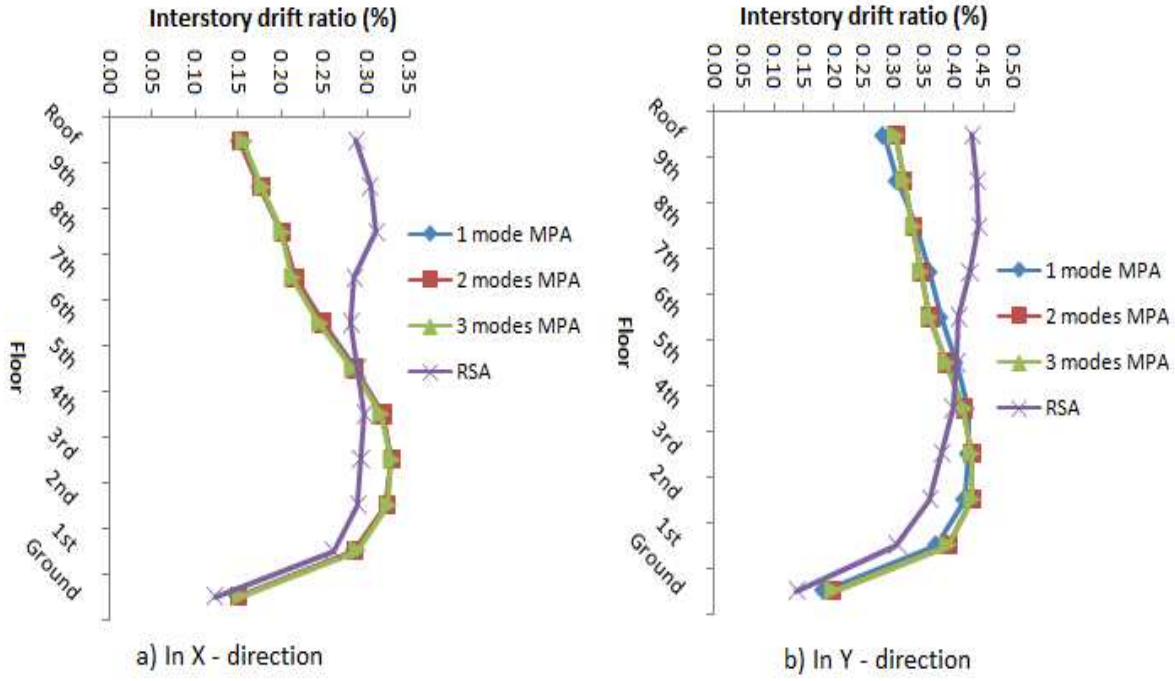

Figure 5.6. Inter-storey drift ratio profile for ten storey RC building

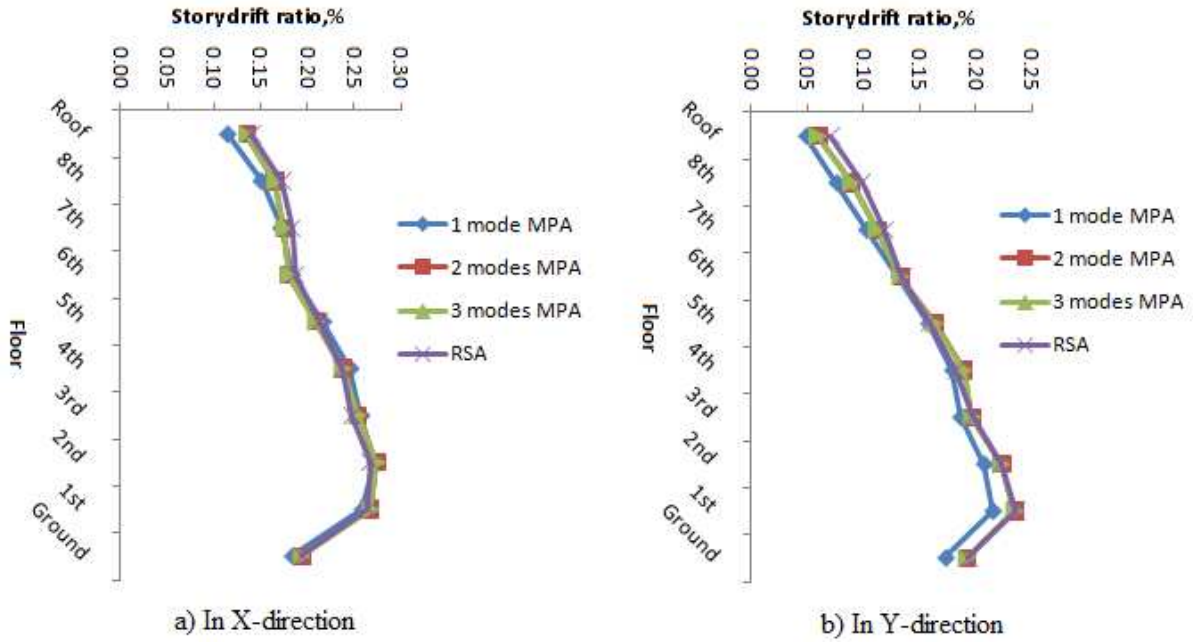

Figure 5.7. Inter-storey drift ratio profile for B + nine storey RC building

5.3.5 Storey shear comparison

In this section, the storey shear values obtained from the conventional and modal pushover analysis method were compared; in addition RSA values are also included for better understanding of the MPA methods Figure (5.8, 5.9 and 5.10). The contribution of higher modes is significant to storey shear than the other responses discussed above. The effect of higher modes decreases from B+9-storey building towards 10 and 5-storey buildings respectively. As seen from Figure 5.9 and 5.10 the contribution of higher modes to the storey shear as the number of storey increases is significant and cannot be ignored. In such a case the conventional pushover analysis may lead to unsafe results. In regular five storey building the values of RSA are larger than MPA results since the contribution of higher modes are significant to storey shear force. i.e. (Twelve modes were included in RSA but only the three significant modes are included in MPA). In 10 storeys regular and irregular buildings the values of MPA generally gave higher responses than RSA since these buildings are pushed into inelastic range, in which nonlinear analysis can give better results. From the results it can be concluded that if equal modes for both RSA and MPA are used in the analysis, MPA can give better results for regular and irregular buildings especially when they are pushed far into

inelastic range. For tall and/or irregular buildings, MPA with few first significant modes included can give better results of storey shear than CPA and RSA methods.

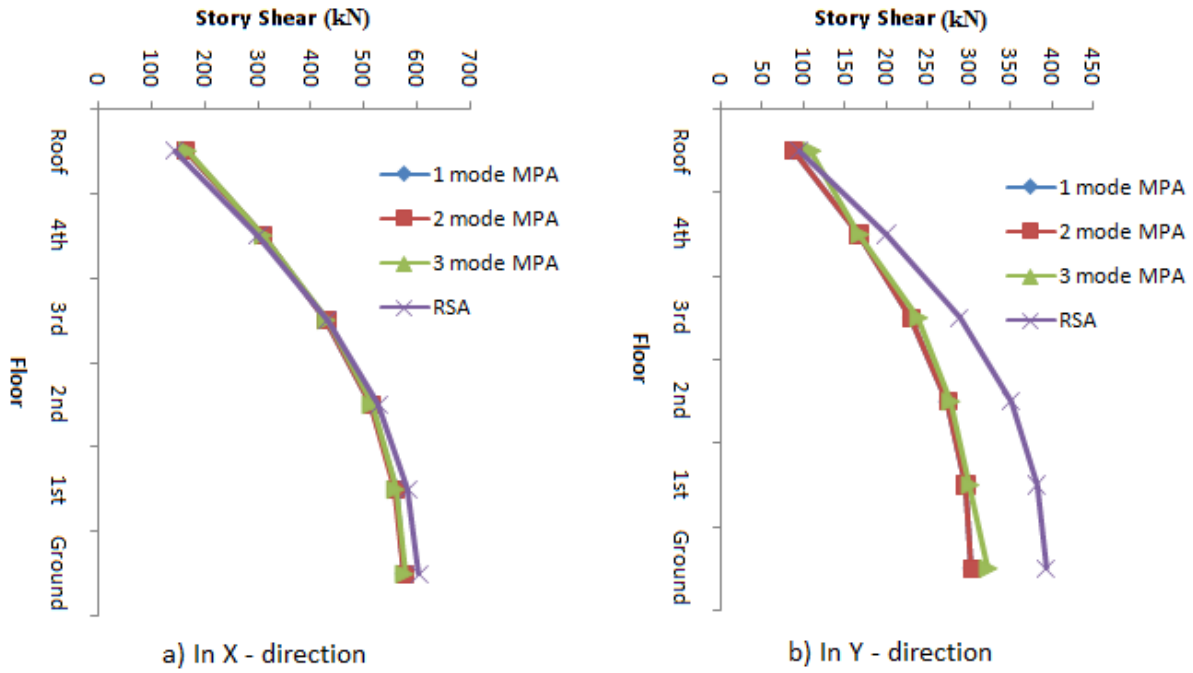

Figure 5.8. Storey shear for five storey RC building

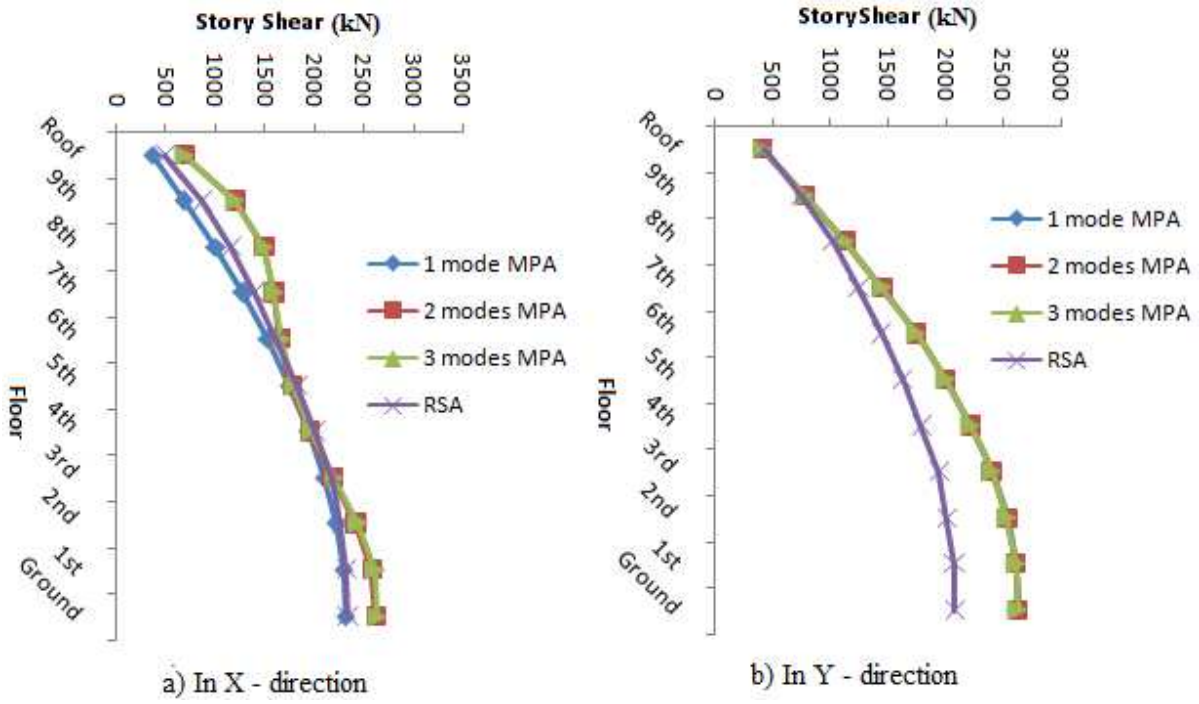

Figure 5.9. Storey shear for ten storey RC building

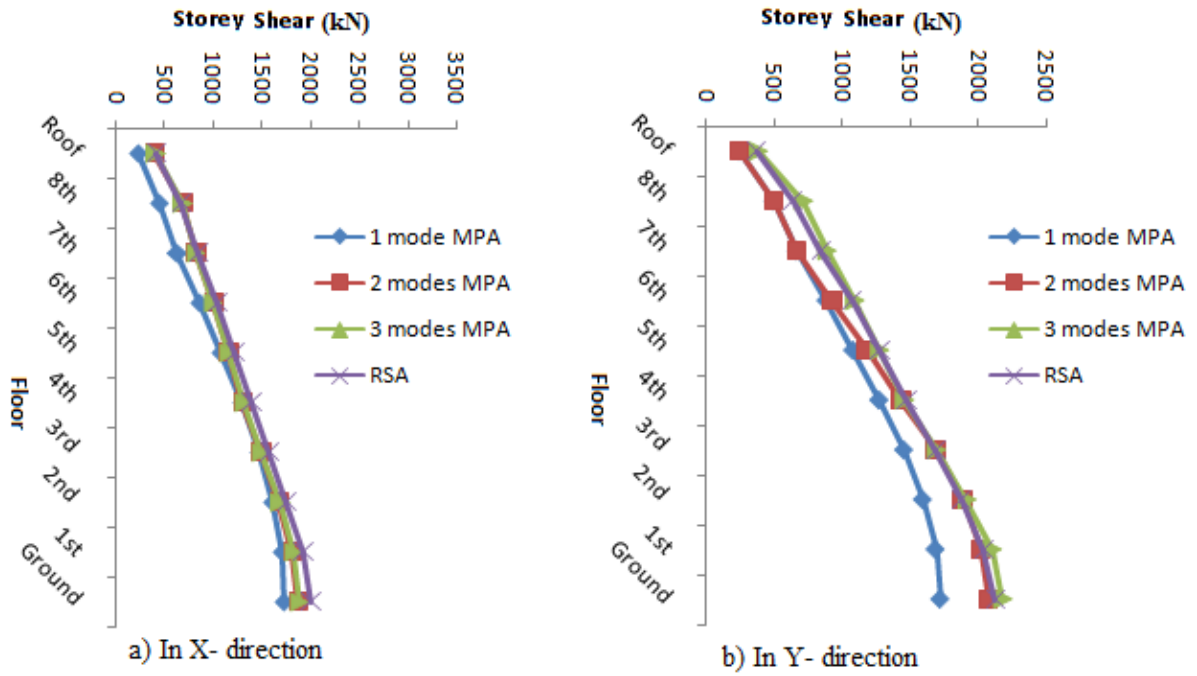

Figure 5.10. Storey shear for B + nine storey RC building

5.4 Plastic Hinge Formation

Eventhough, asymmetrical structures are subjected to pair of actions at a time when subjected to horizontal earth quake forces, pushover analysis is carried out only in the direction of larger displacement. Generally, it has been found that the investigated structures in both X and Y direction subjected the appropriate load combination have remained within the immediate occupancy performance level. The formation of hinges at the last step of pushover analysis; for the 5, 10 and B+9 storey RC buildings subjected to design earthquake at the life safety target displacement level is shown in Figure (5.11-5.16). The life safety performance level is selected because the buildings are designed according to EBCS-8, 1995 which is intended to protect the life safety of the people. Most of the hinges formed in the selected buildings are in the linear range at performance level B which shows that the buildings are safe for expected earthquake forces. On the upper part of the 10-storey building pushed in Y-direction most of the hinges are formed on columns than on beams, which show that the columns on the upper few stories need to be strengthened to assure strong column weak beam principle of capacity design.

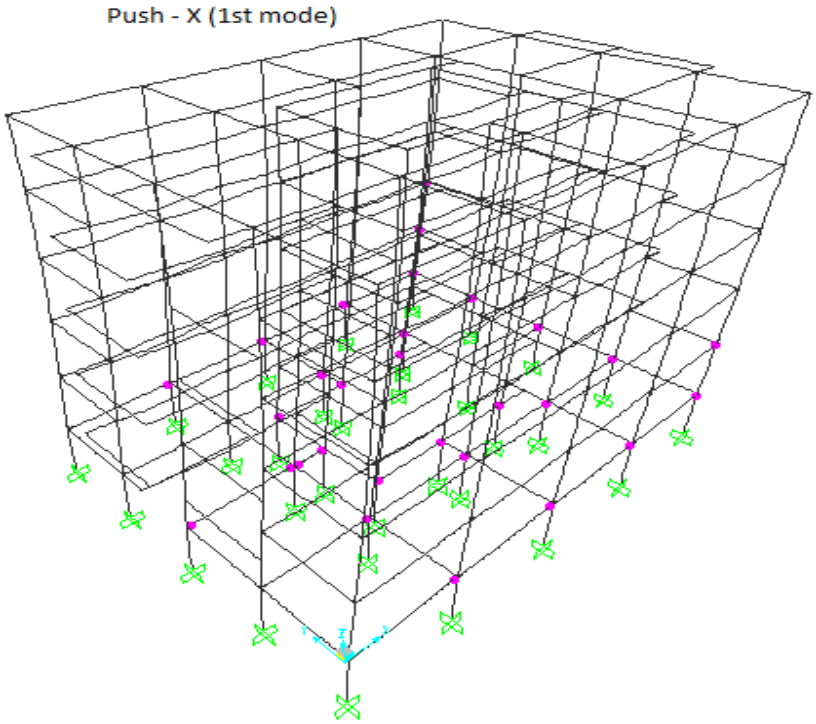

Figure 11. Plastic hinge distribution in five storey RC building in X-direction

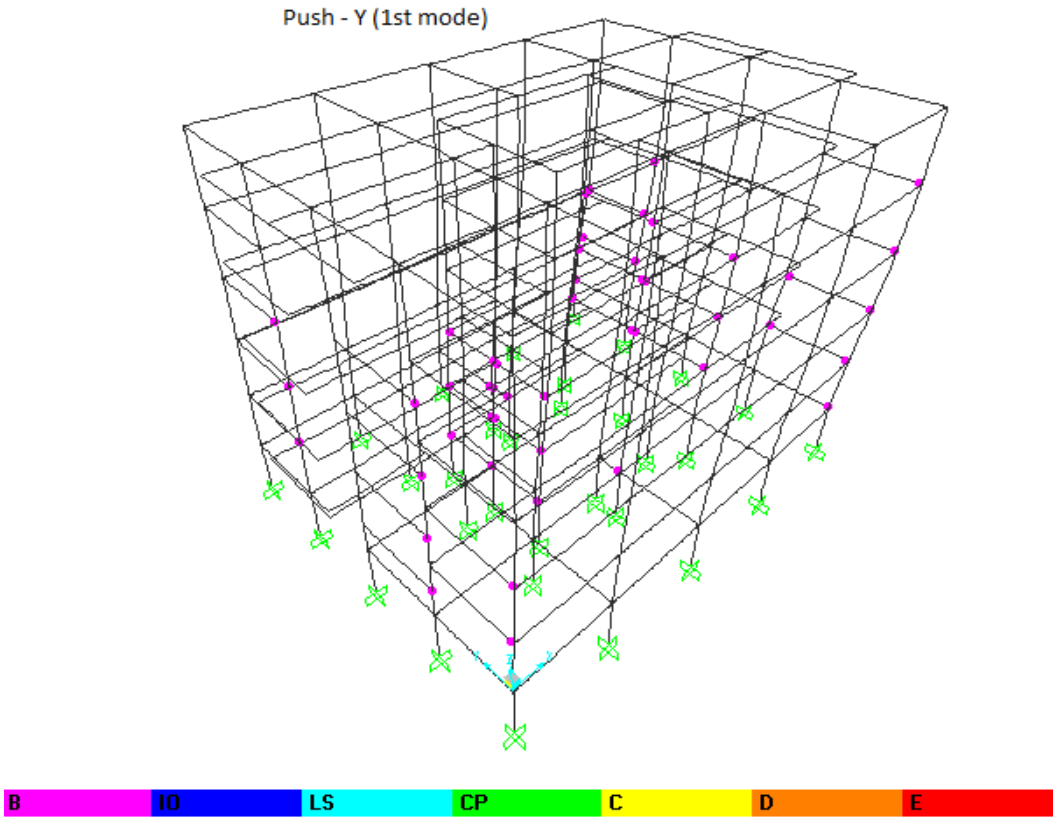

Figure 12. Plastic hinge distribution in five storey RC building in Y-direction

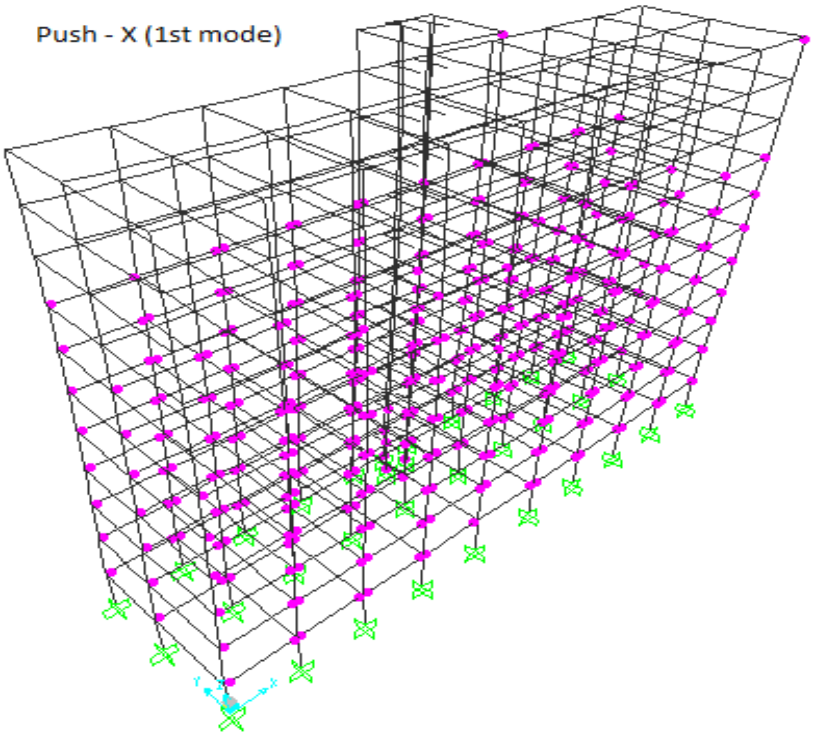

Figure 13. Plastic hinge distribution in ten storey RC building in X- direction

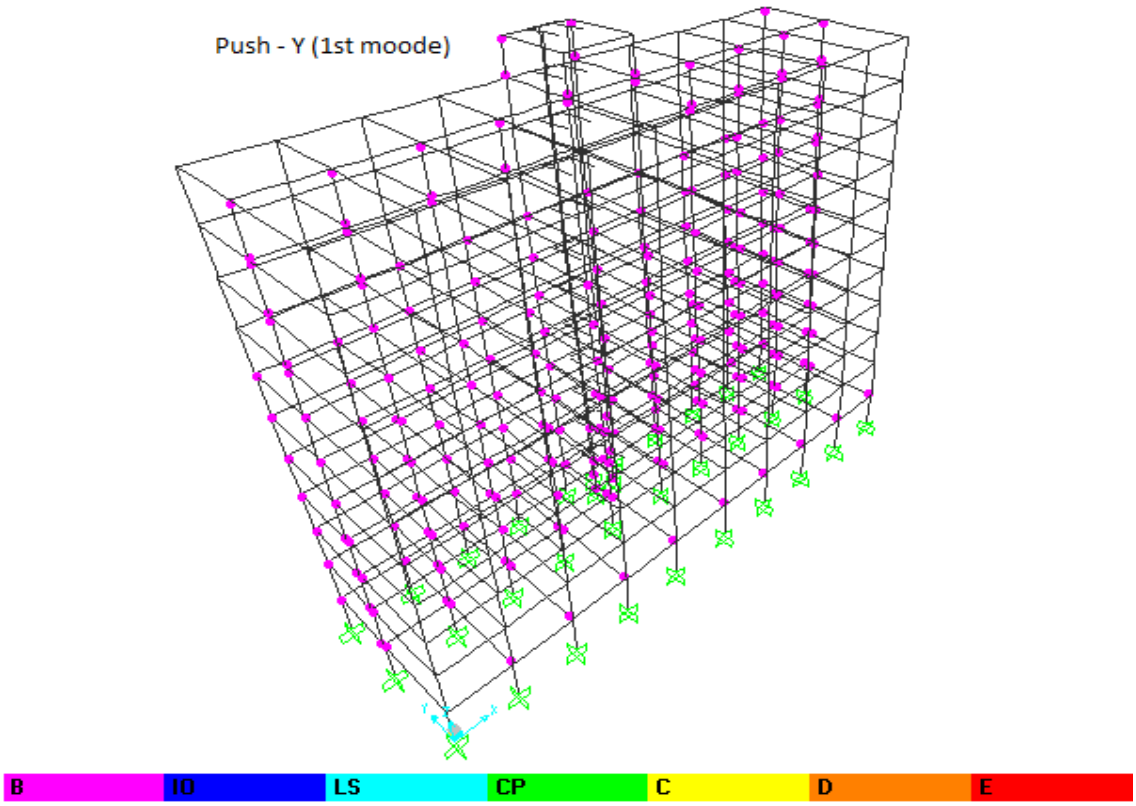

Figure 14. Plastic hinge distribution in ten storey RC building in Y-direction

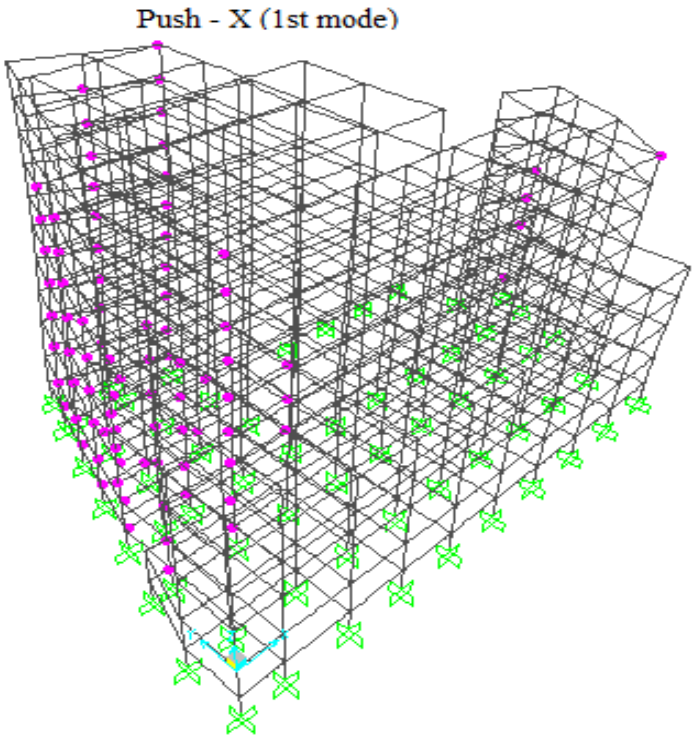

Figure 15. Plastic hinge distribution in B+ nine storey RC building in X-direction

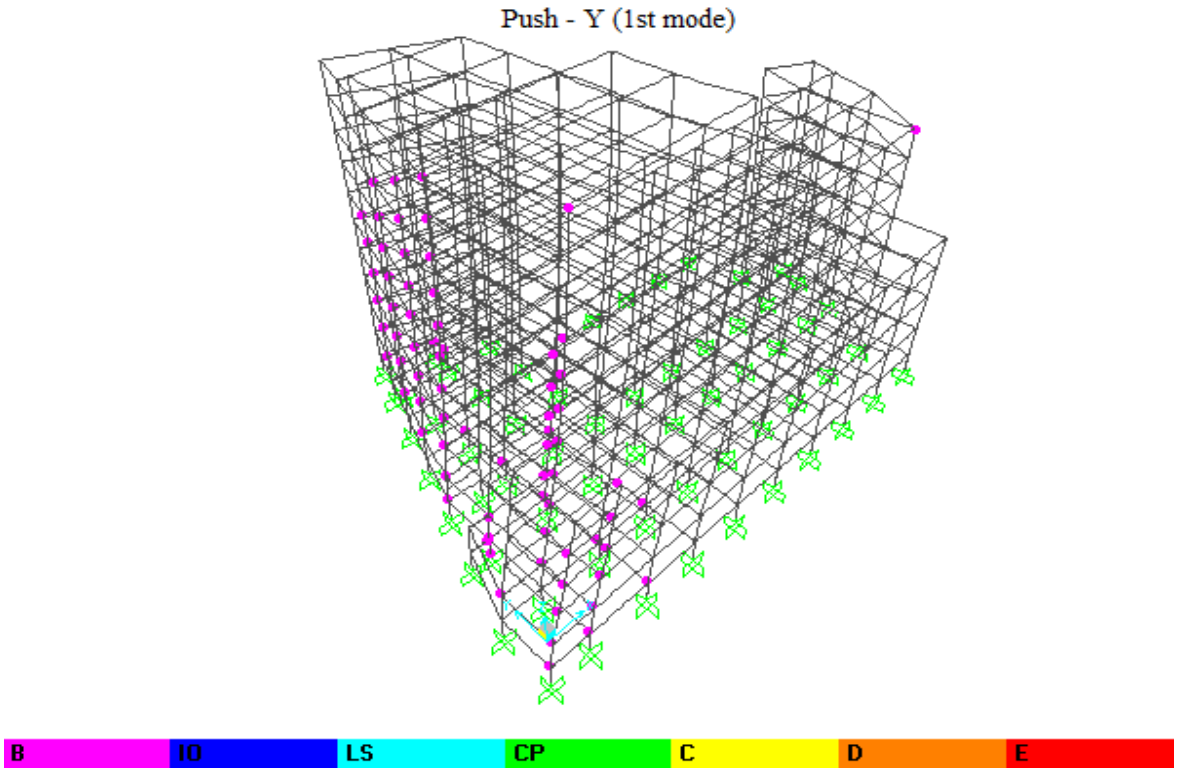

Figure 16. Plastic hinge distribution in B+ nine storey RC building in Y-direction

5.5. Pushover Curves for the Selected RC Buildings

Figure (5.17-5.19) shows the pushover curves from the first significant mode in X and Y direction for the selected RC buildings.

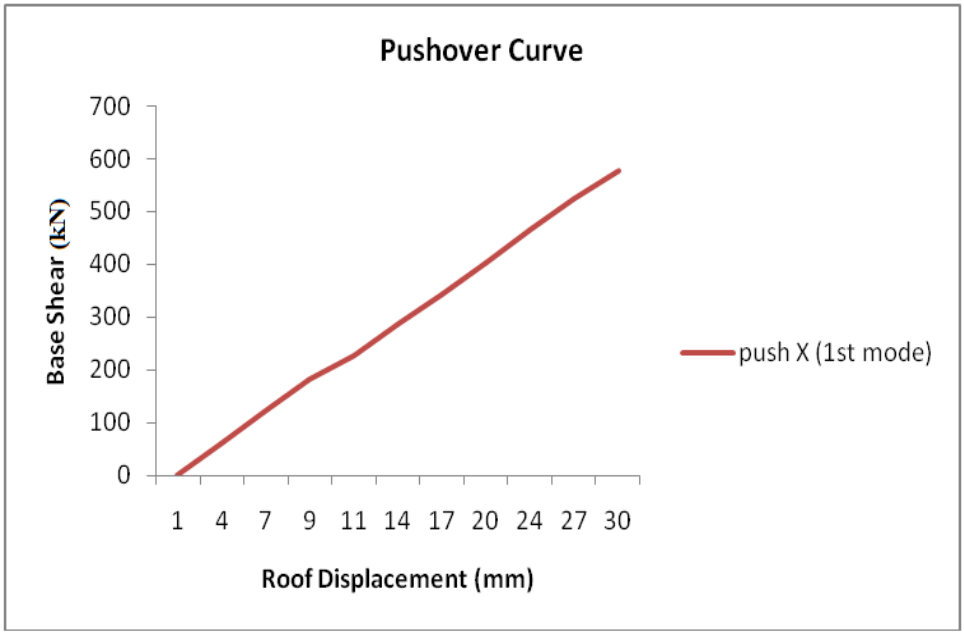

(a)

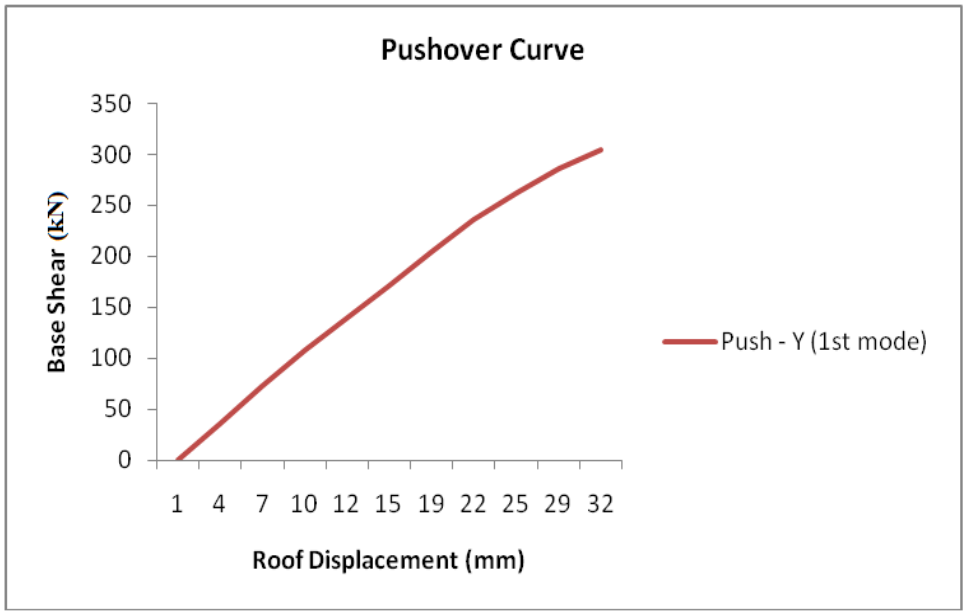

(b)

Figure 5.17. Pushover curves of 5 storey RC building a) In X- direction b) In Y-direction

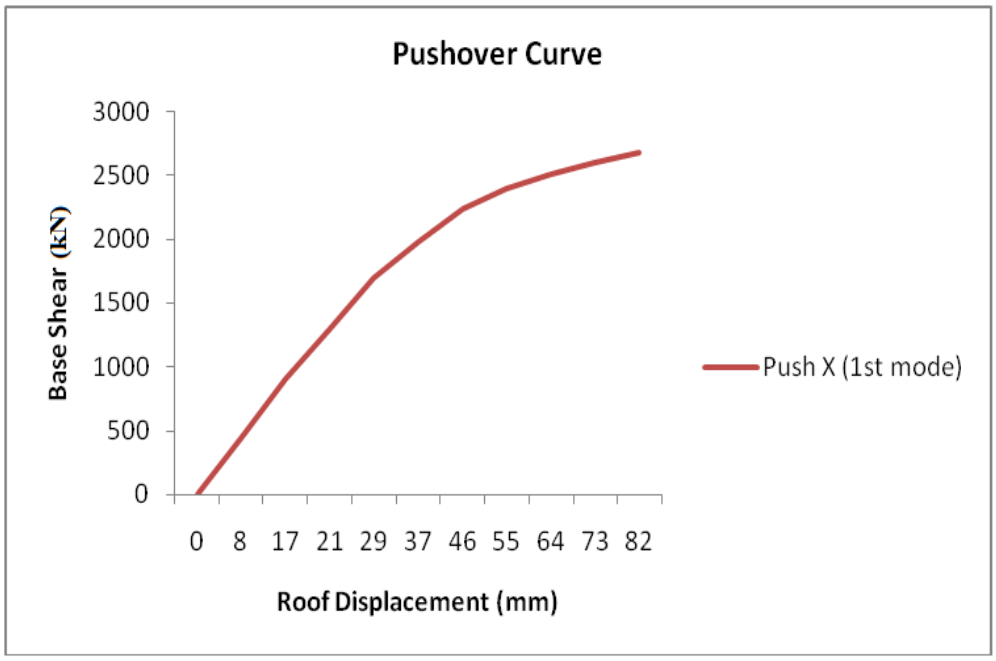

(a)

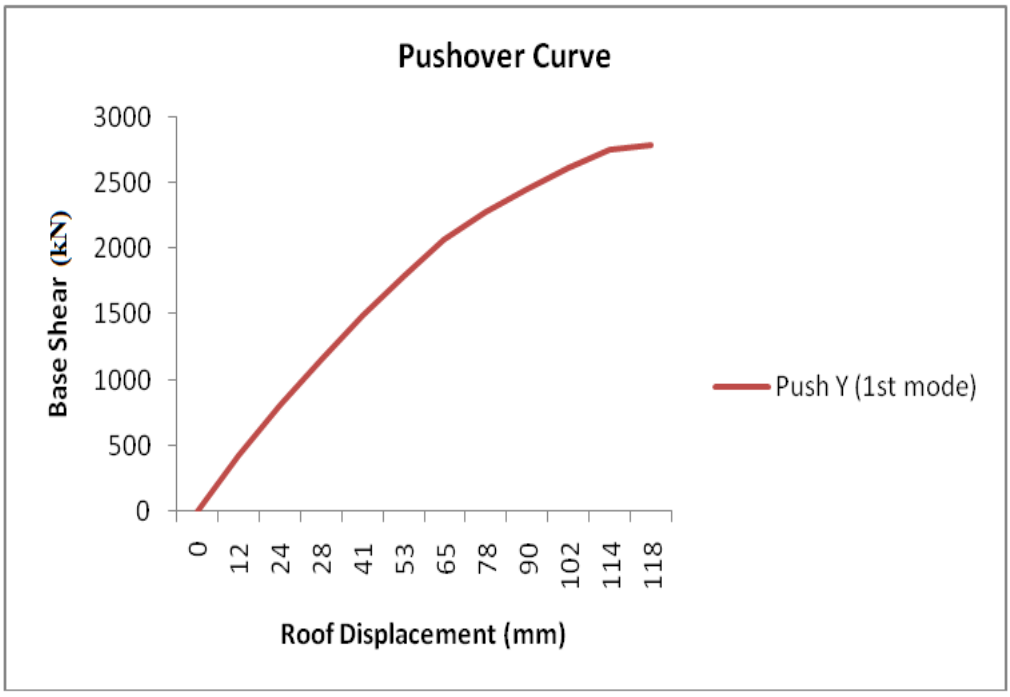

(b)

Figure 5.18. Pushover curves of 10 storey RC building a) In X- direction b) In Y-direction

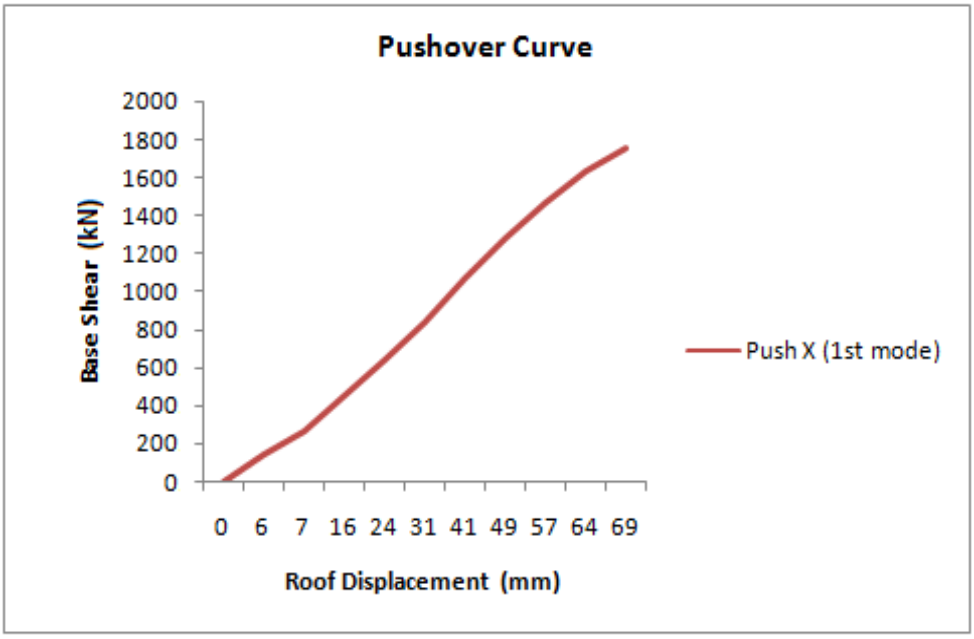

(a)

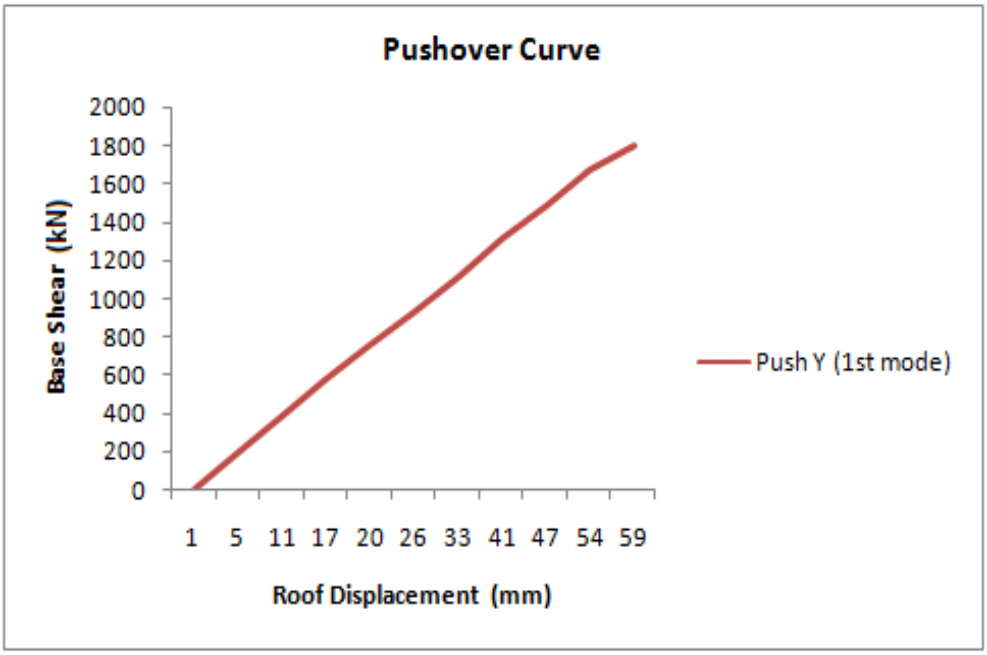

(b)

Figure 5.19. Pushover curves of B + 9 storey RC building a) In X- direction b) In Y-direction

5.5.1 Number of plastic hinges at different performance level

The number of plastic hinges and their formation at target displacement for the first significant mode in X and Y direction, entered in to different performance level at the last step of the pushover analysis output is given in Table (5.14-5.19).

Table 5.14 Number of plastic hinge formation at different performance level for five storey building for Push-X (1st mode)

Step	Displacement (mm)	Base Shear (kN)	A to B	B to IO	IO to E	Beyond E	Total
0	0.75	0.00	847	0	0	0	847
1	3.64	60.22	847	0	0	0	847
2	6.52	120.44	847	0	0	0	847
3	9.41	180.66	847	0	0	0	847
4	11.18	227.47	846	1	0	0	847
5	14.07	287.34	846	1	0	0	847
6	17.23	342.59	845	2	0	0	847
7	20.14	402.40	835	12	0	0	847
8	23.60	467.55	828	19	0	0	847
9	26.62	523.20	823	24	0	0	847
10	29.63	576.89	818	29	0	0	847

Table 5.15 Number of plastic hinge formation at different performance level for five storey building for Push-Y (1st mode)

Step	Displacement (mm)	Base Shear (kN)	A to B	B to IO	IO to E	Beyond E	Total
0	0.57	0.00	847	0	0	0	847
1	3.69	36.20	847	0	0	0	847
2	6.81	72.39	847	0	0	0	847
3	9.93	108.59	847	0	0	0	847
4	11.96	139.13	845	2	0	0	847
5	15.49	171.39	839	8	0	0	847
6	18.76	204.40	835	12	0	0	847
7	22.15	235.66	829	18	0	0	847
8	25.27	261.77	825	22	0	0	847
9	28.58	285.73	810	37	0	0	847
10	31.77	304.28	799	48	0	0	847

Table 5.16 Number of plastic hinge formation at different performance level for ten storey building for Push-X (1st mode)

Step	Displacement (mm)	Base Shear (kN)	A to B	B to IO	IO to E	Beyond E	Total
0	0.19	0	1783	0	0	0	1783
1	8.35	453.33	1783	0	0	0	1783
2	16.51	906.66	1783	0	0	0	1783
3	20.75	1292.42	1782	1	0	0	1783
4	29.01	1691.34	1773	10	0	0	1783
5	37.35	1975.50	1696	87	0	0	1783
6	46.31	2234.36	1568	215	0	0	1783
7	55.09	2393.93	1491	292	0	0	1783
8	63.53	2507.00	1445	338	0	0	1783
9	72.81	2599.64	1397	386	0	0	1783
10	81.79	2674.16	1378	405	0	0	1783

Table 5.17 Number of plastic hinge formation at different performance level for ten storey building for Push-Y (1st mode)

Step	Displacement (mm)	Base Shear (kN)	A to B	B to IO	IO to E	Beyond E	Total
0	0.07	0	1783	0	0	0	1783
1	11.75	427.27	1783	0	0	0	1783
2	23.57	814.53	1783	0	0	0	1783
3	28.13	1159.56	1781	2	0	0	1783
4	40.81	1490.61	1779	4	0	0	1783
5	53.07	1797.10	1742	41	0	0	1783
6	65.21	2065.07	1683	100	0	0	1783
7	77.85	2281.82	1642	141	0	0	1783
8	89.67	2452.96	1615	168	0	0	1783
9	101.82	2610.67	1579	204	0	0	1783
10	114.45	2749.64	1539	244	0	0	1783
11	118.13	2785.52	1525	258	0	0	1783

Table 5.18 Number of plastic hinge formation at different performance level for B+ nine storey building for Push-X (1st mode)

Step	Displacement (mm)	Base Shear (kN)	A to B	B to IO	IO to E	Beyond E	Total
0	0.67	0.00	2771	3	0	0	2774
1	6.29	187.25	2769	5	0	0	2774
2	7.12	209.28	2767	7	0	0	2774
3	15.62	433.79	2761	13	0	0	2774
4	23.66	642.80	2757	17	0	0	2774
5	31.36	841.56	2753	21	0	0	2774
6	40.56	1075.16	2738	36	0	0	2774
7	48.84	1281.55	2728	46	0	0	2774
8	56.69	1472.53	2715	59	0	0	2774
9	63.67	1636.39	2700	74	0	0	2774
10	68.93	1755.81	2688	86	0	0	2774

Table 5.19 Number of plastic hinge formation at different performance level for B+ nine storey building for Push-Y (1st mode)

Step	Displacement (mm)	Base Shear (kN)	A to B	B to IO	IO to E	Beyond E	Total
0	1.22	0.00	2771	3	0	0	2774
1	4.78	192.02	2771	3	0	0	2774
2	10.7	384.04	2771	3	0	0	2774
3	16.78	576.07	2771	3	0	0	2774
4	19.88	675.12	2768	6	0	0	2774
5	26.37	877.21	2755	19	0	0	2774
6	32.94	1074.37	2748	26	0	0	2774
7	40.60	1299.68	2737	37	0	0	2774
8	47.08	1480.92	2724	50	0	0	2774
9	54.04	1670.26	2709	65	0	0	2774
10	58.78	1796.59	2699	75	0	0	2774

6. CONCLUSIONS AND RECOMMENDATIONS

6.1. Conclusions

In this study, different analysis method such as conventional pushover analysis, modal pushover analysis and response spectrum analysis, were utilized for low and mid-rise concrete moment frame structures on stiff soil with existed plan irregularity.

The results obtained show that:

- With sufficient number of 'modal' pairs included, the height-wise distribution of storey shear, storey displacement and inter-storey drifts estimated by MPA is superior to the conventional pushover analysis (first 'modal' pair) result.
- Conventional pushover analysis yields realistic results for five storey regular, fair results in ten storey regular and poor results in ten storey irregular RC buildings. Therefore, the accuracy of the CPA decreases as the height and irregularities of the building increases.
- The contribution of the first two 'modal' pair suffices in most of the cases in MPA and is enough for intended purpose.
- The selected RC buildings met the limits states of design and serviceability (drift) earthquake requirements.
- If equal number of modes is used in RSA and MPA methods, MPA can give higher results for both regular and irregular buildings pushed in to the inelastic range.
- The CPA procedure found to provide close estimates of storey displacement profiles to that estimated by the MPA procedure.
- The contribution of higher modes to the storey shear is significant in both regular and irregular ten storey buildings which cannot be captured by CPA.
- P-Δ effects due to gravity loads in CPA and MPA procedures are small since the buildings are not deformed far into the inelastic range, therefore significant degradation in lateral capacity of the structures is not caused due to gravity load.

6.2 Recommendations for Future Study

- More reinforced concrete structural systems with diverse number of stories and irregularities subjected to several ground motion intensity needs to be assessed to show the superiority extent of MPA over conventional pushover analysis method.
- The effect of soil-structure interaction needs to be adequately addressed in the analyses model to get closer results to the real one.
- Nonlinear dynamic analysis needs to be done to comment on the applicability and accuracy of nonlinear static and linear dynamic methods.
- More refined methods of modeling material nonlinearity and the various lateral load distribution patterns can be used to get more reliable results and to assess the seismic performance of the buildings.

REFERENCES

[1] Applied Technology Council (1996) *"Seismic Evaluation and Retrofit of Concrete Buildings Report, ATC-40"*, Redwood City, California, USA.

[2] Applied Technological Council (2005) *"Improvement of nonlinear static seismic analysis procedures, Report ATC-55"*, Redwood City, California, USA.

[3] Bayer, K., Dazio, A. and Priestley, M.J.N. (2008) "*Seismic Design of Torsionally Eccentric Buildings with U-shape RC walls*", IUSS Press, Pavia, Italy.

[4] Bracci J.M., Kunnath S.K. and Reinhorn A.M. (1997**)** *"Seismic Performance and Retrofit Evaluation of Reinforced Concrete Structures"*, Journal of Structural Engineering, ASCE, Vol. 123, 3-10.

[5] Chintanapakdee C. and Chopra A.K. (2003) *"Evaluation of Modal Pushover Analysis Using Generic Frames"*, Earthquake Engineering and Structural Dynamics, Vol. 32, 417-442.

[6] Chopra A.K. (2001) *"Dynamics of Structures: Theory and Applications to Earthquake Engineering"*, Prentice-Hall: Englewood Cliffs, New Jersey.

[7] Chopra, A. K., and Chintanapakdee, C. (2004) *"Inelastic deformation ratios for design and evaluation of structures: single-degree-of-freedom bilinear systems"*, Journal of Structural Engineering, 130, 1309–1319.

[8] Chopra A.K. and Goel R.K. (2001**)** *"A modal pushover analysis procedure to estimate seismic demands for buildings: theory and preliminary evaluation"*, *Report No. PEER Report 2001/03*, Pacific Earthquake Engineering Research Center, University of California, Berkeley.

[9] Chopra A.K. and Goel R.K. (2002) *"A modal pushover analysis procedure for estimating seismic demands for buildings"*, Earthquake Engineering & Structural Dynamics, Vol.31, pp 561-582.

[10] Computers and Structures, SAP2000. V.14.0 (2009) *"Linear and Nonlinear Static and Dynamic Analysis and Design of Three Dimensional Structures"*, Berkeley, California, USA.

[11] Eberhard M.O. and Sözen M.A. (1993) *"Behavior-Based Method to Determine Design Shear in Earthquake Resistant Walls"*, Journal of the Structural Division, American Society of Civil Engineers, New York, Vol. 119, No.2, 619-640.

[12] EBCS-8 (1995) "*Design of Structures for Earthquake Resistance*", Ethiopian Building Code of Standard by Ministry of Works and Urban Development, Addis Ababa, Ethiopia.

[13] Federal Emergency Management Agency (1997) *"Prestandard and Commentary for the Rehabilitation of Buildings"*, FEMA-273, Washington DC.

[14] Federal Emergency Management Agency (2000) *"Prestandard and Commentary for the Rehabilitation of Buildings"*, FEMA-356, Washington DC.

[15] Goel R.K. (2006) *"Evaluation of nonlinear static procedures using strong-motion building records"*, Survey, Strong Motion Instrumentation Program, SMIP04 Seminar Proceedings.

[16] İnel M., Tjhin T. and Aschheim A.M. (2003) *"The Significance of Lateral Load Pattern in Pushover Analysis"*, İstanbul Fifth National Conference on Earthquake Engineering, Paper No: AE-009, İstanbul, Turkey.

[17] Krawinkler H. and Seneviratna G.D.P.K (1998) *"Pros and Cons of a Pushover Analysis of Seismic Performance Evaluation"*, Engineering Structures, Vol.20, 452-464.

[18] Medhanye B. (2003) "Correlation between Actual Reinforced Concrete Wall Behavior and Its Centerline Model" Master of Science Thesis, Addis Ababa University, Addis Ababa.

[19] Moghadam A.S. (2002) *"A Pushover Procedure for Tall Buildings, 12th European Conference on Earthquake Engineering"*, Paper Reference 395.

[20] Moghadam, A.S. and Tso, W.K. (1996) *"Damage assessment of eccentric multistory buildings using 3D pushover analysis"*, 11WCEE, Elsevier Science, Paper No. 997.

[21] NIST (2010). "*Nonlinear Structural Analysis For Seismic Design*", NIST GCR 10-917-5, prepared by the NEHRP Consultants Joint Venture for the National Institute of Standards and Technology, Gaithersburg, MD.

[22] Oguz S. (2005) *"Evaluation of Pushover Analysis Procedures for Frame Structures"*, Master of Science Thesis, METU, Turkey.

[23] Rana R., Jin L. and Zekioglu A. (2004) "*Pushover Analysis of a 19 Story Concrete Shear Wall Building*" 13th World Conference on Earthquake Engineering Vancouver, B.C., Paper No. 133, Canada.

[24] Sasaki F., Freeman S. and Paret T. (1998) "*Multi-Mode Pushover Procedure (MMP) - A Method to Identify the Effect of Higher Modes in a Pushover Analysis"*, Proc. 6th U.S. National Conference on Earthquake Engineering, Seattle, CD-ROM, EERI, Oakland.

[25] Tso, W.K. and Moghadam, A.S. (1997) *"Seismic response of asymmetrical buildings using pushover analysis"*, In: Fajfar P, Krawinkler, H, Editors. Seismic Design Methodologies for the Next Generation of Codes, Balkema: 311-22.

APPENDIX:

Values of Different Responses of RC Buildings in Tabular Form

Table A.1 Results of Storey displacement for five storey RC building in X-direction

	MPA						RSA
Level	Mode 1	Mode 2	Mode 3	One Mode	Two Modes	Three Modes	U1 (mm)
Roof	29.63	-0.33	-0.19	29.63	29.63	29.63	29.14
4th Floor	26.97	-0.11	0.10	26.97	26.97	26.97	26.15
3rd Floor	22.79	0.14	0.19	22.79	22.79	22.79	21.69
2nd Floor	17.05	0.29	0.00	17.05	17.05	17.05	15.85
1st Floor	10.16	0.27	-0.20	10.16	10.16	10.17	9.13
GF	3.13	0.10	-0.12	3.13	3.13	3.13	2.76

Table A.2 Results of Storey displacement for five storey RC building in Y-direction

	MPA						RSA
Level	Mode 1	Mode 2	Mode 3	One Mode	Two Modes	Three Modes	U2 (mm)
Roof	31.77	-0.16	0.84	31.77	31.77	31.78	33.62
4th Floor	29.41	-0.06	-0.38	29.41	29.41	29.41	28.95
3rd Floor	24.82	0.08	-0.90	24.82	24.82	24.84	23.15
2nd Floor	17.73	0.15	0.00	17.73	17.73	17.73	16.15
1st Floor	9.00	0.13	0.92	9.00	9.00	9.05	8.80
GF	2.26	0.05	0.06	2.26	2.26	2.26	2.62

Table A.3 Results of Storey displacement for ten storey RC building in X-direction

	MPA						RSA
Level	Mode 1	Mode 2	Mode 3	One Mode	Two Modes	Three Modes	U1 (mm)
9th	77.27	-2.25	3.52	77.27	77.30	77.38	83.41
8th	72.02	-0.88	0.84	72.02	72.03	72.03	74.27
7th	65.98	0.66	-1.63	65.98	65.98	66.00	64.92
6th	59.49	1.49	-3.37	59.49	59.51	59.60	56.34
5th	52.02	1.99	-4.44	52.02	52.06	52.25	47.87
4th	43.41	2.20	-4.82	43.41	43.47	43.73	39.16
3rd	33.85	2.11	-4.52	33.85	33.92	34.22	30.22
2nd	23.98	1.77	-3.66	23.98	24.05	24.32	21.42
1st	14.29	1.23	-2.42	14.29	14.34	14.55	12.72
Ground	4.47	0.43	-0.80	4.47	4.49	4.56	3.71

Table A.4 Results of Storey displacement for ten storey RC building in Y-direction

	MPA						RSA
Level	Mode 1	Mode 2	Mode 3	One Mode	Two Modes	Three Modes	U2 (mm)
Roof	118.13	15.40	0.46	118.13	119.13	119.13	125.57
9th	109.65	9.16	0.16	109.65	110.03	110.03	112.64
8th	100.50	2.36	-0.18	100.50	100.53	100.53	99.43
7th	90.43	-4.42	-0.34	90.43	90.54	90.54	86.16
6th	79.62	-9.45	-0.30	79.62	80.18	80.18	73.34
5th	68.28	-12.41	-0.12	68.28	69.40	69.40	61.07
4th	56.18	-13.41	0.16	56.18	57.76	57.76	48.90
3rd	43.51	-12.38	0.37	43.51	45.24	45.24	36.92
2nd	30.80	-9.89	0.42	30.80	32.35	32.35	25.50
1st	18.28	-6.57	0.33	18.28	19.42	19.43	14.69
Ground	5.48	-2.35	0.12	5.48	5.96	5.96	4.15

Table A.5 Results of Storey displacement for B + nine storey RC building in X-direction

	MPA						RSA
Level	Mode 1	Mode 2	Mode 3	One Mode	Two Modes	Three Modes	U1 (mm)
Roof	68.93	12.53	0.99	68.93	70.06	70.07	70.53
8th	65.40	8.28	0.92	65.40	65.92	65.93	66.23
7th	60.77	3.36	0.84	60.77	60.86	60.87	60.92
6th	55.50	-0.93	0.76	55.50	55.50	55.51	55.29
5th	49.86	-3.70	0.68	49.86	50.00	50.00	49.56
4th	43.21	-5.69	0.58	43.21	43.59	43.59	43.03
3rd	34.85	-6.71	0.47	34.85	35.49	35.49	34.98
2nd	26.09	-6.35	0.36	26.09	26.85	26.85	26.54
1st	16.84	-4.78	0.25	16.84	17.51	17.51	17.43
Ground	6.28	-2.01	0.10	6.28	6.59	6.59	6.62

Table A.6 Results of Storey displacement for B + nine storey RC building in Y-direction

	MPA						RSA
Level	Mode 1	Mode 2	Mode 3	One Mode	Two Modes	Three Modes	U2 (mm)
Roof	50.03	20.34	0.55	50.03	54.01	54.01	54.61
8th	48.53	19.16	0.38	48.53	52.18	52.18	52.44
7th	46.21	17.59	0.16	46.21	49.44	49.44	49.41
6th	43.06	16.14	-0.11	43.06	45.99	45.99	45.77
5th	39.03	15.24	-0.30	39.03	41.90	41.90	41.64
4th	34.19	13.84	-0.48	34.19	36.88	36.89	36.76
3rd	28.09	11.72	-0.60	28.09	30.44	30.44	30.56
2nd	21.74	9.51	-0.57	21.74	23.73	23.74	23.83
1st	14.68	6.69	-0.45	14.68	16.13	16.14	16.25
Ground	5.89	2.85	-0.20	5.89	6.55	6.55	6.59

Table A.7 Results of Inter-storey drift ratio for five storey RC building in X-direction

Level	hj (m)	MPA			RSA
		One Mode	Two Modes	Three Modes	
Roof	3.00	0.089	0.089	0.089	0.100
4th Floor	3.00	0.139	0.139	0.139	0.148
3rd Floor	3.00	0.191	0.191	0.191	0.195
2nd Floor	3.00	0.230	0.230	0.230	0.224
1st Floor	3.00	0.234	0.234	0.234	0.212
GF	2.50	0.125	0.125	0.125	0.110

Table A.8 Results of Inter-storey drift ratio for five storey RC building in Y-direction

Level	hj (m)	MPA			RSA
		One Mode	Two Modes	Three Modes	
Roof	3.00	0.079	0.079	0.079	0.156
4th Floor	3.00	0.153	0.153	0.153	0.193
3rd Floor	3.00	0.236	0.236	0.237	0.233
2nd Floor	3.00	0.291	0.291	0.289	0.245
1st Floor	3.00	0.225	0.225	0.226	0.206
GF	2.50	0.090	0.090	0.090	0.105

Table A.9 Results of Inter-storey drift ratio for ten storey RC building in X-direction

Level	hj (m)	MPA			RSA
		One Mode	Two Modes	Three Modes	
Roof	3.00	0.151	0.152	0.156	0.288
9th floor	3.00	0.175	0.176	0.178	0.305
8th Floor	3.00	0.201	0.201	0.201	0.312
7th Floor	3.00	0.216	0.216	0.213	0.286
6th Floor	3.00	0.249	0.248	0.245	0.282
5th Floor	3.00	0.287	0.286	0.284	0.290
4th Floor	3.00	0.319	0.318	0.317	0.298
3rd Floor	3.00	0.329	0.329	0.330	0.293
2nd Floor	3.00	0.323	0.323	0.326	0.290
1st Floor	3.45	0.285	0.286	0.289	0.261
G. Floor	3.00	0.149	0.150	0.152	0.124

Table A.10 Results of Inter-storey drift ratio for ten storey RC building in Y-direction

Level	hj (m)	MPA			RSA
		One Mode	Two Modes	Three Modes	
Roof	3.00	0.283	0.303	0.303	0.431
9th floor	3.00	0.305	0.317	0.317	0.440
8th Floor	3.00	0.336	0.333	0.333	0.442
7th Floor	3.00	0.360	0.345	0.345	0.427
6th Floor	3.00	0.378	0.359	0.359	0.409
5th Floor	3.00	0.403	0.388	0.388	0.406
4th Floor	3.00	0.422	0.417	0.417	0.399
3rd Floor	3.00	0.424	0.430	0.430	0.381
2nd Floor	3.00	0.417	0.431	0.431	0.360
1st Floor	3.45	0.371	0.390	0.390	0.306
G. Floor	3.00	0.183	0.199	0.199	0.138

Table A.11 Results of Inter-storey drift ratio for B + nine storey RC building in X-direction

Level	hj (m)	MPA			RSA
		One Mode	Two Modes	Three Modes	(x dir.)
Roof	3.06	0.115	0.135	0.135	0.141
8th Floor	3.06	0.151	0.165	0.165	0.174
7th Floor	3.06	0.172	0.175	0.175	0.184
6th Floor	3.06	0.184	0.180	0.180	0.187
5th Floor	3.06	0.217	0.209	0.209	0.213
4th Floor	3.40	0.246	0.238	0.238	0.237
3rd Floor	3.40	0.258	0.254	0.254	0.248
2nd Floor	3.40	0.272	0.275	0.275	0.268
1st Floor	4.08	0.259	0.268	0.268	0.265
G. Floor	3.40	0.185	0.194	0.194	0.195

Table A.12 Results of Inter-storey drift ratio for B + nine storey RC building in Y-direction

Level	hj (m)	MPA			RSA
		One Mode	Two Modes	Three Modes	(y dir.)
Roof	3.06	0.049	0.060	0.060	0.071
8th Floor	3.06	0.076	0.090	0.090	0.099
7th Floor	3.06	0.103	0.113	0.113	0.119
6th Floor	3.06	0.132	0.134	0.134	0.135
5th Floor	3.06	0.158	0.164	0.164	0.160
4th Floor	3.40	0.179	0.190	0.190	0.182
3rd Floor	3.40	0.187	0.197	0.197	0.198
2nd Floor	3.40	0.208	0.223	0.224	0.223
1st Floor	4.08	0.215	0.235	0.235	0.237
G. Floor	3.40	0.173	0.193	0.193	0.194

Table A.13 Results of Storey shear for five storey RC building in X-direction

	MPA						RSA
Level	Mode 1	Mode 2	Mode 3	1 Mode	2 Modes	3 Modes	Vx(kN)
Roof	165.56	-17.39	-25.75	165.56	166.47	168.45	144.73
4th Floor	310.98	-20.81	-3.47	310.98	311.68	311.69	302.47
3rd Floor	430.41	-10.68	25.27	430.41	430.54	431.28	433.61
2nd Floor	515.36	6.44	17.37	515.36	515.40	515.69	529.87
1st Floor	561.30	20.30	-16.85	561.30	561.67	561.92	586.15
GF	576.86	26.13	-39.24	576.86	577.45	578.78	605.56

Table A.14 Results of Storey shear for five storey RC building in Y-direction

	MPA						RSA
Level	Mode1	Mode 2	Mode 3	1 Mode	2 Modes	3 Modes	Vy(kN)
Roof	88.86	4.90	-64.90	88.86	88.99	110.15	94.89
4th Floor	167.49	5.98	-14.92	167.49	167.60	168.26	200.74
3rd Floor	231.24	2.87	60.76	231.24	231.26	239.11	288.93
2nd Floor	275.17	-2.27	41.06	275.17	275.18	278.23	351.11
1st Floor	297.27	-6.20	-48.05	297.27	297.33	301.19	383.86
GF	304.28	-7.80	-108.33	304.28	304.38	323.08	393.93

Table A.15 Results of Storey shear for ten story RC building in X-direction

	MPA						RSA
Level	Mode 1	Mode 2	Mode 3	1 Mode	2 Modes	3 Modes	Vx(kN)
Roof	366.66	-585.49	50.73	366.66	690.82	692.68	486.48
9th floor	692.70	-972.35	103.50	692.70	1193.86	1198.34	860.02
8th Floor	989.60	-1105.90	151.84	989.60	1484.02	1491.77	1161.35
7th Floor	1266.22	-948.51	-196.88	1266.22	1582.09	1594.29	1389.72
6th Floor	1523.51	-648.73	-238.13	1523.51	1655.88	1672.91	1615.71
5th Floor	1749.83	-267.56	-274.41	1749.83	1770.17	1791.31	1826.24
4th Floor	1940.79	147.04	-305.01	1940.79	1946.35	1970.10	2013.06
3rd Floor	2103.76	568.77	-330.76	2103.76	2179.29	2204.25	2182.47
2nd Floor	2227.23	923.39	350.23	2227.23	2411.06	2436.36	2261.60
1st Floor	2306.25	1165.92	361.77	2306.25	2584.21	2609.41	2325.79
G. Floor	2320.06	1210.16	363.40	2320.06	2616.71	2641.82	2336.19

Table A.16 Results of Storey shear for ten story RC building in Y-direction

	MPA						RSA
Level	Mode 1	Mode 2	Mode 3	1 Mode	2 Modes	3 Modes	Vy(kN)
Roof	414.56	-41.99	9.45	414.56	416.68	416.79	433.93
9th floor	784.92	-71.16	11.24	784.92	788.14	788.22	761.99
8th Floor	1127.41	-86.85	5.38	1127.41	1130.75	1130.76	1032.20
7th Floor	1451.70	-82.61	-4.86	1451.70	1454.05	1454.06	1245.09
6th Floor	1748.43	-62.87	-12.80	1748.43	1749.56	1749.61	1445.64
5th Floor	2006.13	-35.85	-15.66	2006.13	2006.45	2006.51	1632.66
4th Floor	2221.23	-3.58	-12.66	2221.23	2221.23	2221.27	1798.19
3rd Floor	2401.67	32.51	-4.60	2401.67	2401.89	2401.90	1947.79
2nd Floor	2533.59	62.71	4.57	2533.59	2534.37	2534.37	2016.82
1st Floor	2613.38	78.49	10.22	2613.38	2614.56	2614.58	2070.98
G. Floor	2626.13	81.16	11.94	2626.13	2627.38	2627.41	2079.29

Table A.17 Results of Storey shear for B + nine story RC building in X-direction

	MPA						RSA
Level	Mode 1	Mode 2	Mode 3	1 Mode	2 Modes	3 Modes	Vx(kN)
Roof	231.26	308.35	96.67	231	385	397	408.35
8th Floor	454.96	497.84	77.92	455	674	679	663.70
7th Floor	619.00	531.05	-65.01	619	816	818	842.39
6th Floor	866.19	502.78	-95.84	866	1002	1006	1046.03
5th Floor	1087.85	378.81	-122.73	1088	1152	1158	1217.75
4th Floor	1293.30	166.05	-148.83	1293	1304	1312	1386.92
3rd Floor	1480.36	-133.48	178.36	1480	1486	1497	1576.38
2nd Floor	1617.25	-409.38	200.17	1617	1668	1680	1756.42
1st Floor	1706.65	-620.06	214.71	1707	1816	1828	1920.87
G. Floor	1737.29	-701.72	219.90	1737	1874	1887	2000.70

Table A.18 Results of Storey shear for B + nine story RC building in Y-direction

	MPA						RSA
Level	Mode 1	Mode 2	Mode 3	1 Mode	2 Modes	3 Modes	Vy(kN)
Roof	243.09	16.63	-295.26	243	244	383	375.86
8th Floor	493.75	17.71	-515.69	494	494	714	641.18
7th Floor	666.45	62.80	-581.33	666	669	887	848.69
6th Floor	884.20	276.02	-576.04	884	926	1091	1079.47
5th Floor	1081.24	476.76	-473.14	1081	1182	1273	1282.44
4th Floor	1274.69	656.73	-263.76	1275	1434	1458	1479.20
3rd Floor	1457.95	-854.53	34.89	1458	1690	1690	1694.26
2nd Floor	1596.45	-1007.56	326.50	1596	1888	1916	1882.24
1st Floor	1690.54	-1115.32	559.85	1691	2025	2101	2045.34
G. Floor	1725.26	-1155.41	657.12	1725	2076	2178	2128.41

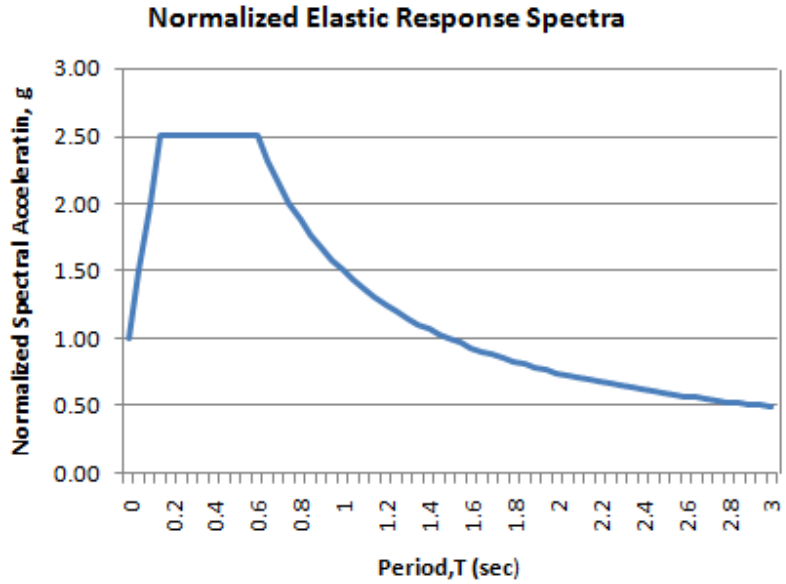

Figure A.1. Normalized Elastic Response Spectra from EBCS-8, 1995 for Soil Class-B

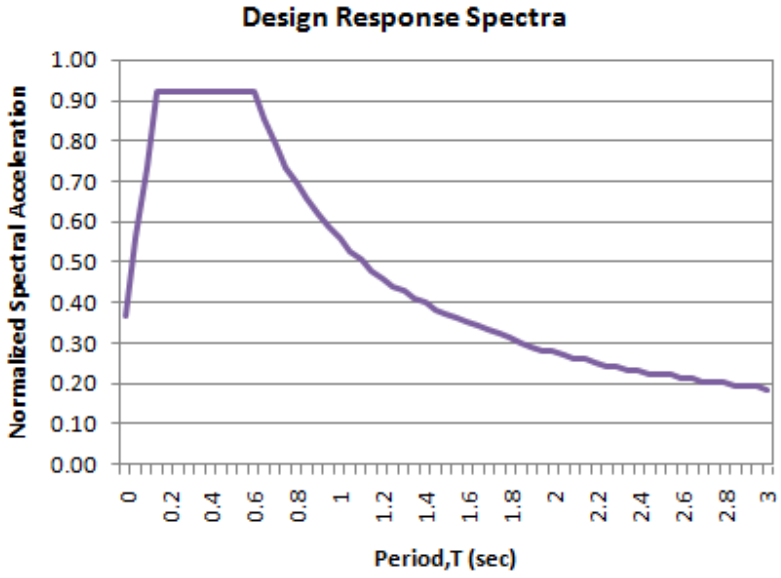

Figure A.2. Design Response Spectra of Soil Class-B for PGA= 0.1g

DECLARATION

I, the undersigned, declare that this thesis is my work and all sources of materials used for the thesis have been duly acknowledged.

Name:	Abdi Mohammed
Signature	_____
Place	Addis Ababa University
	Addis Ababa Institute of Technology
Date of submission	March 2012